Structural control of void formation in dual phase steels

Azuma, Masafumi

Publication date:
2013

Document Version
Publisher's PDF, also known as Version of record

Structural control of void formation in dual phase steels

DTU Vindenergi
PhD Rapport 2013

Masafumi Azuma
DTU Wind Energy PhD-0015 (EN)

April 2013

DTU Vindenergi
Institut for Vindenergi

Author: Masafumi Azuma

Title: Structural control of void formation in dual phase steels

Division: Section for Materials Science and Advanced Characterization

Department of Wind Energy

This thesis is submitted in partial fulfillment of the requirements for the Ph.D. Degree at the Technical University of Denmark.

DTU Wind Energy PhD-0015 (EN)

April 2013

Abstract

The objective of this study is to explore the void formation mechanisms and to clarify the influence of the hardness and structural parameters (volume fraction, size and morphology) of martensite particles on the void formation and mechanical properties in dual phase steels composed of ferrite and martensite. Two dual phase steels (Fe-0.099mass%C-1.63mass%Mn and Fe-0.148mass%-1.60mass%Mn) with martensite particles of different hardness values, volume fractions, sizes and shapes were produced by hot rolling and annealing. Mechanical properties were characterised by Vickers hardness and nanohardness measurements, tensile tests and hole-expansion tests. The initial microstructure and the deformed microstructure were characterized by means of scanning electron microscopy (SEM) and transmission electron microscopy (TEM). In situ tensile tests in a SEM were applied for direct observation of the void formation behaviour.

In this study it is found that most voids form in martensite particles and few voids form in the ferrite matrix. The void formation in the martensite is related to plastic deformation and cracking of martensite particles. The voids in ferrite predominantly form near the end of the martensite particles but are not caused by the decohesion of martensite/ferrite interfaces. Three key factors that control the void formation behaviour in dual phase steels have been established: (i) a critical strain for void formation in the martensite, (ii) strain partitioning between the martensite and ferrite and (iii) strain localization. The critical strain for void formation depends on hardness of the martensite, but is independent of the volume fraction, shape, size and distribution of the martensite. The strain partitioning between the martensite and ferrite depends on the volume fraction and hardness of martensite particles. The strain localization is related to the morphology of the martensite particles and the strength of the ferrite.

Softening of the martensite significantly retards void formation in the martensite, but does not change the void formation mechanisms. The increase of volume fraction of the martensite accelerates the void formation in the martensite by enlarging the size of voids both in the martensite and ferrite. It is suggested that controlling the hardness and structural parameters associated with the martensite particles such as morphology, size and volume fraction are the essential approach to retard the void formation in the dual phase steels.

ISSN: 0106-2840

ISBN: 978-87-92896-40-7

Sponsorship:

Nippon Steel Corporation

Danmarks Tekniske Universitet

DTU Vindenergi

Nils Koppels Allé

Bygning 403

2800 Kgs. Lyngby

www.vindenergi.dtu.dk

Structural control of void formation in dual phase steels

Masafumi Azuma

Supervised by Xiaoxu Huang and Grethe Winther

Section for Materials Science and Advanced Characterization
Department of Wind Energy
Technical University of Denmark
April 2013

Contents

Preface

This report is submitted in partial fulfilment of the requirements for the PhD degree at the Technical University of Denmark. The project was started within the Center for Fundamental Research: Metal Structures in Four Dimensions (M4D), Materials Research Division, Risø DTU, under the supervision of senior scientists, Drs. Xiaoxu Huang, Niels Hansen and Grethe Winther. The study was conducted during the period from September 2009 to November 2012. From January 2012, my main supervisor, Dr. Xiaoxu Huang, joint the Department of Wind Energy, after the reorganization of DTU.

I am grateful to Head of the Materials Research Division Dr. Dorte Juul Jensen and Head of the Center Dr. Henning Friis Poulsen who gave me the opportunity to work within the M4D Center. I am thankful to my supervisors Xiaoxu Huang, Niels Hansen and Grethe Winther, who have provided me with constant discussion, encouragement and much useful support through my PhD study. In particular, Niels Hansen and Xiaoxu Huang are encouraging me all the time. I am also thankful to Stergios Goutianos, who has helped me to do in-situ observations and discussed my PhD work with me. I would like to thank Professors Brian Ralph, Johannes Weertman, Julia Weertman and Nobuhiro Tsuji for their help and discussion. I would like to thank Drs. Wolfgang Pantleon, Oleg Mishin, Leon Mishnaevsky Jr., Yubin Zhang, Xiaodan Zhang and Chuanshi Hong, and PhD students Tianbo Yu and Fengxiang Lin and Jacob Kidmose for their help. Special thanks to the very skilful technicians, Gitte Christiansen, Preben Olesen, Lars Lorentzen, Steen Bang, Frank Adrian, Ove Rasmussen and Erik Vogeley.

Finally, I would like to thank Nippon Steel Corporation for financial support and for producing the steel sheets used in this study and to thank Japanese colleagues, Hiroyuki Kawada, Naoki Maruyama and Naoki Yoshinaga who supported producing the steel sheets and carried out some experiments.

Publications

Paper 1 Azuma M., Hansen Goutianos, S., Hansen N., Winther G. and Huang X. In-situ observation of void formation in dual phase steel. In *30th Risø International Symposium on Material Science* (eds N. Hansen et al.), 2010, 243-251. Roskilde, Denmark: Risø National Laboratory.

Paper 2 Azuma M., Hansen Goutianos S., N., Winther G. and Huang X. Effect of hardness of martensite and ferrite on void formation in dual phase steel. *Mater. Sci. Tech.*, 2012, 28, 1092-1100.

Paper 3 Azuma M., Hansen N., Winther G. and Huang X. In-situ observation of void formation in dual phase steel. *CAMP-ISIJ*, 2012, Vol.25, 417.

Paper 4 Azuma M., Hansen N., Winther G. and Huang X. Effect of martensite hardness on void formation during plastic deformation of a dual phase steel. *CAMP-ISIJ*, 2012, Vol.25, 1132.

Paper 5 Matsuno T., Azuma M., Maeda D., Uenishi A. and Suehiro M. Mechanism Analysis of Micro Voids Nucleation in Ferrite-Martensite Dual Phase Steel by FEM. *CAMP-ISIJ*, 2012, Vol.25, 1065.

Paper 6 Azuma M., Hansen N., Winther G. and Huang X. In-situ observation of void formation during plastic deformation of dual phase steel (in preparation).

Chapter 1

Introduction

Metals have been widely used as structural materials in buildings, ships and automobiles for the last two hundred years. Modern society requires light strong materials for economical, environmental and safety reasons. Therefore, a great effort has been put into developing light strong materials. Advanced high strength steels are one of the answers to the complicated question. As a carbon addition into iron enables to apply phase transformations, precipitation and recrystallization to control microstructures and textures, a wide variety of high strength steels have been produced. Whereas the strength is an important issue, the formability is also required to apply high strength steels for automobiles and electrical appliances. In particular, as components for automobile and electrical appliances are often deformed by stamping and bending, formability is required. However, as strengthening generally reduces the formability such as elongation in tension poor formability should be improved in order to apply for complicated components. Advanced high strength steels such as dual phase steels consisting of a soft ferrite matrix and hard martensite particles, are one of the answers to the complicated question as they have a good balance of elongation, in particular uniform elongation, and high strength. The soft ferrite matrix ensures uniform elongation and hard martensite particles contribute high strength and large work hardening rate. Whereas the uniform elongation is one of the most important parameters for the formability, formability for hole-expansion tests and bending tests is also required to apply steels for complicated automobile components. On the other hand, it is well-known that void formation leads to ductile fracture of metals. For instance, many dimples related to void formation are observed on fracture surfaces of metals after tensile tests at ambient temperature. In general, most voids start to nucleate in single-phase metals after the onset of necking. However, many voids form in metal matrix composites, which consist of a metal matrix and carbides, nitrides, sulphides and oxides, due to a weak bonded interface and brittle reinforcements before necking. As strain and stress encourage voids to form in metals and composites, void formation has a larger effect on post-necking elongation in tension, the formability for hole-expansion tests and bending tests. As dual phase steels have poor formability for hole-expansion tests and bending tests, the formability should be improved. However, even though void formation has a large effect on the formability, the void formation mechanism and effect of metallurgical parameters on void formation in dual phase steels are still ambiguous.

This project is to study the void formation mechanism and the influence of metallurgical parameters including hardness, volume fraction and size of martensite particles in dual phase steels. This thesis is structured as following: Chapter 2 gives a short review of the background; Chapter 3 introduces the materials and experimental procedures used in this study; Chapter 4 demonstrates void formation behaviour in a dual phase steel during in-situ loading; Chapter 5 reports the influence of martensite hardness on the void formation behaviour and main parameters for void formation in a dual phase steel; Chapter 6 suggests the influence of volume fraction; Chapter 7 shows the influence of the morphology of martensite particles on the deformation behaviour of martensite particles in the dual phase steel; and Chapter 8 gives conclusions and outlook.

Chapter 2

Background

2.1 Formability for automobiles

Most steel sheets are cut mechanically, deformed through stamping and applied as automobile components. Therefore, the steel sheets need to have a good formability for the stamping. Typically the following formability for i) deep drawing, ii) stretching, iii) stretch flanging and iv) bending is required due to complicated shapes. In particular, applications for outer panels such as doors, side panels and roof panels require the formability for deep drawing and stretching as shown in Fig. 2.1. In order to improve the formability for deep drawing, textures of steel sheets are controlled by chemical composition, thermomechanical treatments and heat treatments. In addition, smoothness of the surface is also an important property and mild steels are often used for panels due to low yield stress and excellent deep drawability. On the other hand, structural components such as cross-members, wheels and pillars are deformed through bending, hole-expansion and stretch flanging after cutting. It is suggested that the formability for stretch flanging, hole-expansion and bending is strongly related to void formation, growth and coalescence in steel sheets as a large number of dimples related to void formation are observed on the fracture surface of the specimens (e. g. Nishimoto et al. 1981, Hasegawa et al. 2004, Toji et al. 2009, Tasan et al. 2009, Hayashi et al. 2012). In particular, during hole-expansion and bending tests deformation localizes at the edge of the sheets and strains at the edge are much larger than uniform elongation in tensile tests as stress gradients retard the onset of necking. Even though uniform elongation is an important parameter, the formability for stretch flanging and bending is also important. As voids form with strain (e. g. Maire et al. 2008, Landron et al. 2010, Avramovic et al. 2010) and reduce the area of cross section in specimens, reduction in area and thickness is also related to void formation. Therefore, a great effort to clarify void formation mechanisms and control void formation is explored.

2.2 Advanced High Strength Steels

Typically the following high strength steels; i) solid solution hardened steel, ii) precipitation hardened steel, iii) dual phase steel, iv) TRIP (Transformation Induced Plasticity) steel, v) bainite (martensitic) steel, are often applied for automobiles components. Solution hardened steels are typically strengthened by a solid solution of phosphorus (P), manganese (Mn) and silicon (Si). However, the strengthening is limited as P has a negative effect on weldability (e. g. Saito et al. 1987) and Si leads to defects on the surface (e. g. Takada et al. 2009, Shimada et al. 2009). The solid solution hardening contributes to 270-540MPa grade steel sheets (Fig. 2.2). Precipitation hardened steels are strengthened by titanium carbides, niobium carbides and vanadium carbides. The precipitations increase the yield stress and ultimate tensile strength as precipitations disturb dislocation motion, counterbalanced by a reduction of elongation. As shown in Fig. 2.2, the precipitation hardened steels have poor elongation compared with other high strength steels. Dual phase steels consisting of a soft ferrite phase and hard a martensite phase are more attractive for automobile components due to better combination of strength and elongation. As the hard martensite contributes to the strength and a soft ferrite matrix ensures elongation and it follows that the grain size of ferrite, the volume fraction and hardness of martensite are important parameters. These are controlled through the chemical composition of the steel and the conditions under which it is heat treated. TRIP steels have more complicated microstructures consisting of ferrite, bainite and retained austenite. Retained austenite attributes to a large work hardening rate and strength as plastic deformation assists retained austenite to transform to martensite strengthening the steels. After deformation, the microstructures consist of the ferrite matrix, bainite and martensite phases. Dual phase steels and TRIP steels

have a large elongation, in particular, large uniform elongation (Fig.2.2). On the other hand, bainitic steels and martensitic steels have homogeneous microstructures composed of a single microstructure. Bainite and martensite containing a large number of dislocations have a large strength, which is larger than 980MPa (Morito et al. 2003), but the elongation is the smallest of all (Akisue and Hata 1995, Kishida 2000). While the uniform elongation is an important parameter, the formability of the material depends on the response to localized deformation. Parameters to characterize this include the local elongation in the necking zone of a tensile test, the hole-expansion ratio determined by pushing a cone through a punched hole and the elongation through bending (e. g. Hasegawa et al. (2004), Yamazaki et al. (1995)). Fig. 2.2 exemplifies the formability for hole-expansion tests of high strength steels. The hole-expansion tests are used to estimate formability for automobile components. In general, a strain after hole-expansion tests by a conical punch is much larger than uniform elongation and the better formability at a large strain is required. It is well-known that bainitic and martensitic steels have a better formability for hole-expansion tests due to the homogeneous microstructures. On the other hand, dual phase steels and TRIP steels have a poor formability and the formability should be improved to apply dual phase steels for more complicated components.

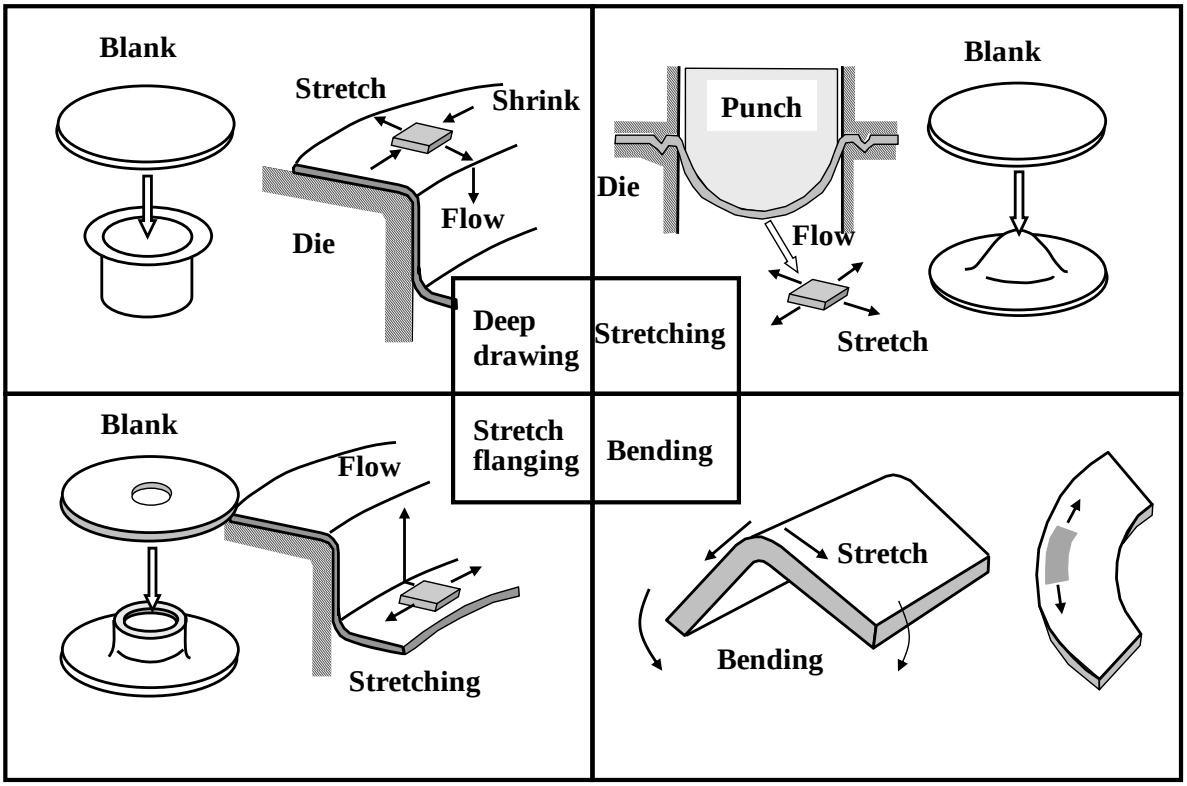

Fig. 2.1 Typical formation process for automobile components: 1) deep drawing, 2) stretching, 3) stretch flanging and 4) bending. The formability for deep drawing and stretching is more important for outer panels such as doors and front panels. Structural components such as pillars and wheels require more the formability for stretch flanging and bending.

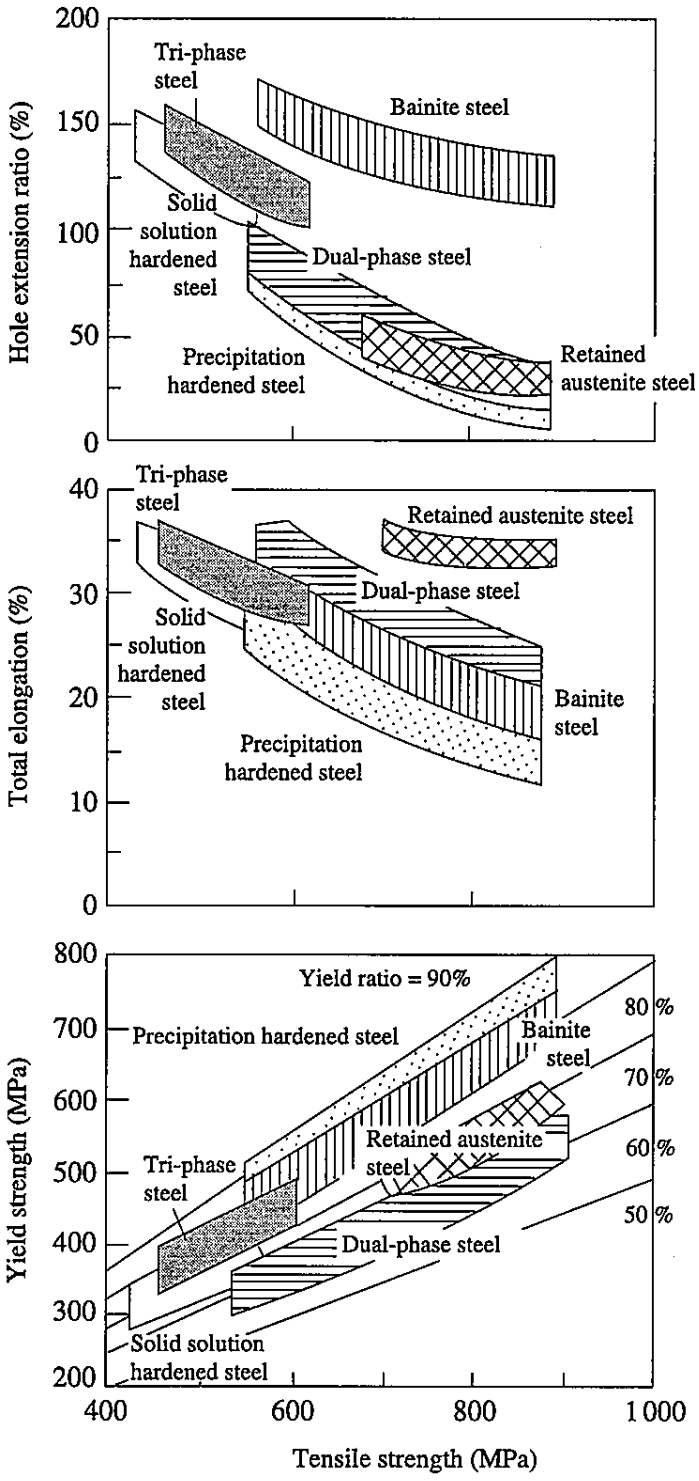

Fig. 2.2 Relationship between tensile ultimate tensile strength and formability of hot rolled high strength steel sheets. Reproduced from Kishida (2000).

2.3 Voids in metals

It is well-known that void formation in metals and metal matrix composites affects the strength, uniform elongation and total elongation. Voids are empty space, void formation leads to a reduction of a cross section of specimens and thereby affects mechanical properties. For instance, Vasudevan et al. (1989) showed that in a

metal matrix composite (Al-20vol.%SiC), where voids start to appear before the onset of necking, void formation decreases the flow stress, ultimate tensile strength, uniform elongation and fracture elongation through tensile tests under hydrostatic pressure as shown in Fig. 2.3. On the other hand, Fig. 2.4 shows that the yield stress, ultimate tensile stress and uniform elongation do not depend on hydrostatic pressure in aluminium as voids form after necking. In addition, González et al. (2002) demonstrated that hydrostatic pressure affects the work hardening rate due to void formation and thereby retards the onset of necking in a metal matrix through a finite element modelling (FEM) analysis (Fig. 2.5). It is obvious that void formation accelerates ductile fracture. For instance, a large number of voids are observed in the necking zone of tensile specimens and near the fracture surface of the specimens. As mentioned above, in metals without hard particles and inclusions, void formation mainly affects the post-uniform elongation, which is defined as an elongation after necking, as voids form in the necking zone of tensile specimens. It is well-known that decohesion at interfaces between metals and particles and particle cracking leads to void formation in metal matrix composites. For instance, Babout et al. demonstrated that decohesion at interfaces between Al and ceramics particles, which consisted of a mixture of zirconia (70% in weight) and silica (30% in weight), and particle cracking of the ceramics dominates in Al alloy-ceramic composites through X-ray tomography (2001, 2004). Decohesion often occurred at the interface facing to the tensile axis and cracks in the particles propagated perpendicular to the tensile axis. As cracks at the interface and in the particles developed into voids and grew in the tensile direction, the morphology of voids depended on strain applied to specimens. Finally, they coalesced with each other and macro-crack formation led to fracture of the specimens. It appears that particle cracking and decohesion are important mechanisms for void formation in composite structures.

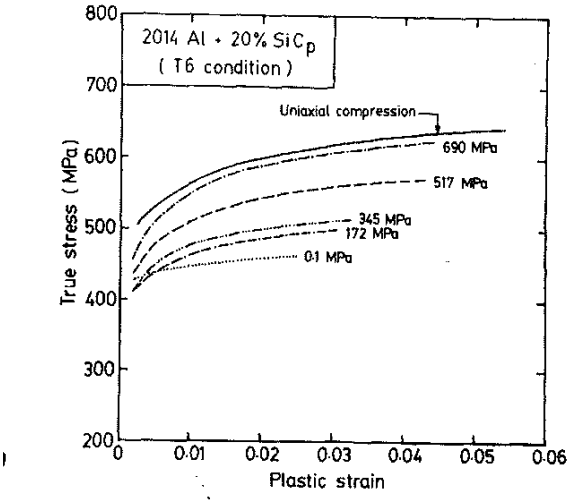

Fig. 2.3 Influence of hydrostatic pressure on stress-strain curves of reinforced 2014 aluminum alloy. Reproduced from Vasudevan et al. (1989).

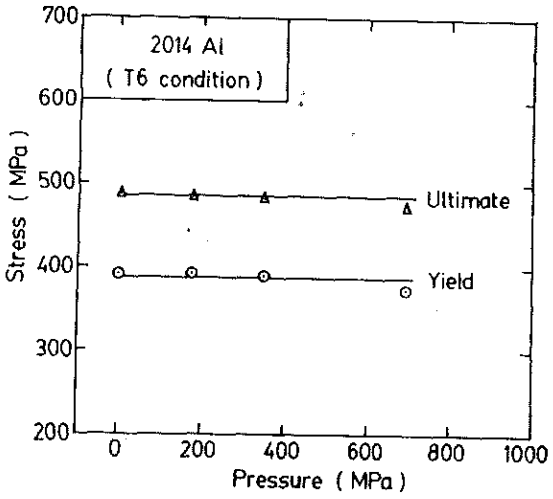

Fig. 2.4 Influence of hydrostatic pressure on the yield stress and ultimate tensile strength of the unreinforced 2014 aluminum alloy. Reproduced from Vasudevan et al. (1989).

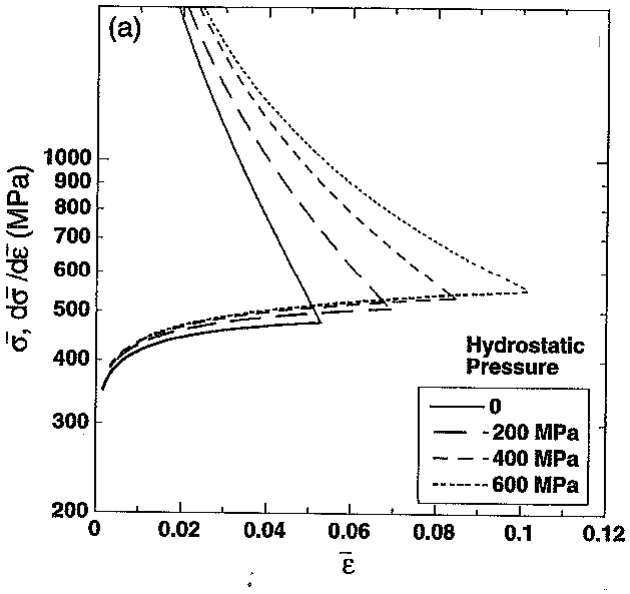

Fig. 2.5 Influence of hydrostatic pressure on the flow stress (σ) and the work hardening rate (dσ/dε) in a metal matrix composite. Reproduced from González et al. (2002).

In dual phase steels, void formation has also been an important objective as a large number of voids are observed near the fracture surface of specimens after tensile tests, bending tests and hole-expansion tests. Many investigations have shown that voids can form in the martensite, in the ferrite and at inclusions and that void formation related to the martensite particles dominates. Therefore, void formation behaviour in dual phase steels is investigated in order to clarify void formation mechanisms and the influence of metallurgical parameters, such as hardness, volume fraction and shape of martensite particles, on void formation in dual phase steels.

Chapter 3

Materials and techniques

3.1 Mechanical tests

3.1.1 Hardness test

A micro-hardness test was carried out to evaluate the hardness of the martensite and ferrite phases in the dual phase steels. Hardness is one of the important methods to evaluate mechanical properties of materials even though it is an intrinsic material property. The hardness increases linearly with tensile strength of materials insofar as the sizes are in a same order. In particular, as dual phase steels are a mixture of a soft ferrite matrix and hard martensite particles, it is difficult to evaluate the mechanical properties of each phase by a tensile test. On the other hand, micro-hardness tests enable one to measure the hardness of each grain/particle easily. Therefore, a micro-hardness test was carried out.

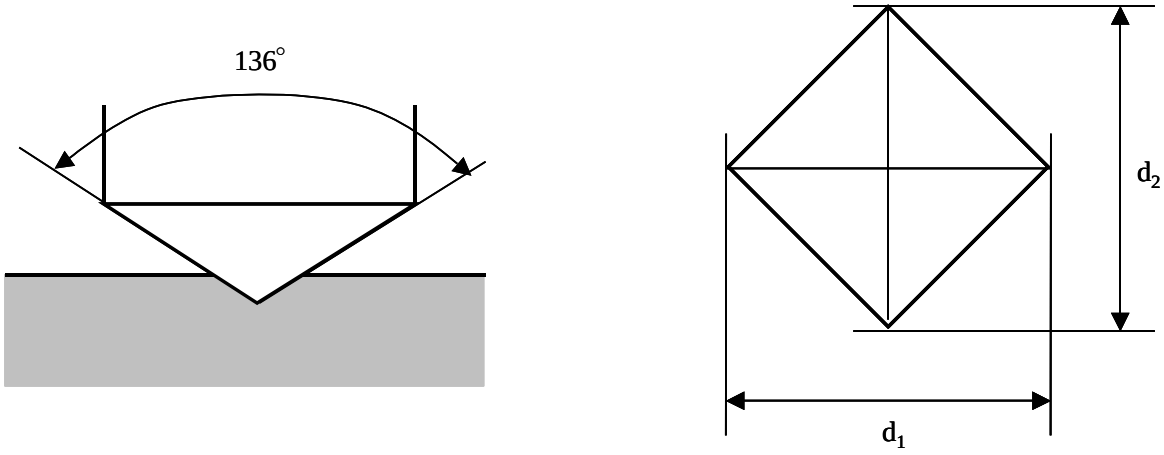

Fig. 3.1 An illustration of Vickers hardness test and an indent by the test.

In this study, the hardness of the martensite and ferrite was characterized by a Vickers hardness test. The Vickers hardness test consists of indenting the test materials with a diamond indenter, which has a pyramidal shape and an angle of 136°. After the indentation, the diameters (d1 and d2 in Fig. 3.1) of the indent were measured and the Vickers hardness (kgf/mm^2) is given by the following equation:

$$Hv = 2F \sin \frac{\frac{136^\circ}{2}}{\left(\frac{d_1 + d_2}{2}\right)^2} \qquad \text{Eq. [1]}$$

The specimen was polished and etched with nital to distinguish the martensite with ferrite. For the micro-hardness test, a Struers DuraScan 70 Hardness test was used with a load of 10gf applied for 10 seconds. For each phase 10 particles/grains were measured and the values were averaged. The indent size was about 5-10μm and were often larger than the ferrite grains and martensite particles as shown in Fig. 3.2. In particular, in deformed specimens martensite particles were stretched in the tensile direction and were thin (Fig. 3.2c). The large grains/particles were chosen to evaluate the hardness by the indents.

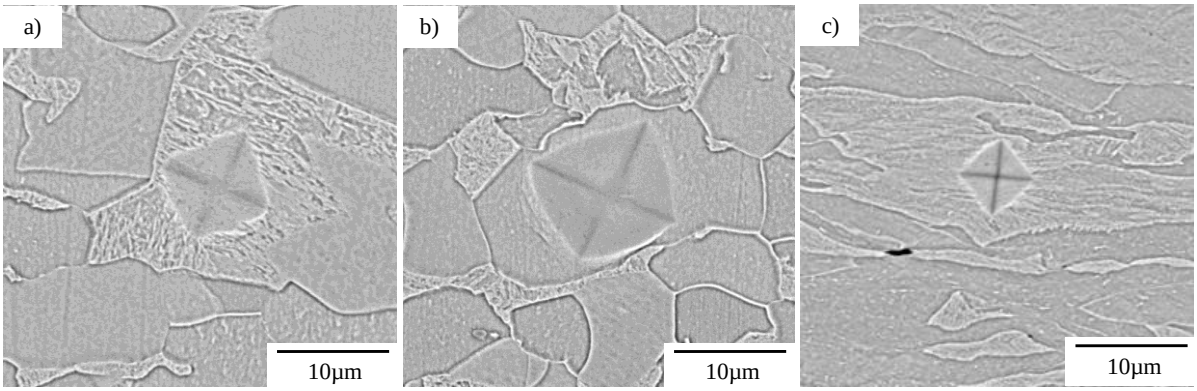

Fig. 3.2 Indents by Vickers hardness tests: a) in the martensite before a tensile test, b) in the ferrite before a tensile test and c) in the martensite after a tensile test.

It is well-known that the hardness depends on the indent size (e.g. Stelmashenko et al. 1993, Miyahara et al. 2001). The hardness measured by smaller indents tends to be large due to relatively large elastic deformation. On the other hand, if the indent size is smaller than the grain size of materials, the hardness tends to be smaller than the macro-scale hardness as the hardness does not contain the effect of grain boundary hardening. In the present study, the hardness of the ferrite does not contain effect of grain boundary hardening, but that of the martensite is affected by grain boundary hardening as the martensite consists of small laths of martensite (the width are about 200nm).

3.1.2 Tensile test

Flat dog-bone specimens of dimensions 3 mm × 35 mm × 180 mm were deformed in tension. The gauge length was 50 mm and the gauge width was 25 mm. The strain rate was controlled by the motion of a cross head and the cross head speed was 3.3×10^{-3} (s^{-1}). The tensile direction (TD) was parallel to the transverse direction of the rolled sheet. During tensile testing, after the stress overcame the ultimate tensile strength, the extensometer was removed. The total elongation was instead estimated based on measurement of gauge length changes after the tensile test. The following parameters have been determined: yield stress (YS), ultimate tensile strength (UTS), uniform elongation (U-El.), total elongation (T-El.) and post-uniform elongation (P-El.) in the necking zone. The uniform and total elongations were estimated based on the nominal strain. Void formation mainly affects the P-El. which is the elongation of the specimen from the start of necking to fracture.

The work hardening rate of the stress-strain curves in Fig. 3.3 was analysed in more detail in order to clarify which phenomenon affect the work hardening rate in the dual phase steels. For the analysis, the modified Crussard-Jaoul analysis (e.g. Lian et al. 1991, Jiang et al. 1995) which is based on the Swift formula, was carried out. In the formula, a stress-strain relationship is given by the following:

$$\varepsilon = \varepsilon_0 + c\sigma^m \qquad \text{Eq. [2]}$$

where ε_0 is an initial true strain, m is a work-hardening exponent and c is a material constant. An integrated form of Eq. [2] with respect to ε, is transformed into a logarithmic form:

$$\ln\left(\frac{d\sigma}{d\varepsilon}\right) = (1-m)\ln(\sigma) - \ln(cm) \qquad \text{Eq. [3]}$$

The slope of the $ln(d\sigma/d\varepsilon)$ vs $ln(\sigma)$ curve equals to $(1-m)$ and the intersection with $ln(s)=(\sigma)$ is given by $ln(cm)$.

In general, as the stress-strain relationship of dual phase steels is affected by the deformation of the ferrite phase and martensite phase, the work hardening behaviour of dual phase steels is divided into two regions (Fig. 3.3); (i) plastic deformation of the ferrite phase and elastic deformation of martensite phase, and (ii) plastic deformation of ferrite and martensite phases. In the first region, the work hardening rate is relatively large as a

large number of dislocations pile up at the martensite/ferrite interfaces because the martensite can deform elastically. In the second region, the work hardening rate is relatively small due to strain accommodation by plastic deformation of the martensite phase. It is also suggested that the slope of Eq. [3] changes suddenly in dual phase steels when the plastic deformation of the martensite contained in the dual phase steel starts. Based on the modified Crussard-Jaoul analysis, the start of the martensite phase contained in bulk specimens is estimated.

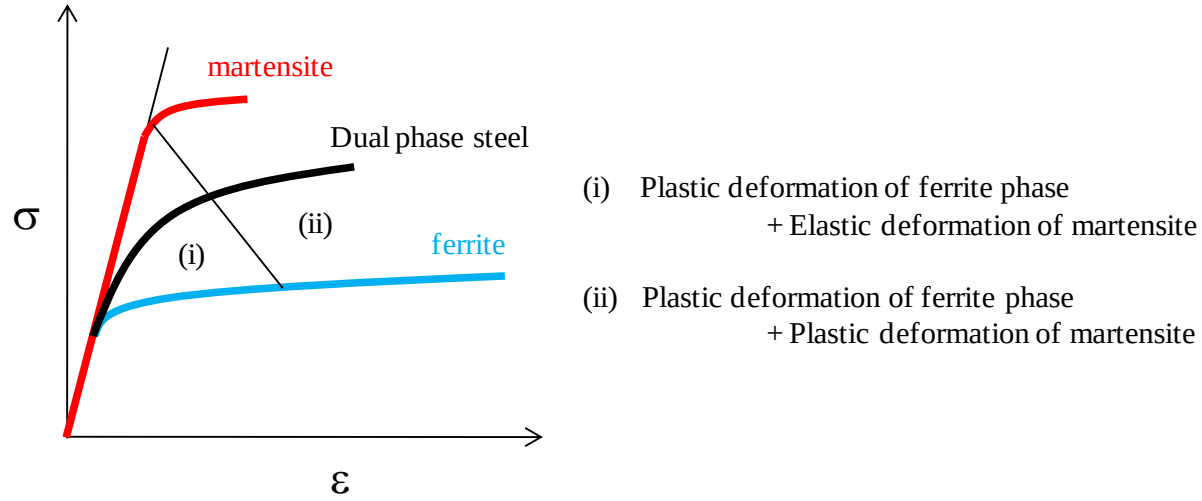

Fig. 3.3 Work hardening behaviour of a dual phase steel. The work hardening behaviour depends on the start of plastic deformation of the martensite phase.

3.1.3 Hole-expansion test

A hole-expansion test was used to estimate the formability for stretch-flanging and hole-expansion. The hole-expansion tests are engineering tests to estimate the formability for automobile components and two types of hole-expansion test are suggested. The first one is used for panels of automobiles during deep drawing (Fig. 3.4a) and another is used for structural components and under car body components (Fig. 3.4b). In both tests steel sheets are punched and a hole is expanded mechanically by a cylindrical punch or a conical punch.

The difference between the two tests is the stress distribution around a hole. In the test by the cylindrical punch (Fig. 3.4a), stress concentrates at the edge of hole, but it is assumed that the specimen at the edge of the hole is under a uniaxial tensile stress during loading. Necking occurs at the edge of the specimen and thereby accelerates fracture of the specimen. Therefore, the formability tested by the cylindrical punch depends on uniform elongation more even though macro crack formation affects the formability.

On the other hand, in the test by the conical punch (Fig. 3.4b), stress distributes in the radial and thickness direction. As the large stress gradient generally retards necking, the specimen can be deformed without necking and the strain at the edge of the specimen is much larger than the uniform elongation. Voids appear at the edge of the specimen and lead to fracture of the specimen. Therefore, the formability strongly depends on void formation in a material. As dual phase steels are applied for structural components, the formability is estimated by the hole-expansion test in Fig. 3.4b.

At first, steel sheets are punched, clamped by a holder and the hole is expanded by the conical punch. In the present study, the diameter of the punch was 10mm and the diameter of the blank was10.6 mm. During loading the edge of the hole is observed and the test is stopped when a crack passes through the sheet. The formability is given as a hole-expansion ratio according to the following equation:

$$\text{Hole-expansion ratio} = (d - d_0) / d_0 \times 100\% \qquad \text{Eq.[4]}$$

where, d_0 is the initial diameter of the hole and d is the diameter of the hole after the hole-expansion test.

In addition to void formation during loading, the formability also depends on damage induced by punching. As the specimen is deformed heavily during punching, the specimen often contains voids. Voids induced by punching and plastic deformation by punching lead to early fracture of the specimen. Besides, a rough fracture surface, which often contains dimples and scratches, after punching accelerates crack formation due to stress

concentration. Therefore, machining and cutting by a laser are suggested as a method to make a hole in components, as they damage less the specimens. The study is a future experiment.

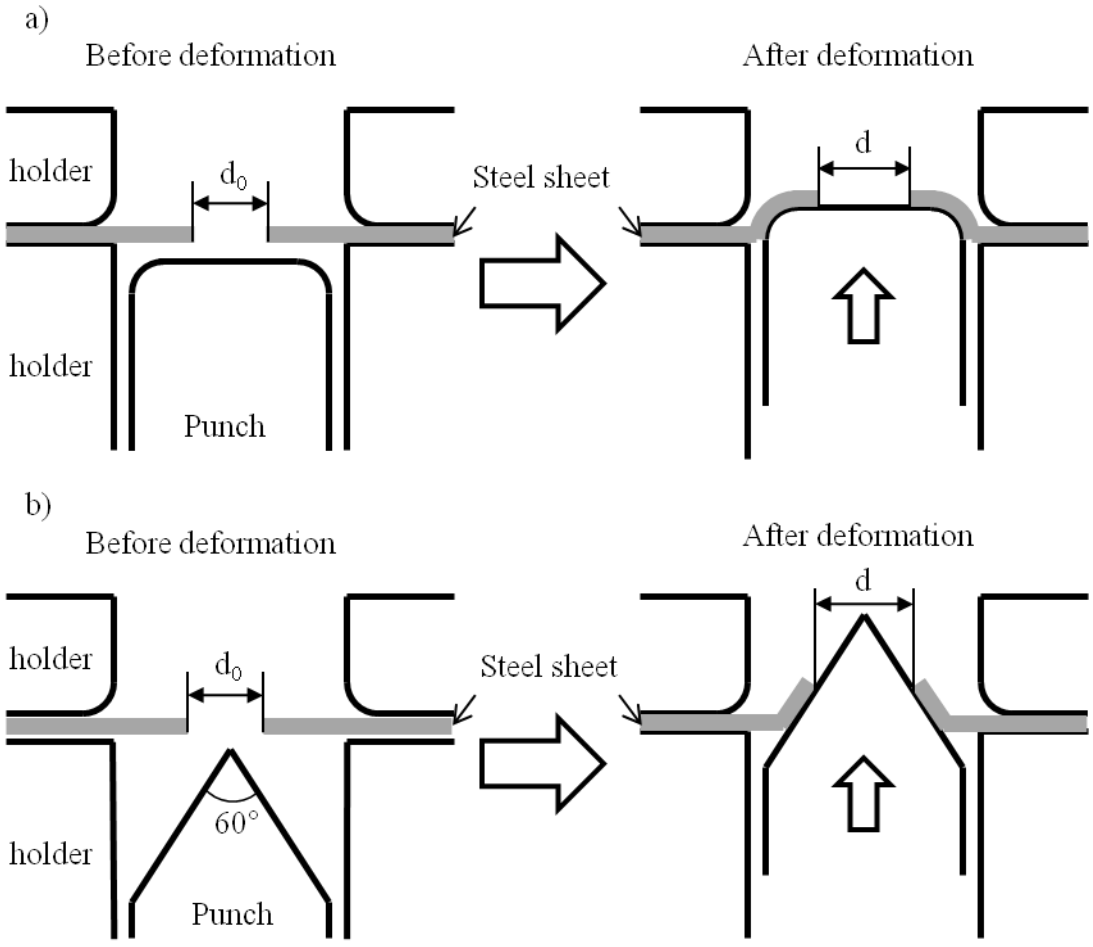

Fig. 3.4 Hole-expansion tests for a) panels (stress distributes in the radical direction.) and b) structural components (stress distributes in the radical direction and the thickness direction).

3.2 Scanning electron microscopy

Scanning electron microscopy (SEM), which images by scanning with a high energy electron beam, is one of the most appropriate methods to observe materials, whereas an optical microscope is also a helpful instrument for structural evolution. The SEM has a much higher spatial resolution than observations by optical microscopy (OM) due to the smaller wavelength of an electron beam. The spatial resolution of the SEM is typically 1-100nm and 100 times as much as optical microscopes. In the SEM observations, some signals generated from specimens when an electron beam interacts with specimens are used to follow structural evolution. There are two familiar signals; (i) secondary electrons (SEs) and backscattered electrons (BSEs). The contrast of SE images mainly depends on the specimen topography and it is, therefore, suitable to observed deformation and fracture behaviour on the surface of specimens as during plastic deformation steps appear on the surface due to plastic deformation and crack formation. On the other hand, the contrast of BSE images predominantly depends on the atomic number and crystal orientation of constituents in specimens. The orientation contrast in BSE images originates in electron channelling contrast (ECC) and is frequently used for lattice defects and boundary structure.

In this study, a Zeiss EVO60 was used for structural evolution of the initial and deformed microstructures. The Zeiss EVO60 was operated at an accelerated voltage of 20kV. In order to characterize the initial

microstructures, the steel sheets were cut parallel to the rolling direction, polished and etched by nital ($96\%C_2H_5OH + 4\%HNO_3$), the surfaces are observed from the transverse direction. Nital can help to distinguish the martensite particles from the ferrite matrix. Five areas were observed at a magnification of 2000×. However, the microstructure at the centre of the specimen was not included to avoid a possible effect of Mn segregation. The grain size was measured in the transverse direction and in the direction normal to the rolling direction by a linear intercept method, and the average value was defined as the grain size. In addition, the size distribution and the aspect ratio of the martensite particles were estimated, because the morphology of the particles was somewhat irregular and they were elongated in the transverse direction. The aspect ratio was determined as the length in the transverse direction divided by the length in the normal direction. The volume fraction of each phase was measured by a point counting method. The deformed microstructures after testing were studied from the transverse direction to estimate the characteristics of voids including (i) initiation site, (ii) number density and (iii) size. In order to detect void initiation sites, the microstructure was etched by nital. Comparisons of the etched and unetched microstructures established that etching does not generate etch pits or affect the shape and size of the voids. Void initiation sites were observed in areas with a limited elongation because a large deformation resulted in microstructures which were too complex to characterize.

Electron backscattered diffraction (EBSD) is also frequently used for the structural evolution of crystalline materials in the last two decades. In an EBSD observation, a Kikuchi diffraction pattern is generated from the specimen when the electron beam hits on the specimen, is automatically analysed by computers and determined the crystal orientation of each point as the pattern strongly depends on crystal orientation of constituents in specimens. Tungsten and lanthanum hexaboride (LaB_6) used to be common as filament materials and field emission guns (FEGs) are more frequent recently due to the better special resolution. In the EBSD with a FEG, the angular resolution is about 20nm and 1°. It is suitable to study crystalline materials. In particular, the FEG-SEM is more useful to estimate deformation behaviour in dual phase steels as a large number of dislocations induced by martensite transformation and plastic deformation leads to large rotations of crystal lattices.

In the present study, a Zeiss Supra-35 FEG scanning electron microscope, equipped with a HKL Channel 5 EBSD system, was used for the observation of initial microstructures and deformed specimens. The specimens were observed from the transverse direction. For the observation of deformed microstructure, the specimen was deformed in tension. The applied strain was 0.05 and smaller than the uniform elongation. The SEM was operated at an accelerated voltage of 20kV and a step size of 50nm. EBSD data were pre-processed using the HKL 5 EBSD software to reduce noise and to smooth the orientation. A critical angle for boundary detection was set to 2° defined as low angle boundaries and grain boundaries, which misorientations over 7°, was defined as high angle boundaries. Based on the experimental data, the strain distribution is estimated macroscopically and locally in specimens deformed in tension.

First of all, the macroscopic strain distribution was evaluated based on the deviation of the Euler angle at each point form the average value of each ferrite grain. For the analysis, a program, which is established by Andy Godfrey (e. g. Li et al. 2002), was used. Ferrite grains and martensite particles were detected by the HKL 5 EBSD software and then the average Euler angle in each ferrite grain was calculated but the martensite phase was neglected. For boundary detection, a critical angle for boundary detection was set to 7°. At each point, the deviation from the average angle was calculated and exemplified in Fig. 3.5. In the map, yellow regions have a small misorientation of 0°, blue regions have a larger misorientation and green regions have a misorientation of over 7°. Since the difference of orientation in a grain is related to geometrically necessary dislocations, it is assumed that the difference means plastic strain in ferrite grains. Based on the contour map, the macroscopic plastic strain distribution; where strain localized and how frequently strain localized, was estimated.

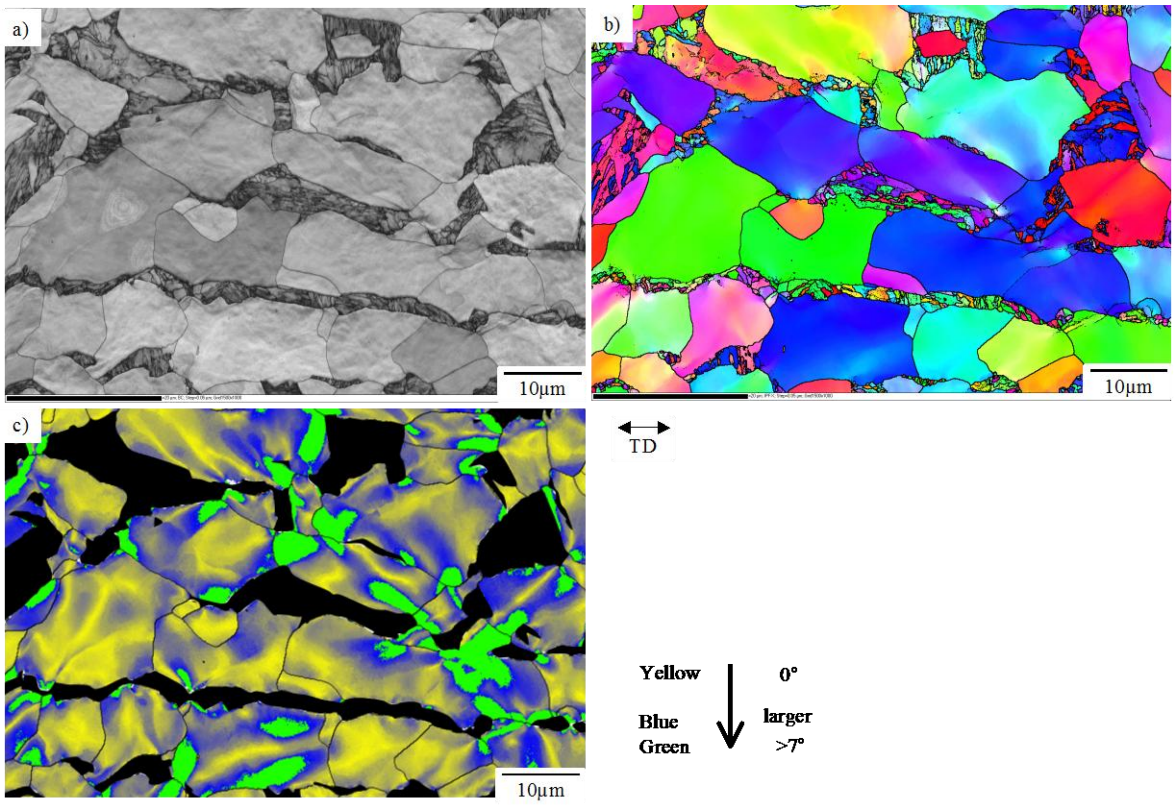

Fig. 3.5 Measurement of strain distribution by a SEM-EBSD method: a) Image Quality map, b) Orientation map and c) a contour map of strain distribution in the ferrite phase. In the contour map, a yellow region has a small strain, a blue region has a larger strain and the strain in green regions is the largest of all. The tensile direction is marked.

In addition, the local strain distribution is evaluated at each martensite/ferrite interface and ferrite/ferrite grain boundary in more detail. In this study, accumulated misorientation profiles from the martensite/ferrite interface and the ferrite/ferrite grain boundaries were measured. As strain distributes heterogeneously in the ferrite phase and martensite phase, typical areas, where strain localizes, were chosen based on the macroscopic observation of strain localization. The accumulated misorientation profiles were measured in the tensile direction and perpendicular to the tensile direction. As the strain tends to localize very close to the martensite/ferrite interface, the accumulated misorientation at 1µm away from the interface is represented as a local strain. About 20 interfaces/boundaries were measured.

3.3 In-situ mechanical tests in a scanning electron microscope

In-situ mechanical tests in a SEM were used to follow void formation behaviour in dual phase steels. For the tests, a load cell (Fig. 3.6b-d) was installed in a scanning electron microscope (Zeiss EVO60) as shown in Fig. 3.6a. Tensile tests and three point bending tests were carried out in the SEM.

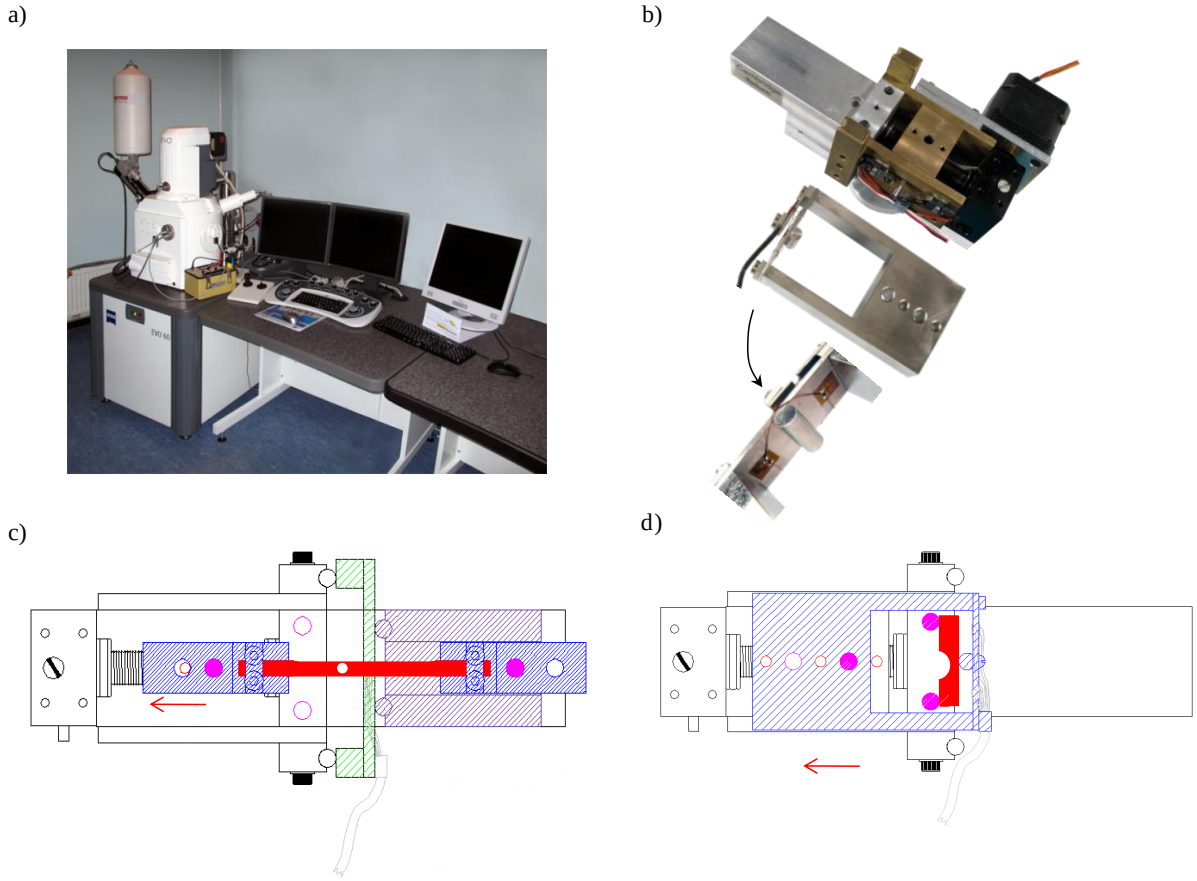

Fig. 3.6 In-situ mechanical tests: a) a SEM (Zeiss EVO60), b) a load cell and sample holders for c) a tensile test and d) a bending test.

For in-situ tensile testing, 0.15 mm × 2.8 mm × 30 mm specimens were machined and a hole with a diameter of 1 mm was made in the centre of the specimen. For bending tests, 2 mm × 3 mm × 26 mm specimens with a notch in the middle were used. The hole and notch allows one to detect void and crack initiation easily. In addition, since the strain distribution around the hole and notch is similar to that at an edge of a tensile specimen after diffusive necking starts and at an edge of a stretch flanging part, the shape of specimens is reasonable to quantify void formation behaviour in the specimens with a hole or a notch. All specimens were polished and etched before deformation. Fig. 3.7 illustrates an in-situ loading test. As shown in Fig. 3.7a, the sample was clamped at both ends and stretched under displacement control in a screw-driven load cell, which was installed inside the microscope. The specimen was strained gradually and the surface structure was characterized during loading. Fig. 3.7b illustrates the gradual bending by a pin of a sample without unloading. In the tests, the deformation concentrates at the edge of the hole and at the bottom of the notch. During the tests the following procedure has been related to nucleation and growth of voids; (i) nucleation density, (ii) size distribution, (iii) length and (iv) area fraction of voids in a area of 25000μm^2. Under each condition, in-situ tests were carried out three times. Void formation behaviour was estimated statistically. The observations have been related to the strain which is defined in the following section.

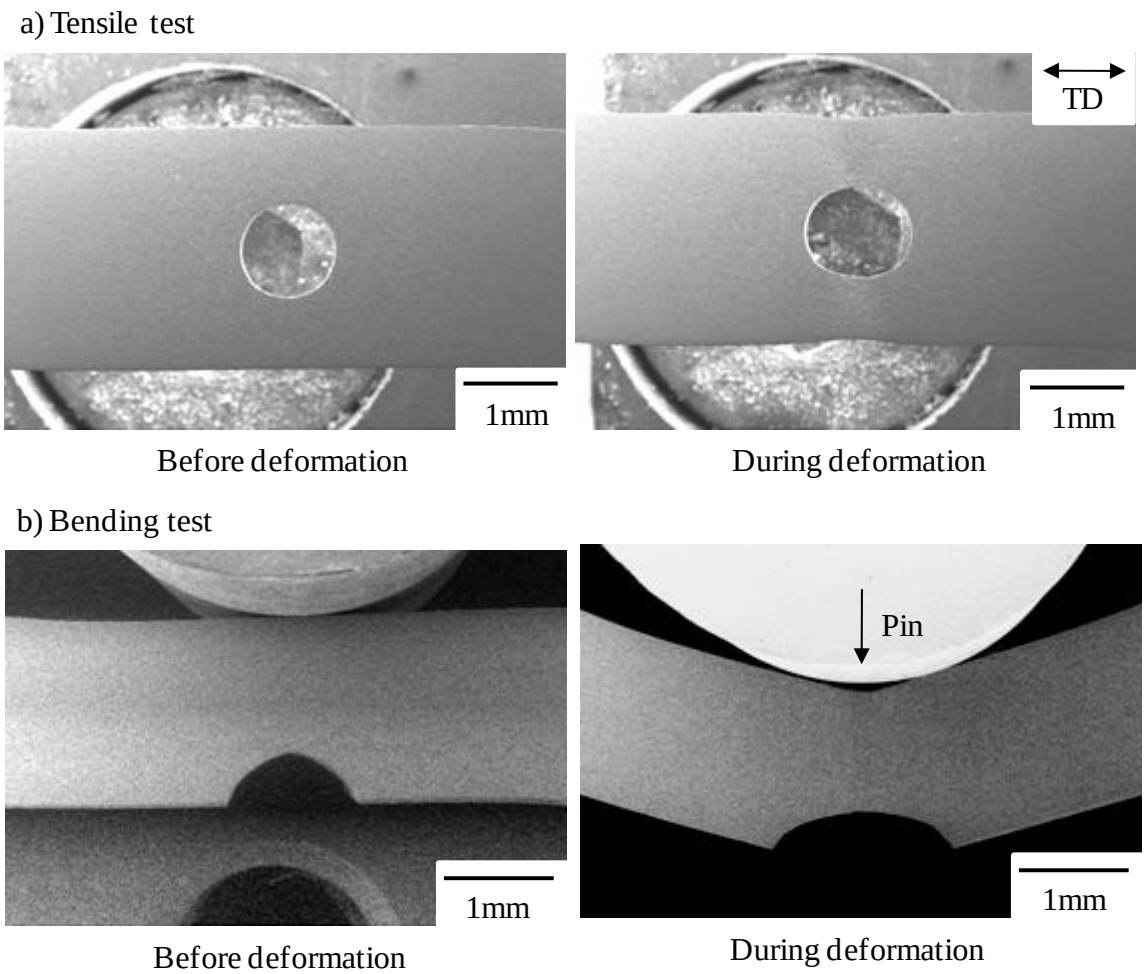

Fig. 3.7 In-situ mechanical tests: a) tensile test in which deformation concentrates near the hole (the horizontal arrow marks the tensile direction, TD), b) bending test in which deformation concentrates near the notch.

3.4 Transmission electron microscopy

Transmission electron microscopy (TEM), which images by transmission and diffraction with a high energy electron beam, is an important method to observe microstructures at a higher resolution, below 0.1 nm for the best instruments. In a TEM observation, a wide variety of signals is generated from specimens when an electron beam interacts with specimens and is used for structural evolution. In particular, bright field images which are produced by a parallel beam, are often used to observe precipitations and dislocations in materials. A diffraction pattern was used to analyse structures of constituents and crystal orientations. A specimen is so thin that an electron beam is transmitted through the specimens which were typically from 100 to 500nm for steels.

In this study, a transmission electron microscope (JEM 2000FX) with a LaB_6 filament and a CCD camera was used. The accelerating voltage was 200kV. The specimens for TEM were prepared by electro chemical polishing. Bright field images were used to observe initial microstructures and deformed microstructures. Dark field images and diffraction patterns were used to characterize precipitations in tempered specimens. In addition, Kikuchi patterns generated convergent electron beam diffraction (CBED) was applied to adjust the tilt angle of the specimen.

The dislocation density in the ferrite phase before deformation, which contains a number of dislocations due to the martensite transformation, was measured by TEM. For all specimens, dislocations were observed from <200> zone axis close to the electron beam direction, making all dislocations visible. In the images many lines are drawn and dislocation number density was counted. Then the dislocation density is given by the following equation:

$$\rho_d = \frac{2N_L}{t} \qquad \text{Eq. [5]}$$

where N_L is the number of intersections at dislocations per unit line and t is a thickness of the observed area. About 10 areas were observed.

3.5 Strains in specimens

Whereas uniform elongation in tensile tests is an important parameter to evaluate the formability, the local strain at the necking zone of specimens both during tensile testing and during in-situ testing is also a key parameter as it is related to macro-crack formation and fracture of the specimen in the necking zone. Generally, since more voids form with strain, void formation has a large effect on the local strain in the necking zone. Post-uniform elongation (P-El) is used to evaluate the formability from the start of necking to fracture of the specimen in tensile tests. However, P-El is an engineering strain and depends on the gauge length, the shape and thickness of specimens as deformation localizes in the narrow necking zone after the start of necking. On the other hand, a thickness strain, which is estimated based on a thickness reduction of specimens, is another parameter to evaluate the strain at each point in the necking zone. In this study the thickness strain (ε_t) in the tensile direction was measured in order to evaluate void formation behaviour in the bulk as shown in Table 3.1a. An initial thickness of a tensile specimen (t_0) is compared with a thickness at each point in the necking zone of the specimen (t_1) after a tensile test. Void formation behaviour in the bulk is evaluated as a function of the thickness strain (ε_t).

During in-situ testing a local strain at the bottom of a hole (ε_h) is estimated based on measurement of a gauge length at the bottom of a hole (Table 3.1b). The hole is helpful to detect void initiation due to stress concentration and retards the onset of local necking due to the stress gradient at the bottom of the hole. The strain in the tensile direction is defined as a local strain during in-situ testing as deformation localizes at the edge of the hole. It seems that the local strain is more related to a thickness strain because deformation localizes at the necking zone in tensile tests. A gauge at the position was defined based on SEM observations. At first, a 100μm gauge and the notch at the bottom of the hole was defined by the SEM observation, in which the distance was estimated based on the microstructure which was visible. The length change of the gauge was directly followed during in-situ tests. If the gauge length is too small, few grains exist in the gauge and a strain does not represent an average value of the specimen because each grain has a different strain due to different crystal orientations and the distribution of martensite particles. On the other hand, since deformation concentrates at the bottom of the hole or notch, a large gauge length might lead to an underestimation of the strain.

Table 3.1 Strains estimated after tensile tests and during in-situ tensile tests.

a) Thickness strain of the specimen after a tensile test: $\varepsilon_t = (t^0 - t^1)/t^1$ Eq.[6]
where, t^0 is an initial thickness of the specimen and t^1 is a thickness at each point after a tensile test.

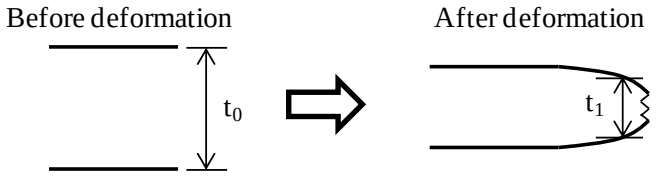

b) Local strain near the hole and at a bottom of a notch during an in-situ test:
$\varepsilon_h = (L_h^1 - L_h^0)/ L_h^0$ Eq.[7]
where, L_h^0 is an initial gauge length (=100μm) and L_h^1 is a gauge length during an in-situ test.

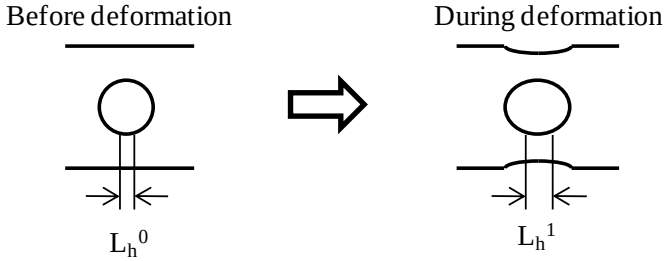

c) Average strain in ferrite grains during an in-situ test: $\varepsilon_F = \Sigma\{ (L_F^1 - L_F^0)/ L_F^0\}$ Eq.[8]
d) Average strain in martensite particles during an in-situ test: $\varepsilon_M = \Sigma\{ (L_M^1 - L_M^0)/ L_M^0\}$ Eq.[9]
where, L_F^0 and L_M^0 are initial length of ferrite grains and martensite particles and L_F^1 and L_M^1 are length of the grains and particles during an in-situ test.

e) Local strain at a necked region of a martensite particle during an in-situ test:
$\varepsilon_L = (L_L^1 - L_L^0)/ L_L^0$ Eq.[10]
where, L_L^0 is an initial length of a necked region of a martensite particle and L_L^1 is the length of a necked region of a martensite particle during an in-situ test.

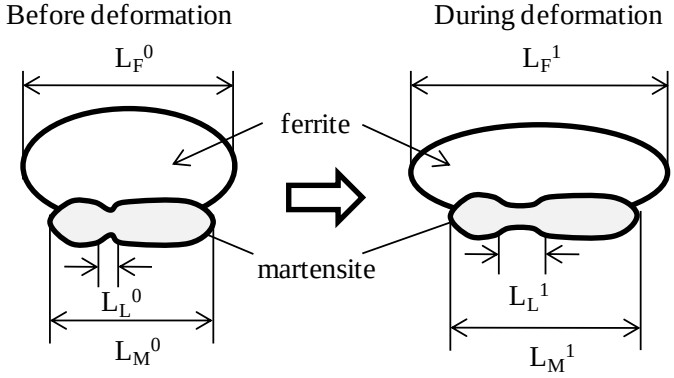

In addition, strains in the martensite and ferrite (ε_M and ε_F) are also important parameters to estimate the effects of metallurgical parameters, such as hardness, volume fraction and shape of the martensite, on void formation in the martensite and ferrite as these parameters represent strain partitioning between the martensite and ferrite (e.g. Shen et al. 1986, Su and Gurland 1987, Tasan et al. 2010). In dual phase steels, as the martensite is much harder than the ferrite, martensite particles are less deformable than ferrite grains. Hardness, volume fraction and morphology of the martensite affect strain in the martensite and ferrite, and are, thereby, related to mechanical properties of dual phase steels. As shown in Tables 3.1c and d and Fig. 3.8, the length

change of ferrite grains and martensite particles were followed during in-situ testing. About 200 grains/particles were measured and the strains were averaged as strains in the martensite and ferrite (ε_M and ε_F).

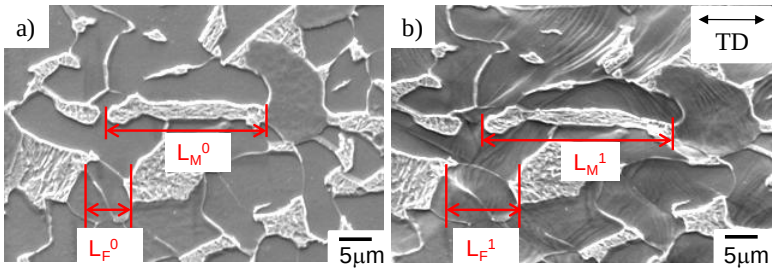

Fig. 3.8 Deformation behaviour in a dual phase steel during an in-situ tensile test: a) before deformation and b) during deformation.

Moreover, a local strain at the necked region of a martensite particle (ε_L) is another key parameter to estimate void formation in the martensite. During tensile testing and in-situ testing deformation localized at the concave part of the martensite particles (Fig. 3.9) and a crack appeared at the necked zone. The local strain at the necked regions is much larger than the average strain in the martensite due to strain localization. Even though a martensite particle does not contain a concave part and a concave part often appeared in the particle during deformation due to necking. Local strain at about 30-180 necked regions was estimated for each condition.

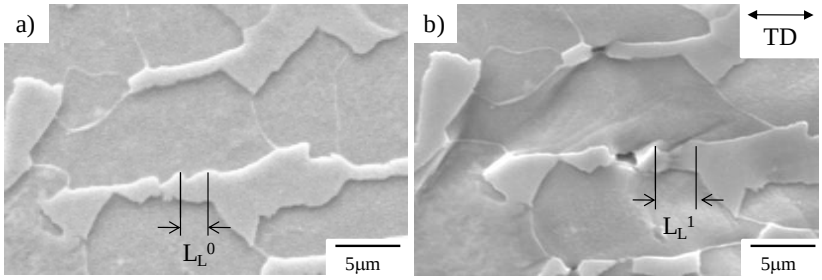

Fig. 3.9 Deformation behaviour at a concave part of a martensite during an in-situ tensile test: a) before deformation and b) during deformation.

3.6 Materials

Four alloys were melted in a vacuum furnace and cast as 20 kg ingots into a crucible to produce the materials which contain different amount of martensite phase (Table 3.2). The chemical compositions are given in Table 3.2. Carbon is one of the most important alloying elements when producing dual phase steels as it affects not only the volume fraction of martensite but also the hardness of the martensite. Dual phase steels with 10-50 vol.% of martensite contain about 0.1-0.2mass% C (e.g. Erdogan 2002, Avramovic et al. 2009 and 2010). In the present steels 0.1-0.2mass% carbon were added to produce a dual phase steel whose matrix is a ferrite phase. Manganese was added to retard the pearlite transformation during cooling, since most of the austenite phase in steels without Mn rapidly transforms to pearlite. However, a large amount of Mn generates zones of Mn segregation in the centre of the ingot, which makes the microstructure heterogeneous and also leads to different void formation behaviour in this zone [Avramovic et al. 2009]. Therefore, the Mn contents were set to 1.6 and 2.0 mass%. Sulphur and oxygen often exist as sulphides and oxides in steels and they have a negative effect on the mechanical properties because of void formation around inclusions (e.g. Nutt and Needleman 1987, Christman et al. 1989, Clyne and Withers 1993, Maire et al. 2008). For this reason, an electrolytic iron with a sulphur content less than 0.001mass% was used. The ingot was annealed at 1200˚C for 1 hour in an argon atmosphere, hot-rolled from 45 to 3 mm thickness at 1100-950˚C, cooled slowly from a hot-rolling finishing temperature of 950˚C to 650˚C to promote ferrite formation, followed by water cooling to ambient temperature and transformation of austenite into martensite. Some specimens were tempered at 300-600˚C for 100s to evaluate the effect of a softened martensite phase.

Table 3.2 Chemical composition / mass%

	C	Si	Mn	P	S	N	O
Steel1	0.099	0.01	1.63	0	0.0007	0.0008	<0.0010
Steel2	0.148	0.01	1.60	0	0.0007	0.0016	<0.0010
Steel3	0.200	0.01	1.59	0.001	0.0006	0.0018	<0.0010
Steel4	0102	0.01	1.99	0.001	0.0008	0.0013	<0.0010

The microstructures after hot rolling are shown in Fig. 3.11. The microstructures were composed of ferrite grains (F) and martensite particles (M) and neither pearlite nor bainite was observed. The martensite was lath martensite, which had hierarchic structure as shown in Fig. 3.10. In general, lath martensite is composed of packets, which consist of parallel blocks. There are three blocks with different orientation in a packet. Each block consists of laths of martensite with Kurdjumov-Sachs (K-S) relationship to prior austenite. Specially, each block consists of two specific K-S groups (sub-block), whose misorientation is about 10 degrees. The initial microstructure was free from voids and cracks. The microstructures strongly depended on the chemical compositions. As shown in Fig. 3.11 and Table 3.3, a ferrite phase occupied majority of the area in Steel 1, 2 and 4, the matrix was the ferrite phase. On the other hand, Steel 3 contained a large amount of martensite particles due to retardation of ferrite formation by the 0.2mass% carbon addition, which stabilizes the austenite phase and retards ferrite formation. In addition, the mechanical properties of Steel 3 were different from others (Table 3.4), Steel 3 was not used for in-situ mechanical tests. In addition, Steel 4 has a band-like structure consisting of the martensite phase at the centre of a specimen due to Mn segregation zones (Fig. 3.12). Avramovic et al. (2009) and Tasan et al. (2010) pointed out that the band-like structure has a negative effect on the formability and void formation behaviour in the zones is different from other regions. Table 3.4 also shows that as Steel 1 and 2 had high ultimate tensile strength and a low yield ratio (0.2%YS/UTS) of about 0.5, the measured tensile behaviour were typical for dual phase steels. Therefore, Steel 1 and 2 were chosen as specimens to estimate the void formation behaviour in dual phase steels. Whereas Steel 1 and 2 have different martensite fraction, the size of ferrite grains and aspect ratio of martensite particles are similar. The steel containing an 0.21 martensite is named SVM (Small Volume fraction of Martensite) and the steel containing an 0.38 martensite is named LVM (Large Volume fraction of Martensite).

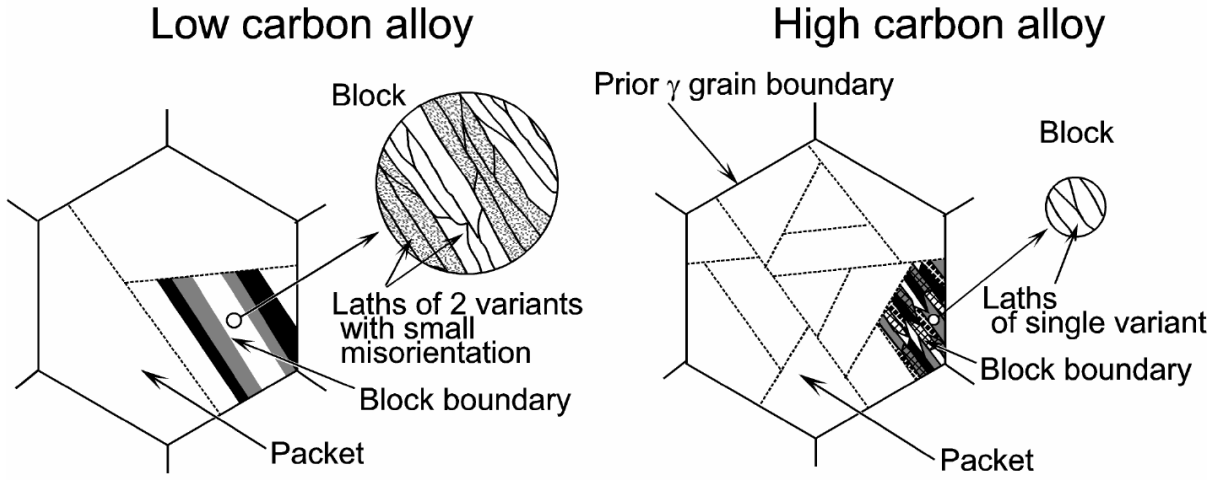

Fig. 3.10 Schematic illustration showing lath martensite structure in (a) a low carbon (0-0.4mass%C) and b) high carbon (>0.6mass%C) alloys. Reproduced from Morito et al. (2003).

The shape of the two phases is also different. Ferrite grains nucleate at triple junctions and grain boundaries of the austenite during cooling and have a polygonal shape. Martensite particles are, on the other hand, transformed from the remaining austenite and they are less regular in shape with concave and convex profiles and some particles are elongated in the rolling direction. As shown in Fig. 3.13, the sizes range from less than 1 to over 20μm and the average aspect ratio of SVM and LVM are 2.1 and 2.2.

A microhardness test shows that the hardness of the martensite and ferrite depends on tempering treatments, but the hardness of the specimens are almost the same at the same tempering temperature, as shown in Fig. 3.14. In particular, the tempering treatments strongly affected the hardness of the martensite due to a large number of carbide precipitates. The standard deviations of the hardness of the martensite were relatively large due to the small size. As these steels (SVM and LVM) have different amounts of martensite, but the hardness of the ferrite and martensite is similar at each tempering temperature, the steels are suitable to estimate the effect of the hardness and volume fraction of the martensite on void formation in the dual phase steels.

The stress-strain curves of SVM and LVM also show that these steels were typical dual phase steels. The stress increases rapidly after yielding and the work hardening rate is very high. 0.2% yield stress (0.2%YS), which is defined as a yield stress in the dual phase steel because the steel never shown yield point phenomenon as shown in Fig. 3.15, is relatively small. They had a larger ultimate tensile strength (UTS). The steels had a low yield ratio, which is given by 0.2%YS/UTS. The steels were typical dual phase steels because it has low yield ratio and high strength.

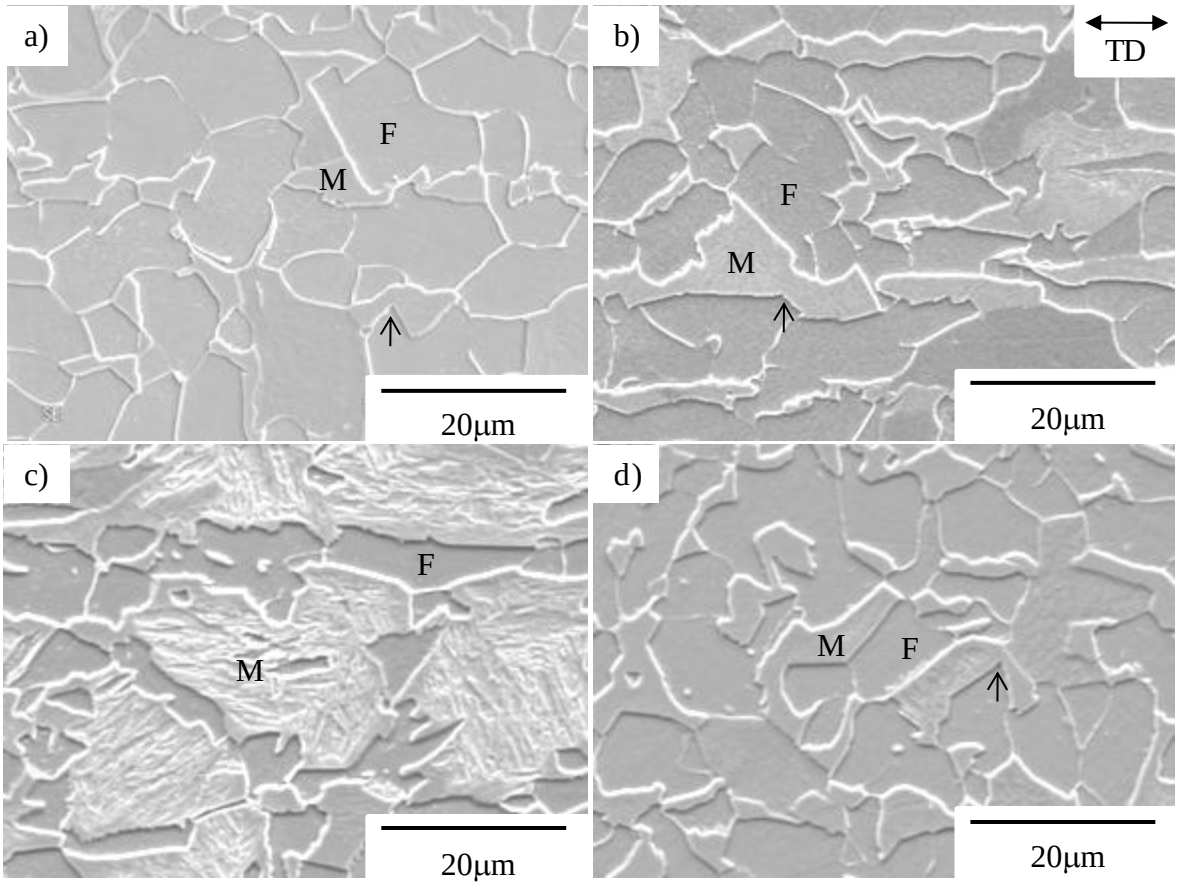

Fig. 3.11 Initial microstructure of dual phase steels: a) Steel 1, b) Steel 2, c) Steel 3 and d) Steel4. Equiaxed grains are a ferrite phase (F) and martensite particles (M) have concave and convex profiles (marked by arrows). In Steel 3 cementite precipitated in the martensite particles due to a high Ms temperature. The rolling direction (RD) is marked.

Table 3.3 Grain size, volume fraction and aspect ratio of martensite particles in the dual phase steels.

	Grain size / μm		Volume fraction		Aspect ratio	Microhardness	
	Ferrite	Martensite	Ferrite	Martensite	of martensite	Ferrite	Martensite
Steel 1 (SVM)	7.3	3.6	0.79	0.21	2.1	162	398
Steel 2 (LVM)	7.1	6.3	0.62	0.38	2.2	163	387
Steel 3	4.8	-	0.34	0.66	-	164	350
Steel 4	6.8	4.3	0.69	0.31	2.4	168	386

SVM: Small Volume fraction of Martensite, LVM (Large Volume fraction of Martensite)

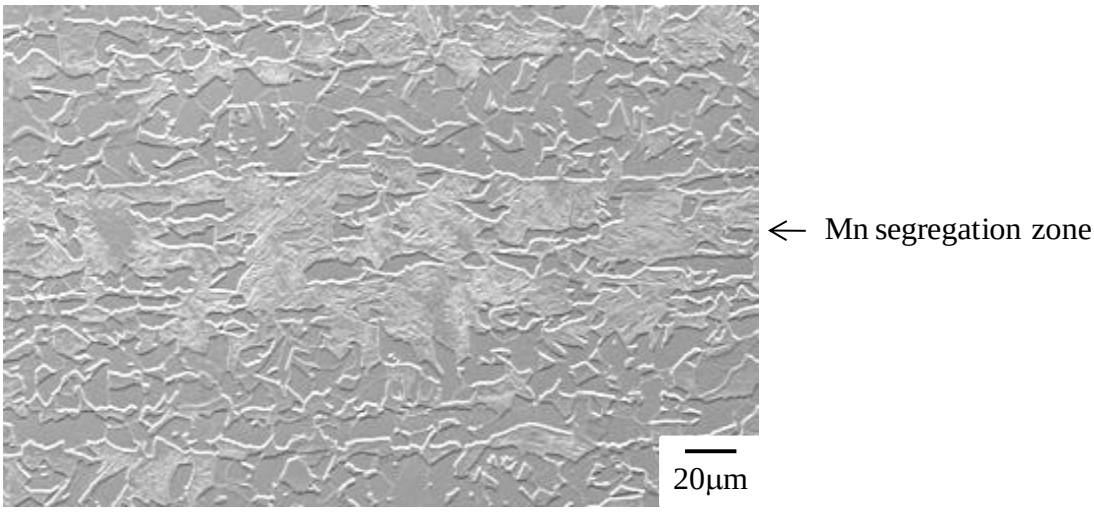

Fig. 3.12 The microstructure at the center of Steel 4. A band-like structure consisiting of martensite particles was observed.

Table 3.4 Mechanical properties of the dual phase steels

	0.2%YS	UTS	El.	U-El.	P-El.
Steel 1	361	683	19.1	10.4	8.7
Steel 2	456	868	13.7	8.4	5.3
Steel 3	603	1077	9.4	6.5	2.9
Steel 4	513	825	20.2	11.0	9.2

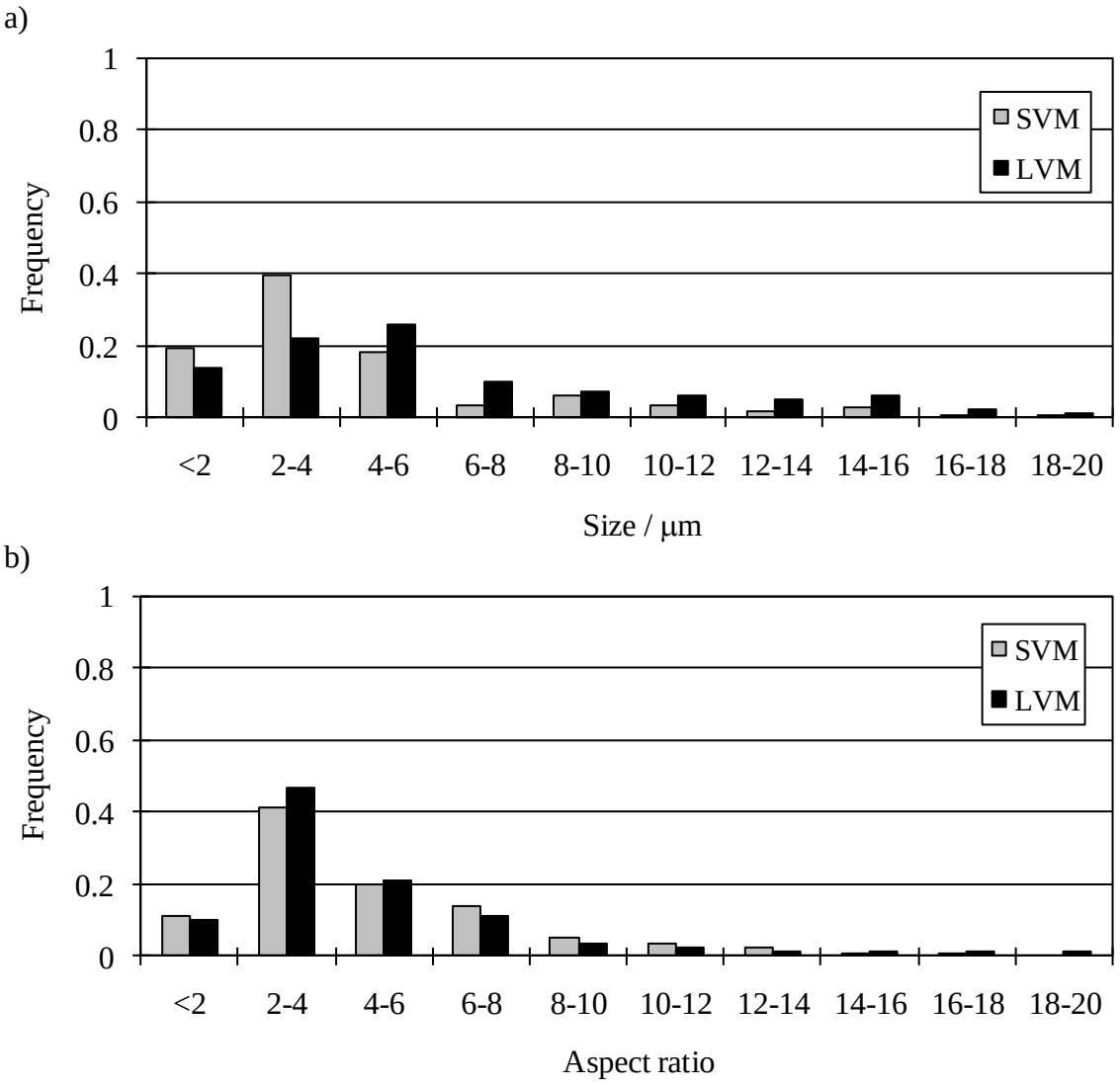

Fig. 3.13 Size distribution (a) and aspect ratio (b) of the martensite particles.

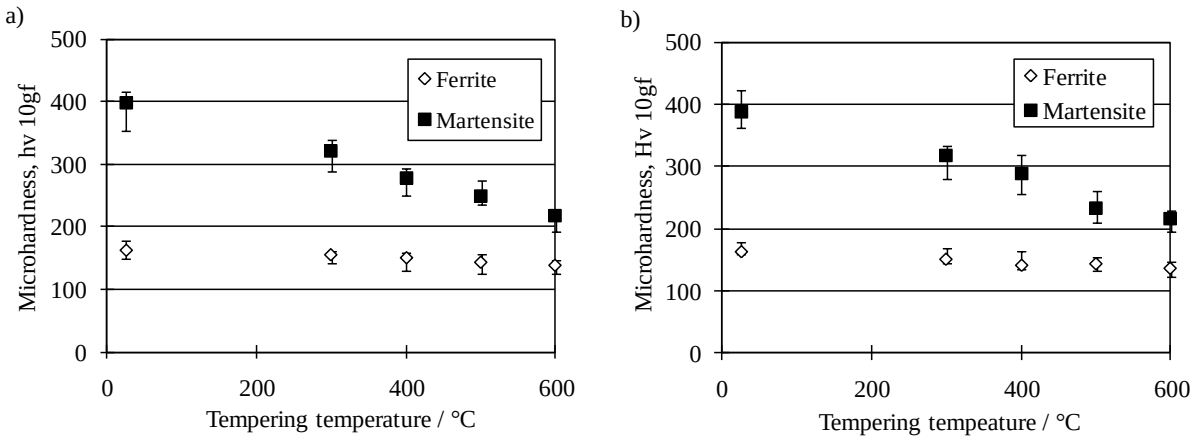

Fig. 3.14 Tempering temperature dependence of microhardness of the martensite and ferrite in a) SVM and b) LVM. The hardness of the martensite mainly depends on the tempering temperature.

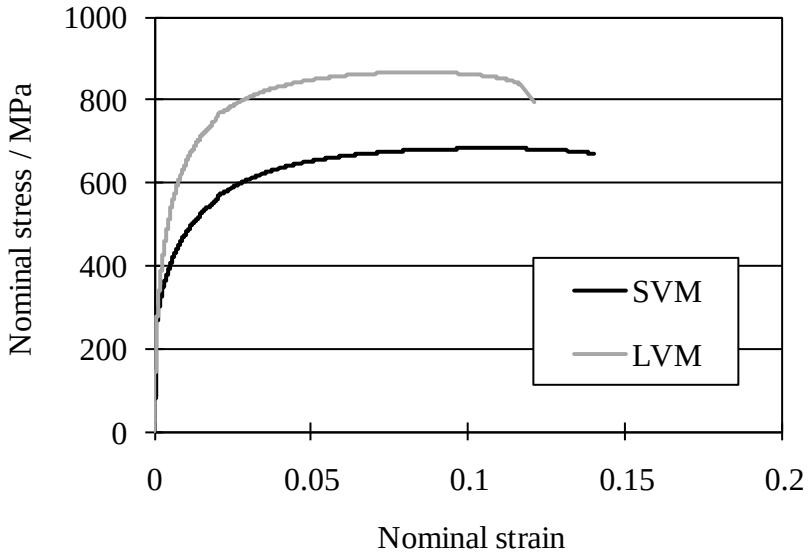

Fig. 3.15 Nominal stress-nominal strain curves of SVM and LVM.

Chapter 4

Void formation mechanism

4.1 Introduction

Void formation in metals affects the strength and the formability for tensile tests, hole-expansion tests and bending tests. Dual phase steels are applied for automobile components as dual phase steels have a high strength and large uniform elongation. The uniform elongation and strength are important parameters but critical to formability is also the response to the crack formation and growth. Parameters to characterize this response include the elongation in the necking zone of a tensile test, the hole-expansion ratio determined by pushing a cone through a punched hole and the elongation during a bending test (e.g. Yamazaki 1995 et al. Hasegawa et al. 2004). To clarify in detail the material behaviours, the focus in the present work is a characterization of the local deformation behaviour during loading the nucleation and growth of voids as studied by in-situ scanning electron microscopy.

It has been suggested that void formation, growth and coalescence lead to fracture of specimens in dual phase steels. Nucleation of voids has been an important objective in many investigations which have shown that voids can nucleate in the martensite, in the ferrite and at inclusions and that void nucleation related to the martensite particles is dominating as shown in Table 4.1. In the previous studies in Table 4.1, voids are classified based on observation of deformed microstructures. Voids elongating perpendicular to a tensile direction tend to be classified as voids in the martensite phase, which form due to cracking of martensite particles. On the other hand, equiaxed voids and voids elongating in a tensile direction are often classified as voids in the ferrite, which form at the martensite/ferrite interface due to decohesion. As a ferrite/ferrite grain boundary often exists between two martensite particles and martensite particles are connected by a void after deformation, decohesion at a ferrite/ferrite grain boundary is suggested as another void formation mechanism. Such observations have been followed by suggestions and discussion of void nucleation mechanism where four are illustrated in Fig. 4.1. The experimental basis for these mechanisms is the observation that most voids in broken specimens are formed between two martensite particles in the necking zone which is illustrated in the last column of Fig. 4.1. Four mechanisms which may lead to this end-scenario are also illustrated in Fig. 4.1a, where the first row shows that voids have their origin in a crack in the martensite particle which breaks the particle into fragments which separate and form the void. Other mechanisms are illustrated in Fig. 4.1b and 1c where the first columns show decohesion at the martensite/ferrite interface leading to void formation. The bases for this suggestion are observations showing that voids nucleation by cracking of the martensite particles are limited whereas large voids are observed between martensite particles near the fracture (e.g. Avramovic et al. 2010). Fig. 4.1d exemplifies that decohesion at the ferrite/ferrite grain boundary leads to void formation between two martensite particles. However, these mechanisms as well as other mechanisms are still ambiguous and mechanisms are still explored as an improvement of the dual phase steels is an important industrial issue. The present study thereby has an objective to study mechanisms behind void nucleation and growth and in-situ testing in a scanning electron microscopy (SEM) has been chosen as an appropriate technique as it enables one to follow the void formation behaviour in a specimen directly as a function of the applied strain and stress. Such observations together with an analysis of cracked specimens have led to classification of cracks and voids allowing quantification of two defects and an analysis of their importance. The study focuses on two types of dual phase steels for which strength of the martensite particles, which is an important parameter, has been varied by tempering treatments at 300-600°C.

Table 4.1 Observation of voids in dual phase steels.

authors	date	Void formation site			
		Martensite*	Ferrite*	inclusion	Ferrite/ferrite grain boundary
Koo and Thomas	1977	O			
Tomota et al.	1977	●	●		
Rashid	1978	▲	▲	-	-
Gerbase et al.	1979		O		
Speich and Miller	1979		O		
Korzekwa et al.	1980		O		
Balliger	1982	O	▲	-	-
Szewczyk and Gurland	1982	-	O		
He et al.	1984	O			
Ray	1984	▲	▲	▲	
Shen et al.	1986	O	-	-	-
Steinbrunner et al.	1988	●(crack and separation)	●		
Han and Margolin	1989	O	▲		
Sarwar et al.	1996	●(crack and separation)	●		
Gladman	1997	O			
Kim et al.	2000	▲	O		
Sun and Pugh	2002	●	●		
Erdogan et al.	2002	●	●	▲	
Hasegawa et al.	2003	▲	O		
Han et al.	2004	O			
Poruks et al.	2006	-	O		
Mazinani and Poole	2007	O	▲		
Kang et al.	2007	O	-	-	-
Uthaisangsuk et al.	2008, 2009	O	-	-	-
Maire et al.	2008	▲	O		
Tasan et al.	2009	O	-		
Kelestemur et al.	2009	O	-	▲	
Ahmed et al.	2009	●	●		
Avramovic et al.	2009	▲	O	▲	
Avramovic et al.	2009	▲(crack and separation)	O	▲	
Toji et al.	2009	▲	O		
Landron et al.	2010		O		
Ghadbeigi et al.	2010	O	-		
Calcagnotto et al.	2011	●	●		
Kadkhodapour et al.	2011			▲	O

O: major void formation site, ▲: minor void formation site, ●: observed void site

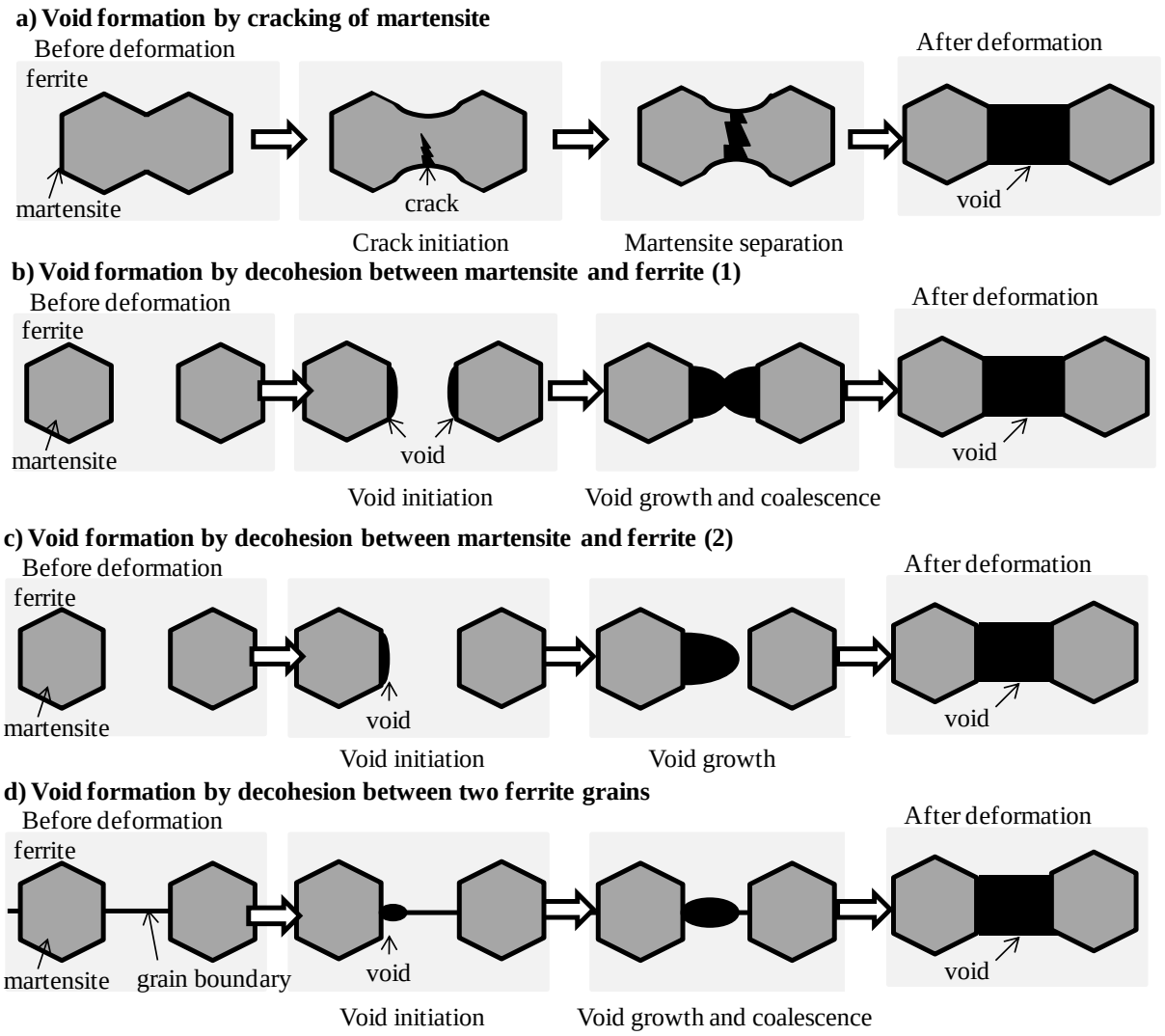

Fig. 4.1 Illustration of four void formation mechanisms between martensite particles in dual phase steels: a) void initiated by cracking of a martensite particle , b) void initiation by decohesion at the interface between ferrite and martensite and coalescence of two voids formed at the end of martensite particles, c) void initiation by decohesion at the interface between ferrite and martensite and growth of a void formed at the end of a martensite particle and d) void formation by decohesion at the ferrite/ferrite grain boundary.

4.2 Experimental procedures

A dual phase steel, SVM, without tempering treatments (see Section 3.6) is used to follow the void formation, growth and coalescence. At first, the deformed microstructure after testing was studied from the transverse direction to estimate the characteristics of voids including (i) initiation site, (ii) number density and (iii) size. In order to detect void initiation sites, the microstructure was etched by nital. Comparisons of the etched and unetched microstructures established that etching does not generate etch pits or affect the shape and size of the voids. Void initiation sites were observed in areas with a limited elongation because a large deformation resulted in microstructures which were too complex to characterize.

In addition, tensile tests and three point bending tests were carried out in a scanning electron microscope (see Section 3.3). All specimens were polished and etched before deformation. During the tests the following procedure has been related to nucleation and growth of voids; (i) nucleation density, (ii) size distribution, (iii) length and (iv) area fraction. The observations have been related to the strain which is defined in Section 3.5.

Voids in the bulk after a tensile test were also characterized based on a classification by mechanisms suggested through in-situ mechanical tests.

4.3 Results

4.3.1 Deformed microstructure after a tensile test

Fig. 4.2 shows typical microstructures after tensile testing at room temperature. In the figure, the horizontal axis is the tensile direction. Most voids, which appear black in the figure, are located between martensite particles (light grey) near the fracture surface or in the bulk. Since the initial microstructure contained no cracks or voids, these voids had formed during the test. Figs. 4.2a and b demonstrate that, near the fracture surface, the number of voids is large and they show a variation in size and shape. In particular, voids elongated in the tensile direction are observed. Figs. 4.2c and d show that in the bulk away from the fracture surface the size and number of voids are relatively small when necking started. Figs. 4.2a and b also show some voids which have coalesced near the fracture surface. It is apparent that void formation and coalescence led to the rupture of the specimen. Since the majority of the voids formed in the necking zone, void formation mainly affects the post-uniform elongation (P-El).

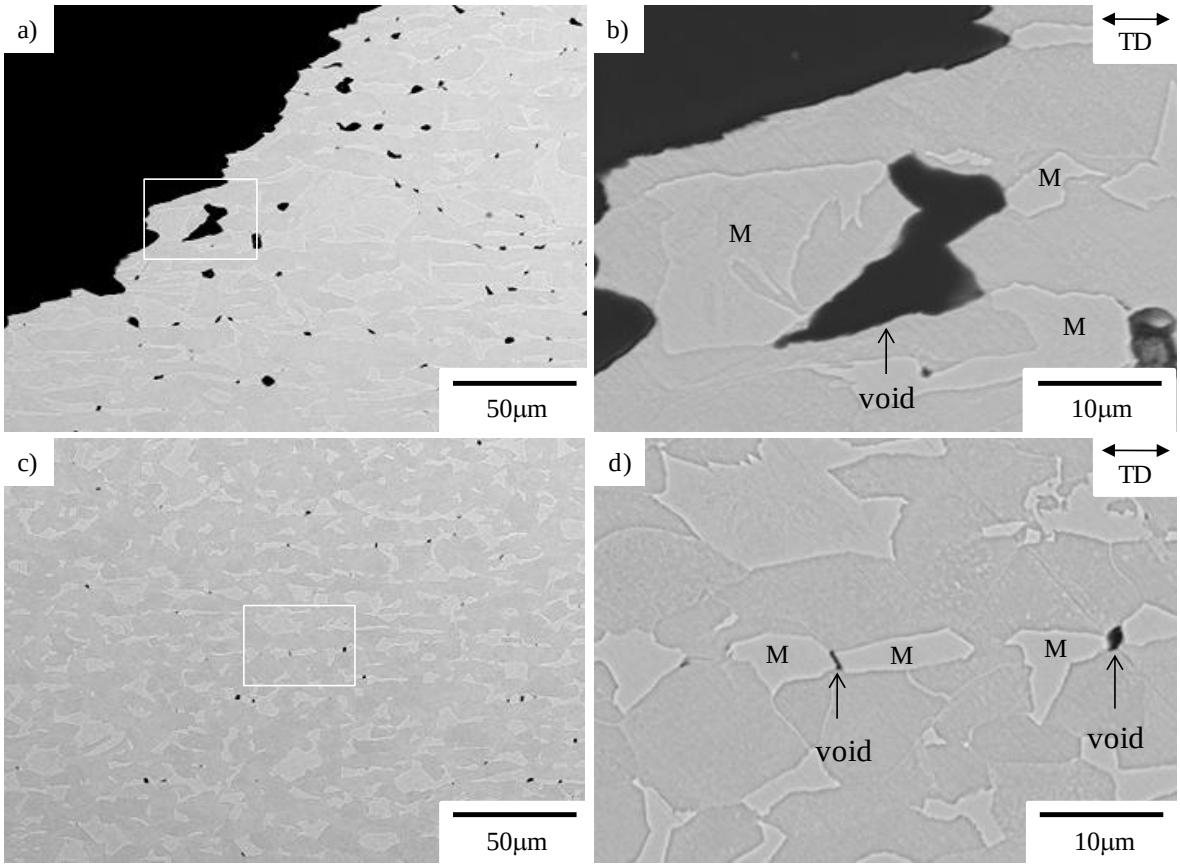

Fig. 4.2 Typical microstructures in the dual phase steel (SVM) after a tensile test: a) and b) near the fracture surface (ε_t =0.429), c) and d) in the bulk (ε_t =0.250). The tensile direction (TD) is marked.

Areas outside the necking zone have also been examined and typical microstructures are shown in Fig. 4.3, illustrating three important crack and void formation sites. Here a distinction is made between a defect which can propagate perpendicular to the maximum tensile direction which is called a “crack”, and a defect which can grow in the tensile direction and the shear direction which is called a “void”. The three sites are the following:

(i) At an interface between ferrite and martensite but located in the martensite phase

(ii) At an interface between ferrite and martensite but located in the ferrite phase
(iii) At an inclusion

Examples of all three sites are given in Fig. 4.3:

(i) : A crack in a martensite particle is illustrated in Fig. 4.3a. The crack tends to form at the concave side of the particle and propagates perpendicular to the tensile direction. Cracks that are not connected with the martensite/ferrite interface are not observed. This type of crack is called "a crack in martensite". The crack often developed as a void due to crack propagation in a martensite particle and separation of the particle fragments. The void is called "a void in martensite".

(ii) : A martensite/ferrite interface void in ferrite is shown in Fig. 4.3b. This type of void initiates at the interface between ferrite and martensite near the end of the martensite particle and grows in the tensile direction without propagating along the interface or into the martensite. This type of void is called "a void in ferrite".

(iii) : A void at an inclusion which may be initiated by decohesion between the ferrite matrix and the inclusion is shown in Fig. 4.3c. In the present samples such voids are few as the sulphur and oxygen content was low.

In general, the three types of voids nucleate and propagate due to the stress and strain which build up at the martensite particles and inclusions. In this respect the behaviour of the dual phase steel will be discussed in Chapter 5.

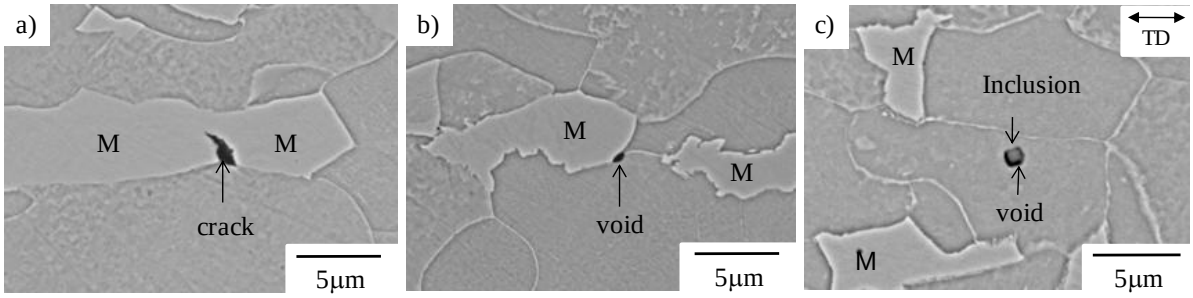

Fig. 4.3 Typical voids in the dual phase steel (SVM) deformed in tension to a thickness strain of $\varepsilon_t = 0.111$: a) void in martensite, b) void in ferrite, c) void at an inclusion. The strain ($\varepsilon_t = 0.111$) is larger than the uniform elongation (U-El = 0.104).

4.3.2 Void formation behaviour during in-situ testing

A typical observation during an in-situ tensile test is shown in Fig. 4.4. The microstructures shown in this figure has been taken from an area near the hole in the specimen. Fig. 4.4a shows neither voids nor cracks in or near the martensite particles before deformation. However, after deformation to a strain of ε_h=0.159, a small crack (crack1) was initiated in a martensite particle (Fig. 4.4b). At a larger strain (ε_h=0.227), an additional crack (crack 2) has divided the martensite particle in Fig. 4.4c into two, and crack1 has propagated in the martensite particle. At a strain of ε_h=0.623, crack1 has propagated perpendicular to the tensile direction and has passed through the martensite particle as shown in Fig. 4.4d. However, once the crack has passed through the particle, it stops and does not propagate into the ferrite even when the strain is raised further.

After propagation, the morphology of the martensite separation (crack1) in Fig. 4.4d is similar to that shown in Fig. 4.4c (crack2). It is therefore possible that crack 2 may also have its origin in a crack in the martensite particle. Fig. 4.4d also shows that the martensite separation around crack2 can lead to void formation at the martensite. After fracture of the particles the two parts of the martensite particle have moved apart in the tensile direction and a void has formed. The width of the void (defined as the dimension perpendicular to the tensile axis) is almost equal to the thickness of the martensite particle after fracture and the width does not depend on strain as the void growth is predominantly in the tensile direction. Most of the voids in the bulk of the tensile sample illustrated in Fig. 4.2 have a similar morphology, suggesting that they have formed by the same

mechanism, involving cracking and separation of martensite particles and in-situ observations also appear to be representative of the bulk behaviour.

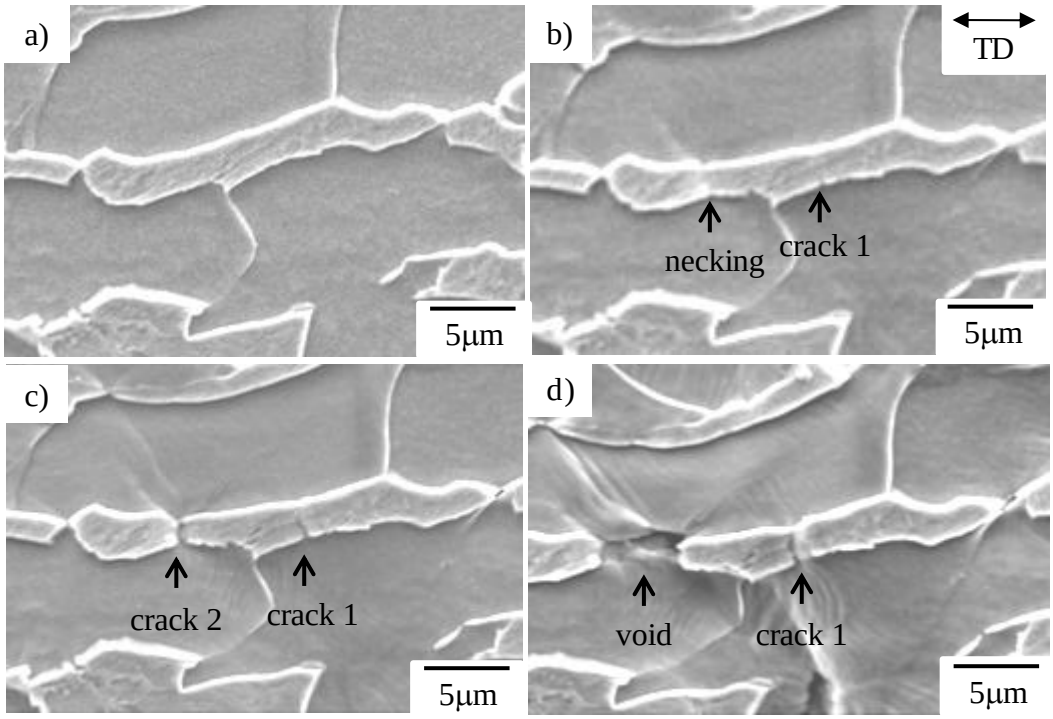

Fig. 4.4 In-situ observation of void formation in the dual phase steel (SVM) during a tensile test: a) initial microstructure without cracks or voids, b) crack initiation in martensite (ε_h= 0.159), c) crack propagation in martensite (ε_h= 0.227) and d) void growth and crack propagation (ε_h = 0.623). A definition of a local strain (ε_h) is given in Table 3.1.

Another example of voids formed during in-situ tensile testing is shown in Fig. 4.5. As for Fig. 4.5 the right column of images are enlarged sections of the left column. Necking of the martensite and multiplicative void formation in the martensite can be observed. The initial microstructure consists of elongated martensite particles which are aligned along the tensile direction (Figs. 4.5a and b). The numbering of the ferrite grains in Fig. 4.5a refers to section 4.4.2 where the strain of each ferrite grain is estimated for further analysis and discussion. After deformation to a strain of ε_h=0.067, a crack has propagated in a martensite particle between the ferrite grains labelled 5 and 7 as shown in Figs. 4.5d and e. At the larger deformation in Figs. 4.5g-h, multiple voids have formed in parallel with necking of the martensite. The voids at the martensite tend to form at the concave parts or the necked regions and multiple void formation in the martensite is often observed. Local strains measured in the necked regions, ε_L^1 and ε_L^2, are 0.23 to 0.28, i.e. larger than the average strain (ε_h) because the deformation concentrates at the concave parts of the martensite particles.

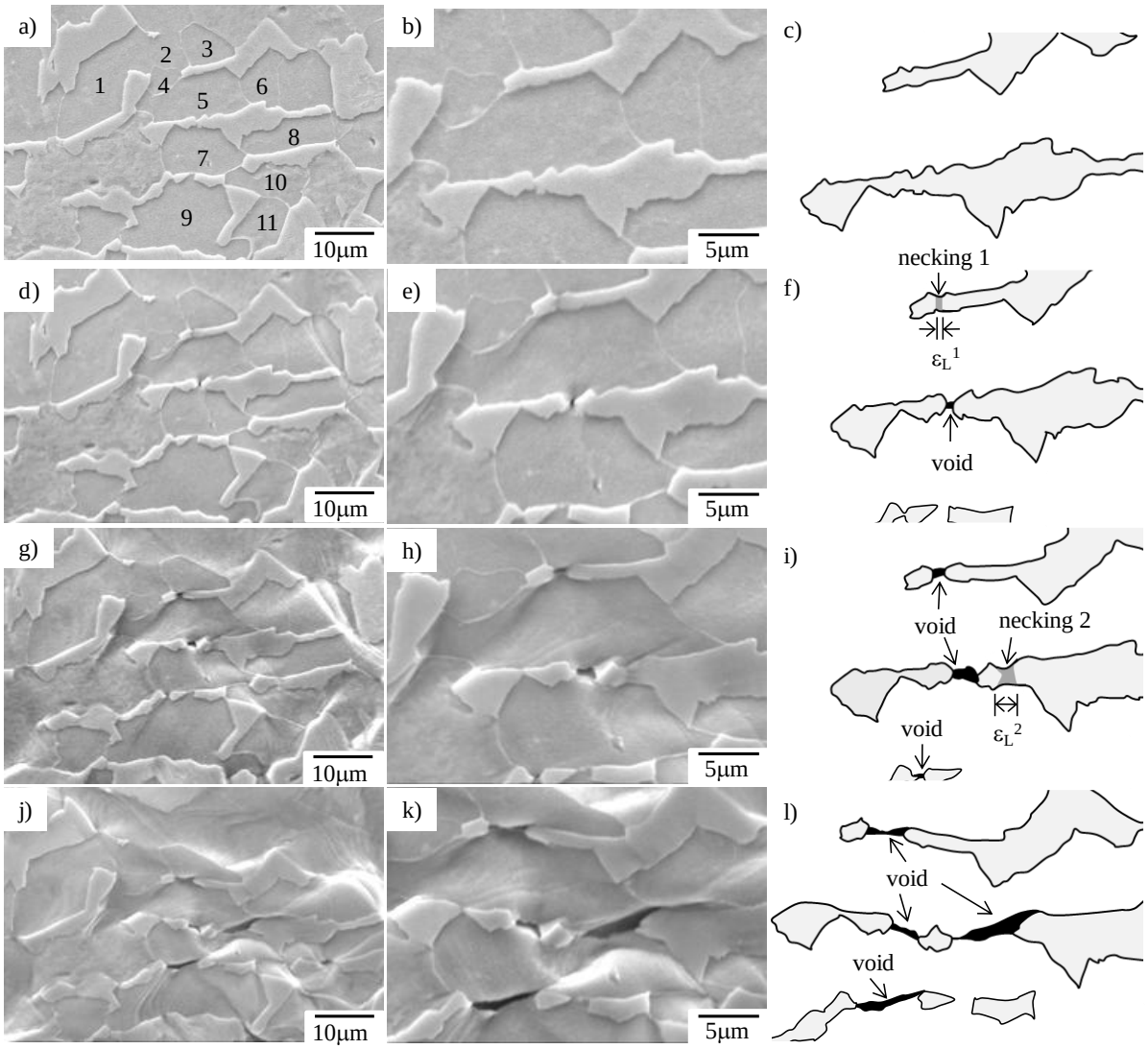

Fig. 4.5 In-situ observation of void formation in the dual phase steel (SVM) during a tensile test at low (left column) and high (right column) magnifications: a) and b) initial microstructure without cracks or voids, d) and e) necking of a martensite particle and void formation in a martensite particle (ε_h= 0.067), g) and h) necking, formation and growth of voids (ε_h= 0.200), j) and k) formation and growth of voids in martensite particles (ε_h = 0.422). ε_L^1 and ε_L^2 show local strain in the necking zone, c), f), i) and l) sketches from b), e), h) and k) of the martensite particles, necked regions and voids. A definition of a local strain at the necked region of a martensite particle (ε_L) is given in Table 3.1.

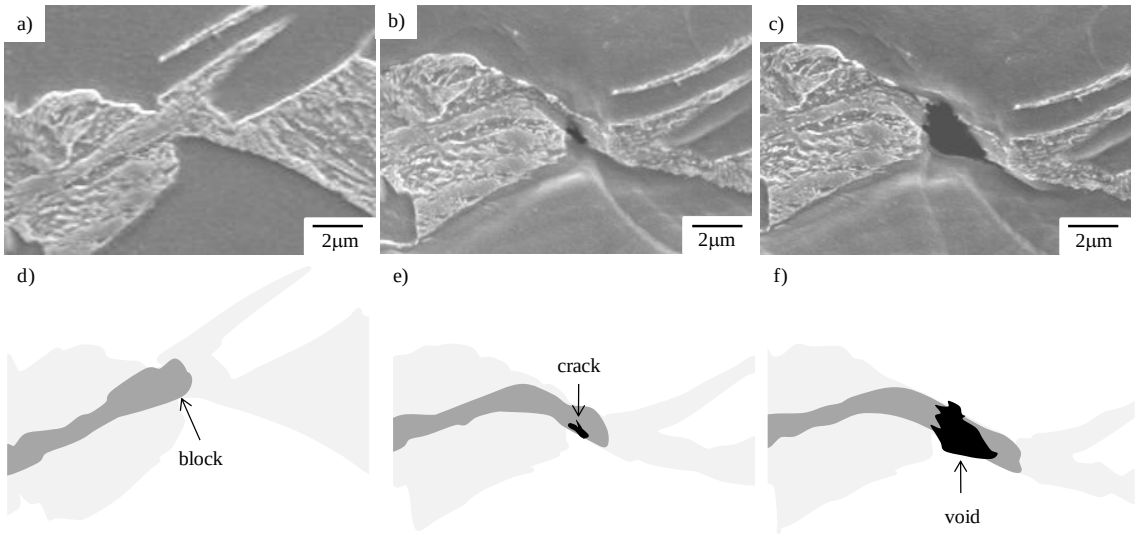

Fig. 4.6 Crack propagation behaviour in the dual phase steel (SVM): a) before deformation (ε_h=0), b) after deformation to ε_h =0.376 and c) ε_h =0.471. d), e) and f) sketches from a), b) and c) of the martensite particle. A crack passed through a block illustrated in d)-f) during the in-situ test.

During crack propagation, cracks often cross block boundaries consisting of a lath of martensite as shown in Fig. 4.6. The specimen was tempered at 300°C for 100s to observe block boundaries. Before deformation, a block was located at a concave part of a martensite particle. Figs. 4.6d-f highlight the deformation and crack propagation behaviour in the block. At a strain of ε_h =0.376, a crack initiated at the martensite/ferrite interface on the martensite side after plastic deformation of the concave part and crossed the block with strain. After deformation to a strain of ε_h =0.471, the crack divided the martensite particle into two but the crack stopped propagation into ferrite grains. As lathes of martensite generally align along the long axis of a block, it appears that the crack passed through lathes of martensite. Steinbrunner et al. and Sarwar et al. suggested that separation of prior austenite grain boundaries leads to crack formation in martensite particles due to segregation of phosphorus on the prior austenite grain boundaries. However, in-situ observations have revealed that cracks in the martensite are not related to prior austenite grain boundaries, but the shape of the martensite particles. In addition, prior austenite grain boundaries are not located in martensite particles in dual phase steels produced through hot-rolling processes as ferrite grains nucleate at prior grain boundaries.

A large deformation leads to void coalescence as shown in Fig. 4.7 observed in a bending test similar to the one shown in Section 3.4. Figs. 4.7a and b show martensite particles without cracks and voids in the undeformed structure. Deformation to a strain of 0.366 led to fracture and separation of the martensite particles at the concave part as shown in Fig. 4.7e. After deformation to a strain of 0.545 in Figs. 4.7g and h, the voids have grown in the shear direction (SD) and coalesced to form an extended void with a length of about 14μm.

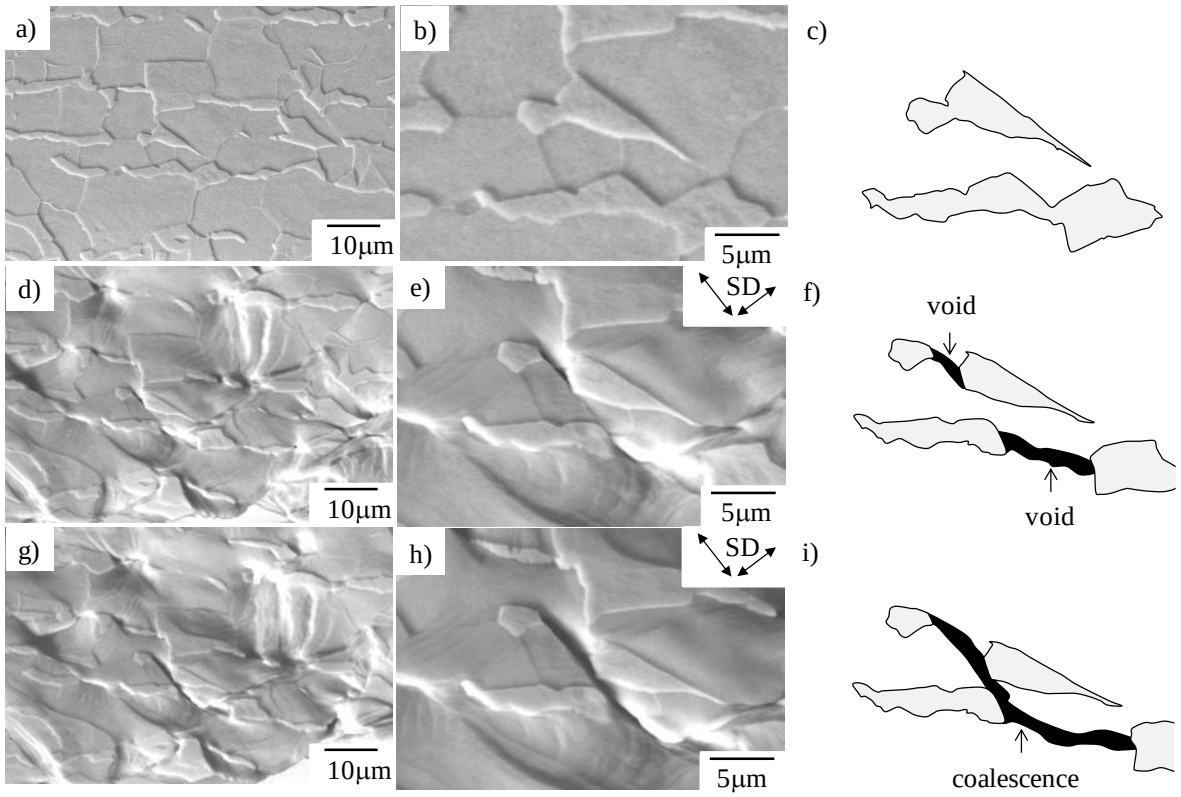

Fig. 4.7 In-situ observation of void formation in the dual phase steel (SVM) during a bending test (shear directions (SD) are marked by arrows): a) and b) initial microstructure without cracks or voids, d) and e) void formation in martensite particles (ε_h= 0.366), g) and h) void coalescence (ε_h= 0.545, c), f) and i) sketches from b), e) and h) of the martensite particles and voids.

Although void formation in the ferrite matrix was rarely observed, Fig. 4.8 shows an example. Before deformation, ferrite grain boundaries are seen but the ferrite matrix does not contain voids (Fig. 4.8a). Deformation to a strain of 0.045 did not produce voids in the ferrite matrix but created slip bands in a ferrite grain at a tip of a martensite particle (Fig. 4.8b). As the strain was increased in Fig. 4.8c, a void has appeared near the end of a martensite particle on the ferrite side. Even though a further strain was applied, the void grew in the tensile direction without propagating along the martensite/ferrite interface and it did not reach another martensite particle on the left side. In the ferrite voids often formed at a triple junction consisting of two ferrite grains and a martensite particle as a ferrite/ferrite grain boundary was frequently located near the tip of the particles. However, decohesion between the ferrite/ferrite grain boundary, which was suggested as a main void formation mechanism in a dual phase steel by Kadkhodapour et al. (2011), was not observed.

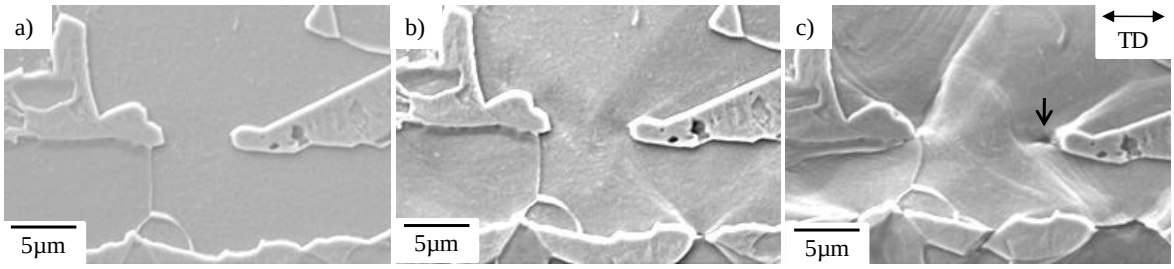

Fig. 4.8 In-situ observation of void formation in the ferrite during a tensile test: a) initial microstructure without cracks or voids, b) slip band formation in the ferrite (ε_h= 0.045) and c) void formation in the ferrite (ε_h= 0.262). The void (marked by an arrow) initiated at the martensite particle on the right side did not reach another martensite particle on the left side.

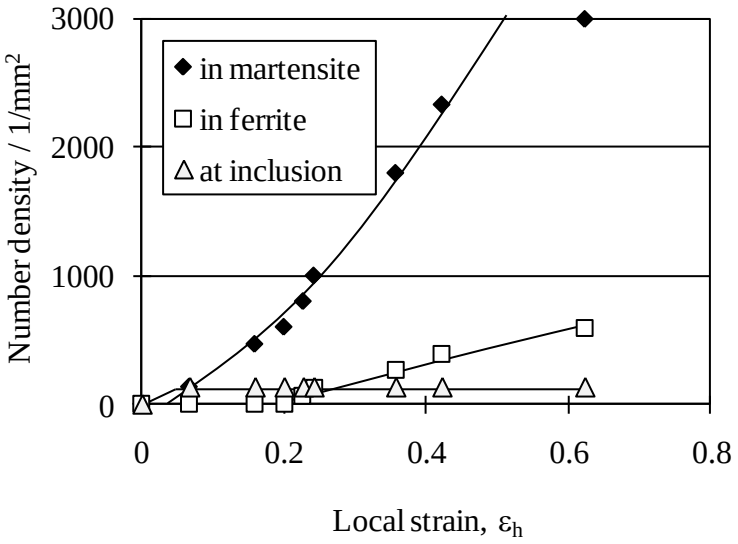

Fig. 4.9 Void number density in the martensite and the ferrite as a function of the local strain (see Table 3.1) in an in-situ test.

To evaluate the effect of void formation during deformation, the number density, size distribution, average length, maximum length and area fraction of voids have been quantified. As an example, Fig. 4.9 shows the void number density in the martensite and the ferrite during an in-situ tensile test. Voids form predominantly in the martensite and already at a low strain whereas few voids form in the ferrite and at a larger strain. This agrees with previous observations showing that cracks can form in martensite before necking of the specimen while voids appear in ferrite after necking (e.g. Erdogan 2002, Avramovic et al. 2009 and 2010, Calcagnotto et al. 2011). In addition, voids started to appear at inclusions at a very low strain and the number density saturated at a strain of ε_h=0.067 due to weak bonded interfaces and a low density.

a)

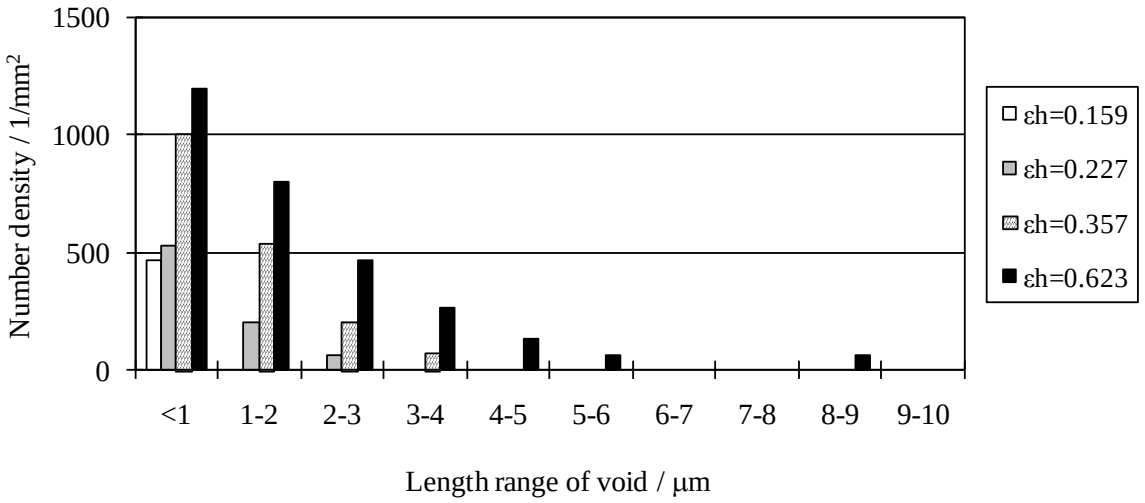

b)

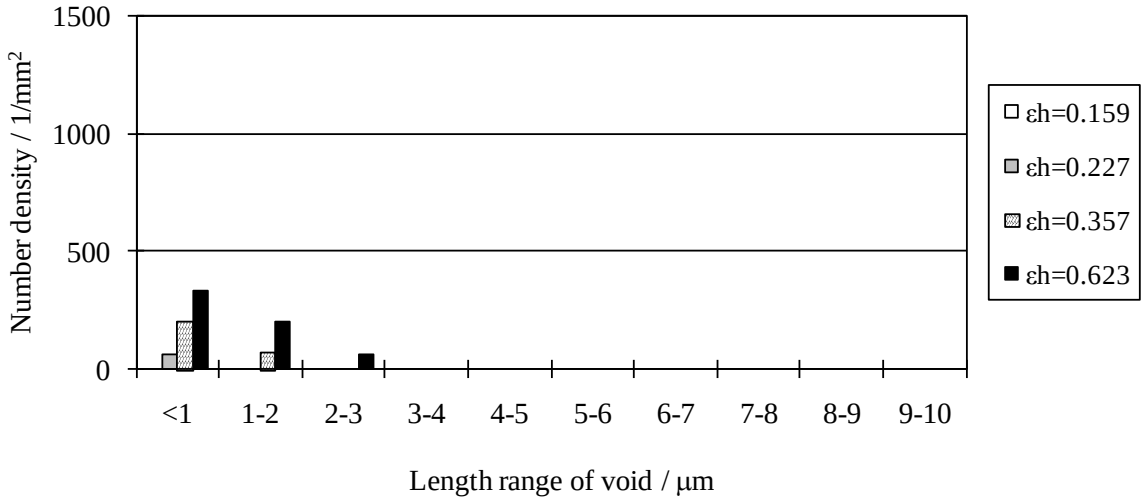

Fig. 4.10 Size distribution of voids formed in the dual phase steel (SVM) during an in-situ tensile test: a) in the martensite, b) in the ferrite.

The size distribution of voids is shown in Fig. 4.10. For all strains, in both the martensite and the ferrite, the number of small voids dominates. This indicates that voids nucleate when the local strain overcomes the critical strain for void formation. The voids grow steadily with strain until the specimen breaks. A continuous void formation was observed in previous works through an observation of a deformed specimen and X-ray tomography (e.g. Maire et al. 2008, Landron et al. 2010, Avramovic et al. 2010). Figs. 4.11a and b show the influence of local strain on void length in the tensile direction. Both the average void length and the maximum void length in the martensite are larger than in the ferrite. However, the difference in average length between the martensite and ferrite is relatively small because many small voids are generated in the martensite during deformation. Also, the strain dependence of the void length in the martensite is larger than in the ferrite. The area fraction of voids is estimated as a function of strain in Fig. 4.11c. The area fraction in both the martensite

and the ferrite increases with strain because of void nucleation and growth. Obviously, voids in the martensite also occupy a relatively large area at a large local strain leading to fracture of the specimen.

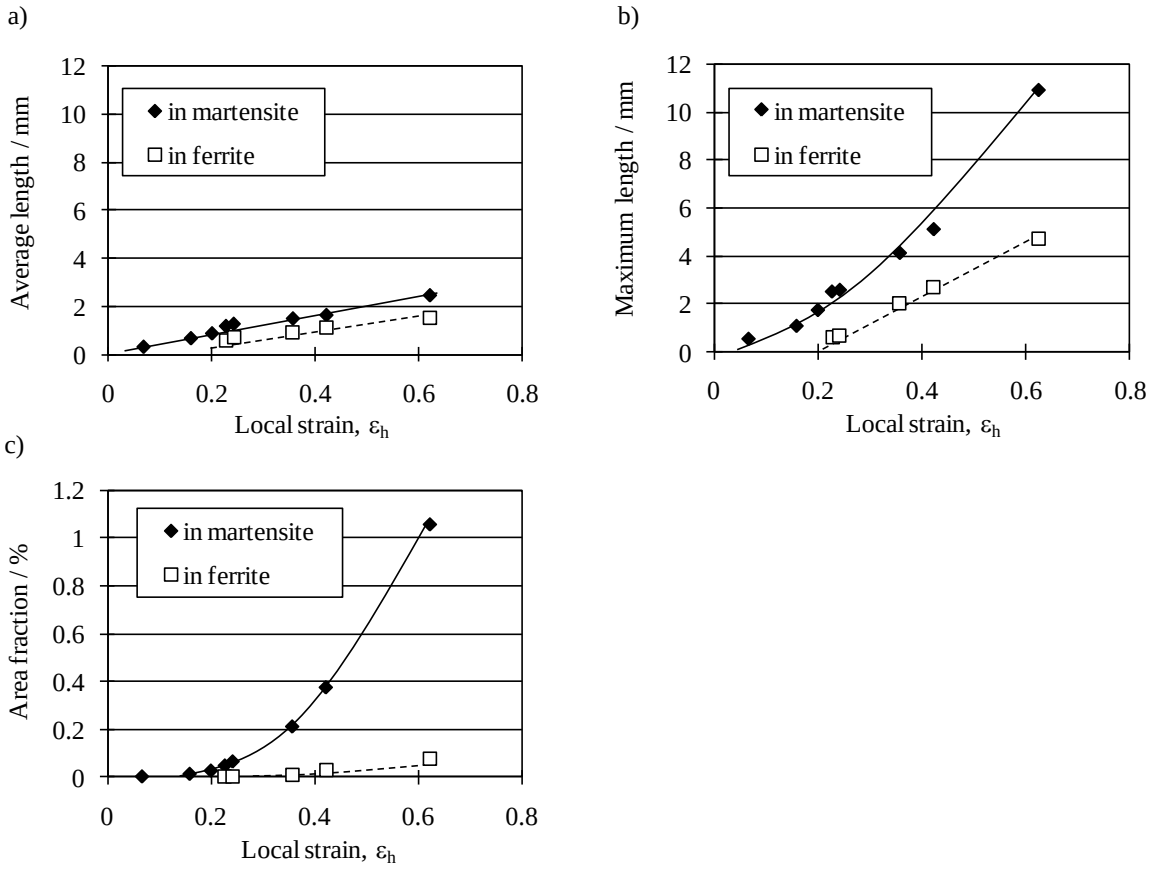

Fig. 4.11 Influence of local strain on void formation behaviour in the dual phase steel during an in-situ tensile test: a) average length, b) maximum length and c) area fraction.

4.4 Discussion

The structure of the tensile deformed specimens and the structural evolution during in-situ testing show that after an initial small strain cracks in the martensite particles start to appear and develop into voids during further straining. At small strains voids also form in the ferrite, however, with a much smaller frequency (see Fig. 4.12). Voids are observed at inclusions but their frequency is low due to the purity of the steel. Based on these microstructural observations, cracks and voids related to martensite particles will be discussed in more detail also considering the hardening behaviour of martensite and ferrite and how this behaviour can be affected through annealing of the dual phase steel. In a final section void formation in ferrite is discussed. The structural evolution has also been studied in bulk specimens tested in tension and the observations indicate that the results obtained by in-situ testing are representative for the bulk behaviour of the dual phase steel.

4.4.1 Plastic deformation of martensite

In an analysis of the deformation behaviour of the dual phase steel an important issue is the individual behaviour of the martensite phase and the ferrite matrix and how interaction takes place in the composite structure. In particular, deformation of the martensite is related to void formation in the martensite. For

example, plastic deformation of martensite particles starts at small strains ($\varepsilon_h \approx 0.05$) during in-situ loading and takes place preferentially at the concave part of the particles before cracks are initiated (Fig. 4.5). A hardness test also demonstrates that martensite and ferrite can deform plastically due to the hardening behaviour (Fig. 4.12). However, the hardening rate of the martensite is smaller than the ferrite due to a small work hardening behaviour of the martensite phase and strain partitioning between the martensite and ferrite (e.g. Shen et al. 1986, Su and Gurland 1987, Tasan et al. 2010, Ghadbeigi et al. 2010). Similar findings are reported after a bending test of a dual phase steel (e.g. Hayashi et al. 2012). It is also found that in the bulk the martensite started to deform plastically at a small strain through an analysis of the work hardening behaviour of the bulk specimen during tensile testing (e.g. Lian, Jiang et al. 1991) and in-situ observation by neutron diffraction (e. g. Morooka et al. 2012) and X-ray diffraction (e.g. Jia et al. 2009). It is obvious that deformation of the martensite is related to void formation in the martensite. In this study the onset of plastic deformation of the martensite in the bulk specimen was estimated based on the stress-strain curve of the dual phase steel (Fig. 3.15) and the modified Crussard-Jaoul analysis (e.g. Lian et al. 1991, Jiang et al. 1995). Fig. 4.13 shows that the work hardening behaviour rate is divided into three regions; (i) the work hardening rate is the highest of all, (ii) the work hardening rate decreases gradually with deformation and (iii) the work hardening rate drops rapidly. The large work hardening rate is related to a large number of dislocations piled up at the martensite/ferrite interfaces because the martensite deforms only elastically. On the other hand, the change of the slope shows that plastic deformation starts in the martensite as pile-up dislocations lead to yielding of the martensite and plastic deformation of the martensite accommodates the work hardening in the ferrite. A transition strain (ε_{trans}) from elastic to plastic deformation of the martensite is 0.03. In previous works, it is shown that the martensite phase starts to deform plastically less than a strain of 0.06 even though a martensite phase is very hard. Before the start of necking, the work hardening rate has already decreased rapidly. The drop of the work hardening rate is related to a reduction of cross section by void formation. It is obvious that void formation before the onset of the necking reduces the work hardening rate and reduces uniform elongation. In parallel with the plastic deformation, deformation of the ferrite grains takes place as illustrated by the observation of coarse slip bands (Figs. 4.4b, 4.5c and h). The observations also show that a fairly large strain is required before the first void appears in the ferrite (Fig. 4.8).

It is also pointed out that plastic deformation of martensite particles is proceeded to separation of the deformed particles (e.g. Steinbrunner et al. 1988). Whereas plastic deformation of the martensite phase has an important role on void formation in dual phase steels, brittle fracture of martensite particles is sometimes assumed to occur in dual phase steels and only plastic deformation of a ferrite matrix is taken into account in order to simulate void formation in dual phase steels (e.g. Kadkhodapour et al. 2011, Vajragupta et al. 2012). The present study has demonstrated that plastic deformation of the martensite is a key factor to improve the formability of dual phase steels. In addition, as shown in Fig. 4.5, the critical strains at the necked region of the martensite particles for void formation in the martensite were about 0.23-28 and the local stain in the martensite for crack formation was much larger than the local strain of the specimen (ε_h), even though the critical local strain for void formation is about 0.05, which is also reported by Steinbrunner et al. (1988). The critical local strain for void formation in the martensite did not depend on volume fraction and morphology of the martensite, but the hardness of the martensite (e.g. Azuma et al. 2012). This result indicates that plastic deformation of the martensite is a key factor to control the formability of dual phase steels. Strain partitioning between soft ferrite and hard martensite depends on the volume fraction of martensite phase and hardness of martensite phase (e.g. Kadkhodapour et al. 2011, Lian et al. 1991, Jiang et al. 1995 and Azuma et al. 2012).

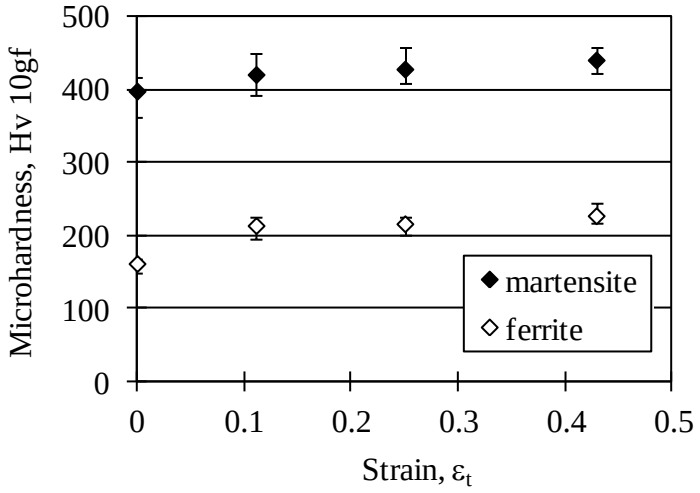

Fig. 4.12 Hardness of martensite and ferrite in the dual phase steel (SVM) after tensile testing.

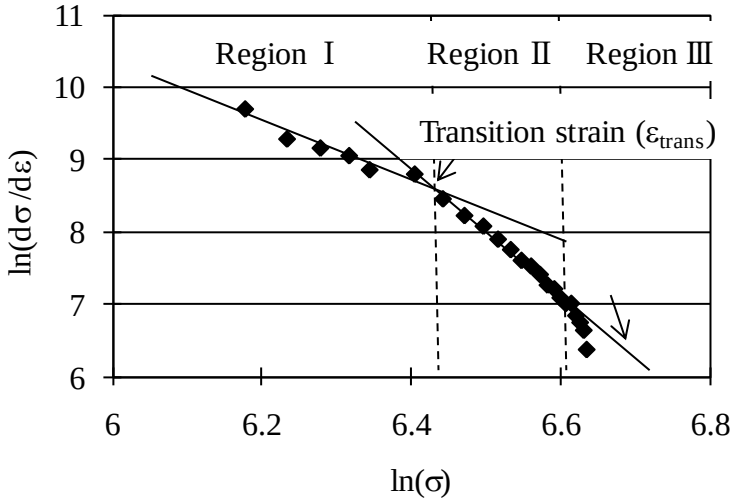

Fig. 4.13 An analysis of the work hardening behaviour in the dual phase steel (SVM) based on the modified Crussard-Jaoul method. In region Ⅰ, the ferrite phase deformed plastically but the martensite deformed elastically. Region Ⅱ means that plastic deformation occurred in the ferrite and martensite. Region Ⅲ is related to a reduction in the area due to void formation.4.4.2 Plastic deformation of ferrite.

In an analysis of the deformation behaviour of the dual phase steel an important issue is the individual behaviour of the martensite particles and the ferrite matrix and how interaction takes place in the composite structure.

In parallel with the plastic deformation of the martensite particles, plastic deformation of the ferrite grains takes place as illustrated by the observation of coarse slip bands (Figs. 4.5b, 6c and h). The void formation is proceeded by localized glide representing slip band formation around the concave part and the tip of the martensite particles. Similar findings have been reported that slip bands formed in the ferrite composing of dual phase steels before cracking of martensite particles. It is apparent that the deformation of soft ferrite grains is related to deformation of hard martensite particles if the grains are constrained by the particles. The application of the in-situ technique has also allowed a monitoring of the strain in the ferrite grains in an area where voids

have been observed. This has been done by following the length change of the ferrite grains (Fig. 4.5). The strains are given in Table 3.1, which reveals that the strains in individual grains increase with the strain of the specimen (ε_h). This shows that the effects of the grain size and the crystallographic orientation of the ferrite grains are of minor importance. However, Table 4.2 also shows that a number of grains have deformed to relatively large strains and that these grains are located next to the broken martensite particles, although some grains, which are not constrained by martensite particle, were heavily deformed. Once a large deformation was induced in the ferrite grains due to crack formation in the particles, other voids formed in other martensite particles locating to opposite side of the broken martensite. It appears that larger strain in the ferrite grains next to broken martensite leads to larger plastic deformation of other martensite particles and multiple void formation. The observation illustrates the complex deformation pattern of the dual phase steel and that the deformation behaviour of both phases as well as the interaction between martensite and ferrite is important since the multiple void formation leads to fracture of specimens.

Table 4.2 Strains of ferrite grains in an area with broken martensite particles as shown in Fig. 4.5.

Grain	ε_h=0.067	ε_h =0.200	ε_h =0.422
1	0.050	0.125	0.150
2	0.125	0.188	0.625
3	0.130	0.261*	0.522*
4	0.067	0.200	0.467
5	0.104*	0.313*	0.750*
6	0.053	0.263	0.947
7	0.111*	0.286*	1.029*
8	0.024	0.122	0.308
9	0.063	0.191*	0.468*
10	0.056	0.167	0.556*
11	0.080	0.240	0.760

* Formation of voids in neighbouring martensite particles

In addition, it is apparent that the deformation of soft ferrite grains is related to deformation of hard martensite particles if the grains are constrained by the particles. The application of the in-situ technique has also allowed a monitoring of the strain in the ferrite grains in an area where voids have been observed. This has been done by following length change of the ferrite grains (Fig. 4.5). The strains are given in Table 4.2, which reveals that the strains in individual grains increase in relatively good accordance with the strain of the specimen (ε_h). This shows that the effects of the grain size and the crystallographic orientation of the ferrite grains are of minor importance. However, Table 4.2 also shows that a number of grains have deformed to relatively large strains and that these grains are localized next to the broken martensite particles, although some are also found in other locations. A more detailed analysis requires a larger experimental basis but the observation illustrates the complex deformation pattern of the dual phase steel and that the deformation behaviour of both phases as well as the interaction between martensite and ferrite is important. Landron et al. pointed out that reduction of a cross section by void formation accelerates void formation based on an engineering model and an observation by X-ray tomography (2010). It supplements that the multiple void formation is an important process in dual phase steels.

4.4.2 Cracks in martensite

Most voids are formed in the martensite particles following cracking of the particles. In the tensile deformed microstructure, cracks initiated at the martensite/ferrite interface on the martensite side after plastic deformation of martensite particles as illustrated in Figs. 4.4-6. In all cases, decohesion and void formation at the martensite/ferrite interface was not observed prior to crack initiation in the martensite. It is apparent that the dual phase steel before deformation is free of cracks and voids but already at a small strain cracks in martensite start to appear following necking of the particles (Fig. 4.4). Many of these cracks form in martensite particles elongated in the tensile direction and they are typically observed where the surface of the particles is concave pointing to an increased stress and strain in such regions. In addition, crack propagation across a block boundary suggests that the shape of the martensite particles has a larger effect on crack formation in the martensite whereas the block boundaries and packet boundaries contribute to the strength and the ductility of

the martensite. In parallel with the initiation of small cracks in the martensite, deformation localizes more in the ferrite grains next to cracks as illustrated by the observation of coarse slip bands (Figs. 4.4c, d and 4.5h). These observations point to a combined effect of strain, particle size and morphology on the crack initiation in the martensite. The findings supplement previous observations showing that cracks form in martensite particles at a smaller strain in a dual phase steel containing large martensite particles, which have elongated shapes and concave profiles, than in a steel with small martensite particles (e.g. He et al. 1984, Erdogan 2002). Similarly cracks in a spheroidized steel, consisting of a ferrite matrix and cementite particles, form in large cementite particles with concave parts and propagate in the particles perpendicularly to the tensile stress direction during tensile tests, compression tests and torsion tests (e.g. Gurland 1972), which has led to the suggestion that large particles are preferred crack formation sites. However, in the present study, cracks did not form in large martensite particles but in elongated particles or at the concave parts of the particles even though the microstructure is composed of both small and large martensite particles. It appears that it is related to deformation of the martensite as the large martensite particles were deformed less than the thinner particles. Tasan et al. (2010) also pointed out that thinner martensite bands are deformed more than thicker martensite bands in a dual phase steel during an in-situ tensile test.

4.4.3 Voids in martensite

The present observations show in agreement with previous studies that voids form in the martensite particles as shown in Table 4.1 (e.g. Koo et al. 1977, Balliger 1982, He et al. 1982, Shen et al. 1986 and Gladman 1997). It is also found that both in the tensile test of the bulk specimen and in-situ testing voids start to form in the martensite at relatively small strains about ε_t , $\varepsilon_h = 0.05$ (Fig. 4.9) which agrees with the findings for a dual phase steel deformed in tension that voids form at a strain of 0.034 (e.g. Calcagnotto et al. 2011). However, application of the in-situ techniques has illustrated void nucleation related directly to plastic deformation of the martensite particle and crack formation in the particles. On the other hand, Avramovic et al. (2011) have suggested that elongated voids between two martensite particles originate in void formation in ferrite phase as voids at the martensite/ferrite interface should grow more than in the martensite. In addition, they have suggested that as fracture occurs in the specimen after void formation in the ferrite, voids in the ferrite have a more negative effect on the formability in the dual phase steel. However, the in-situ test has demonstrated that cracks in the martensite particles develop into voids and voids in the martensite grow in the tensile direction more than in the ferrite. Moreover, the observation has clarified that influence of voids in the ferrite is minor due to the small area fraction even though some voids form in the ferrite in advance of the fracture.

Based on the observations it is suggested that cracks and voids in the martensite particles evolve in four steps: (i) plastic deformation of the martensite, (ii) crack initiation at the martensite/ferrite interface, (iii) crack propagation leading to fracture of the martensite particles and (iv) void formation by separation of the particle fragments. Besides, the in-situ observations have also allowed quantification of the size and number of voids and their area fraction as a function of a given strain. Fig. 4.10 shows that both the fraction of large voids and the area fraction of voids increase rapidly for strains at 0.36 and above. This illustrates the importance of voids in the martensite and also that routes to reduce such voids must be explored in order to increase the formability of a dual phase steel. One such route is discussed in the next section.

4.4.4 Voids in ferrite

The voids in ferrite are typically observed near the end of the martensite particles (Figs. 4.3b and 4.8). It is also found that voids never propagate along the martensite/ferrite interface and the ferrite/ferrite grain boundary but grow in the tensile direction. The absence of decohesion points to a high strength of the martensite/ferrite interface and the ferrite/ferrite interface as decohesion is an indication of a weak interface, for example, between inclusions and ferrite or martensite in steel (e.g. Roberts et al. 1976, Qiu et al .1999, Sabirov and Kolendnik 2005, León-Garcia et al. 2010, Hosseini et al. 2007) and between reinforcement and matrix in metal-matrix composites (e.g. Nutt et al. 1987, Christman et al. 1989, Clyne and Withers 1993, Whitehouse and Clyne 1993). In the present specimens the voids in ferrite may have their cause in a high stress concentration near the end of the elongated hard martensite particle as the interface is faced perpendicular to the tensile direction and deformation concentrates in ferrite grains between martensite particles. The concentrated stress may be partly relaxed by plastic deformation of the ferrite, creating the dislocations and vacancies required for void growth composites (e.g. Lubarda et al. 2004, Traiviratanav et al. 2008, Meyers et al. 2009).

Finally, the void growth has been quantified in more detail based on a structural evolution. Fig. 4.14 shows that the void initiated at the interface, which was shown in Fig. 4.8, grew in the tensile direction, the ferrite grain between two martensite particles was elongated until fracture of the specimen and the void did not reach another martensite particle. Voids at a martensite particle did not reach another particle even though the length between two martensite particles was about 1 μm (Fig. 4.15) and voids formed at a triple junction of two ferrite grains and a martensite particle (Fig. 4.16). In addition, the ferrite grain remained between two martensite particles during the tensile test and decohesion at ferrite/ferrite grain boundaries did not occur in the dual phase steels as shown in Fig. 4.16. The characteristic void formation behaviour in the ferrite also supplements that void formation in the martensite is dominant in the dual phase steels. Moreover, the complicated void formation behaviour in dual phase steels; voids formed in the ferrite are still isolated at the martensite/ferrite interface but cracks initiated in the martensite exist as a void between two martensite particles, makes deformed microstructures confusing. The in-situ scanning electron microscopy is a powerful technique to reveal fracture behaviour in dual phase steels.

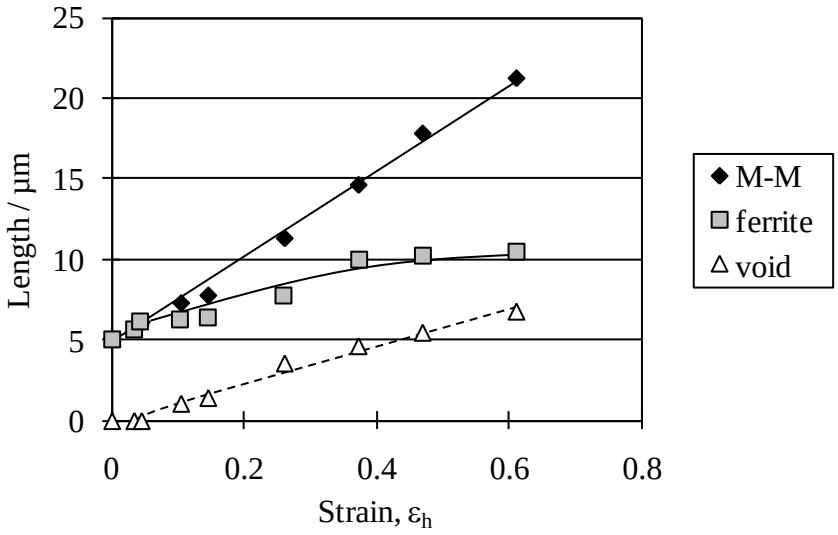

Fig. 4.14 Length change between two martensite particles, of a ferrite grain between two the particles and a void in the ferrite in Fig. 4.8.

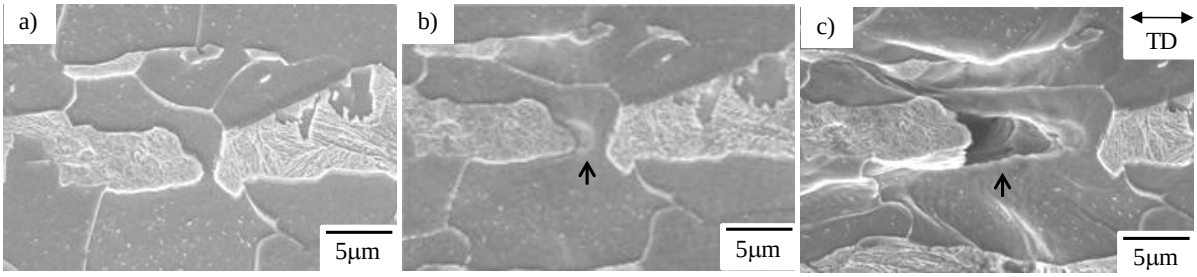

Fig. 4.15 In-situ observation of void formation at a ferrite/martensite interface in SVM tempered at 500°C during a tensile test: a) initial microstructure without cracks or voids, b) slip band formation in the ferrite (ε_h= 0.481) and c) void formation in the ferrite (ε_h= 0.880). The void (marked by an arrow) initiated at the martensite particle on the right side did not reach another martensite particle on the left side.

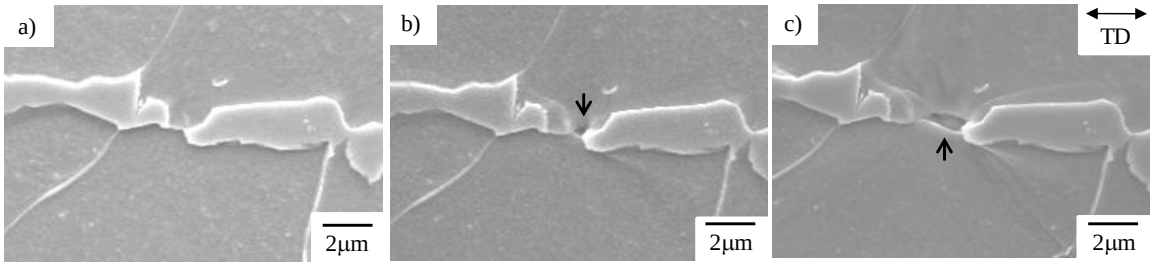

Fig. 4.16 In-situ observation of void formation at a triple junction of two ferrite grains and a martensite particle in LVM during a tensile test: a) initial microstructure without cracks or voids, b) slip band formation in the ferrite (ε_h= 0.118) and c) void formation in the ferrite (ε_h= 0.310). The void (marked by an arrow) initiated at the martensite particle on the right side did not reach the other martensite particle on the left side.

4.4.5 Void formation behaviour at inclusions

Few voids formed at inclusions at smaller strains even though the inclusion density is low. Fig. 4.17 demonstrates typical void formation by decohesion at the martensite/inclusion interface. At a strain of ε_h= 0.046, cracks had already propagated along the interface and voids surround the inclusions. Some voids existed at inclusions before deformation. A crack tended to initiate at the interface facing perpendicular to the tensile direction, propagated along the interface and then plastic deformation of the surrounding ferrite grains allow the crack to develop as a void. It appears that a large stress concentration is at the interface perpendicular to the tensile direction, weak bonded interfaces and stress concentration at a tip of the cracks contributes void formation at inclusions. Kadkhodapour et al. (2011) suggested that stress is large at a metal/inclusion interface facing perpendicular to a tensile axis, once a crack forms at the metal/inclusion, stress concentrates at the tip of the crack and the crack propagates along the interface very rapidly through a FEM analysis. On the other hand, voids at the martensite/ferrite interface did not propagate along the interface, but grew in the tensile direction. The different void growth behaviour indicates that the interfacial strength between the martensite and ferrite is relatively large. In addition, Table 4.3 demonstrates interfacial strength, which is estimated by comparison experimental results with a physical model, between ferrite matrixes and inclusions, ferrite grains and martensite particles. Interfacial strength between martensite and bainite (lathes of ferrite) is about 2-2.4GPa and interfacial strength between ferrite and inclusions is about 1-2GPa. It is obvious that the ferrite/inclusion interfaces, such as carbide, nitride, sulphide and oxide, are weak, but the martensite/ferrite interface is strong. Therefore, the large interfacial strength between the martensite and bainite contributes to the absence of decohesion between the martensite and ferrite. Plastic deformation of the surrounding ferrite grains allow a crack to develop as a void. It, therefore, appears that the voids in Fig. 4.16 and Fig. 4.3c surrounded inclusions. The rapid void formation at inclusions leads to saturation of the number density of voids at inclusions at a small strain (ε_h<0.05) as shown in Fig. 4.9.

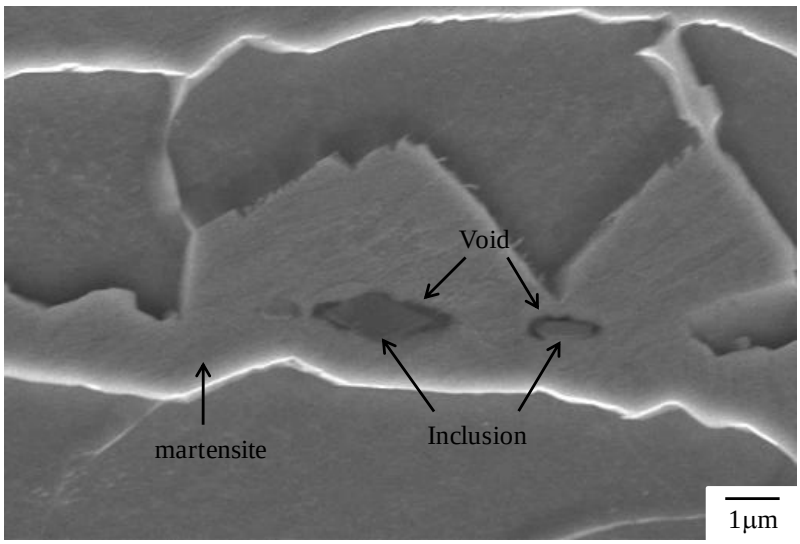

Fig. 4.17 Void formation at inclusions (ε_h= 0.046) in the dual phase (SVM). The voids, inclusions and martensite are marked by arrows. The inclusions are surrounded by voids as the voids have already formed at a small strain, propagated along the interface between the inclusions and martensite.

Table 4.3 Interfacial strength between ferrite and martensite, inclusions.

Particle	Volume fraction	ε_{nuc}	Interfacial strength / GPa	Reference
martensite	0.10	0.9	2.4-2.5	Poruks P. Et al.
Y_2O_3	0.02-0.10	0.02-0.13	1-1.6	Kosco J. B. et al.
MnS	0.0023	0.36	1.1-1.4	Qiu H. Et al.
Fe_3C	0.02-0.14	0.45-0.62	1.2-2.0	LeRoy G. Et al., Kwon D.

4.4.6 Void formation behaviour in the bulk

Void formation behaviour in the bulk after the tensile test was also estimated. Each void in the bulk was characterized based on the classification by the in-situ observation; voids induced by a crack in the martensite exist between two broken martensite particles, and voids formed in the ferrite touch only a martensite particle. It is assumed that voids touches only one martensite particle are characterized as a void in the ferrite because simultaneous void formation was not observed at the tip of two martensite particles, which faced each other, due to heterogeneous morphology of the particles and stress relaxation by single void formation. Fig. 4.18 demonstrates that, in the bulk specimen, voids in the martensite are more frequent and larger than in the ferrite, and occupy the majority of the area. It is apparent that the voids in the martensite mainly contribute to the formability in dual phase steels. Hosseini et al. (2007) and Roberts et al. (1976) pointed out that in steels with MnS same mechanisms such as crack formation in MnS or decohesion between steels and MnS dominate void formation on the surface of specimens and in the bulk. However, crack formation and decohesion occurs more frequently on the surface due to out of plane deformation. On the other hand, X-ray observation has exemplified that voids form more frequently in the centre of specimens than near the surface after the start of necking (e. g. Maire et al. 2008). It appears that necking affects the stress distribution in the bulk specimen and more voids form at the centre of the specimen. Specially, a stress distribution, such as stress triaxiality and hydrostatic stress, is one of the most important parameters to affect void formation in materials.

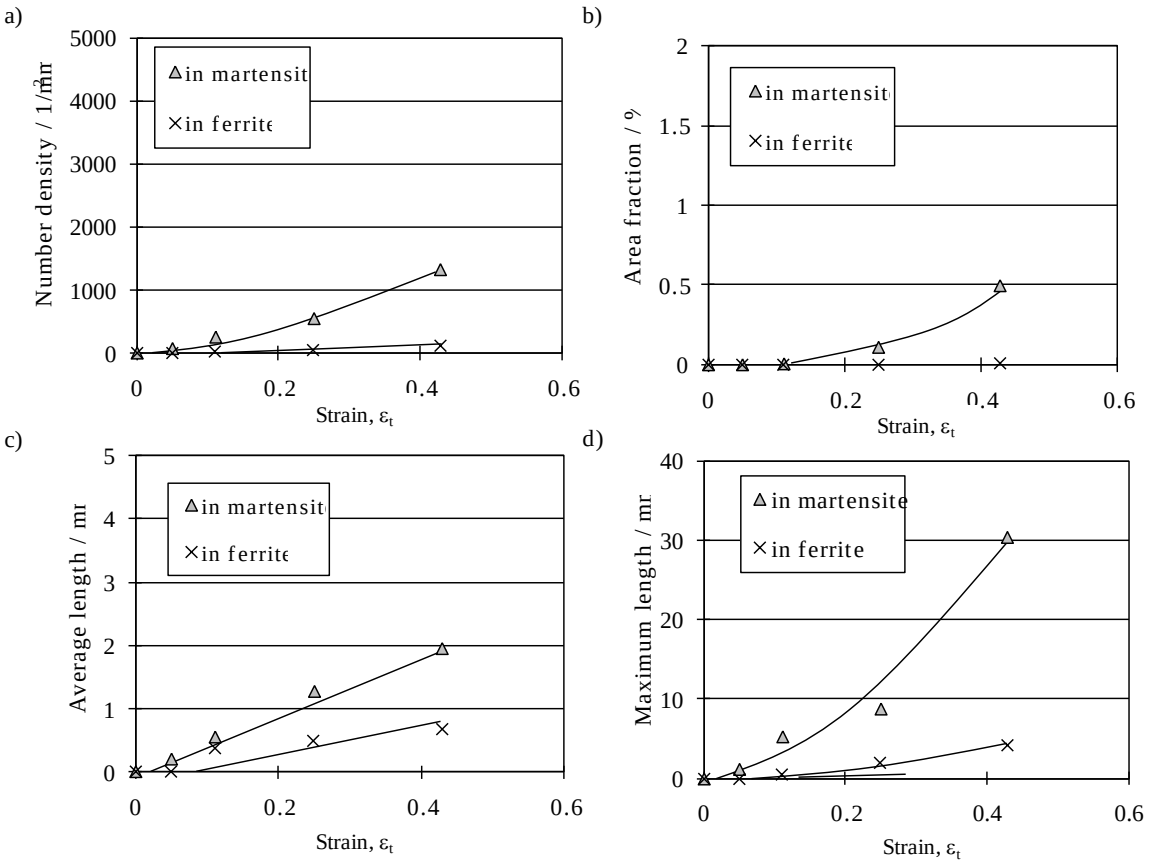

Fig. 4.18 Void formation behaviour in the bulk of the dual phase steel: a) number density, b) maximum length, c) average length and d) area fraction of voids. Each void is characterized by the following classification. Voids induced by cracking of martensite particles exist between two broken martensite particles and voids formed in the ferrite touch at only a martensite particle.

4.5 Summary

Crack and void formation during deformation of a dual phase steel (SVM) has been followed by tensile testing of bulk specimens and by in-situ loading in a scanning electron microscope. The following conclusions are reached.

1. Cracks and voids have been observed at different sites; (i) in the martensite phase, (ii) in the ferrite phase and (iii) at inclusions. At a given strain both the frequency and the area fraction of voids in martensite dominate.

2. The cracks and voids in the martensite particles evolve in four steps; (i) plastic deformation of the martensite, (ii) crack initiation at the martensite/ferrite interface, (iii) crack propagation leading to fracture of martensite particles and (iv) void formation by separation of particle fragments. The in-situ observations have allowed void nucleation to be related directly to plastic deformation and cracking of martensite particles.

3. The in-situ observations have revealed the absence of decohesion at the martensite/ferrite interface and ferrite/ferrite grain boundary. The voids on a martensite particle do not reach another martensite particle even though voids grow in the tensile direction.

4. The voids in ferrite are predominantly formed at the tip of elongated martensite particle interfaces perpendicular to the tensile axis and grow in the tensile direction.

5. Characteristic void morphology enables one to distinguish voids in the ferrite from voids in the martensite in bulk specimens. Martensite cracks exist as elongated voids between martensite fragments and voids in the ferrite are still isolated.

Chapter 5

Effect of martensite hardness

5.1 Introduction

As mentioned in the last chapter, a majority of voids formed in the martensite, but voids rarely formed in the ferrite by the tensile tests of bulk specimens and in-situ tensile tests in a SEM. In particular, as more voids form after the onset of necking, void formation strongly affects post-uniform elongation. In composite structures, as a matrix interacts with reinforcements, a number of parameters related to martensite have been suggested which may affect the crack and void formation, especially the hardness of the martensite and the grain size of the ferrite based on a concept that void formation has an origin in the difference of mechanical properties of the martensite and ferrite.

Mazinani and Poole (2007) suggested that softening of the martensite through intercritical annealing at high temperature, where the carbon content in the austenite is low and thereby makes the martensite soft, improves the true fracture strain. However, as intercritical annealing affects the volume fraction, shape and size of the martensite, which might affect void formation, the effect of the hardness of the martensite is still ambiguous.

Tempering treatments are also suggested as a method to improve the formability, counterbalanced by a reduction of the ultimate tensile strength. Fang et al. (2003), Samuel (1985), Joarder et al. (1990) and Hasegawa et al. (2004) reported that softening of the martensite through tempering treatments increases the elongation and hole-expansion ratio. In particular, post-uniform elongation is significantly improved by the treatments. However, they did not observe the void formation behaviour in the dual phase steels in detail even though void formation leads to fracture of the specimen. Jardim et al. (1984) and Tomota et al. (1977) suggested that softening of the martensite assists plastic deformation of the martensite and retards void formation in the dual phase steels. However, criteria for void formation and how the hardness of the martensite affects void formation are still ambiguous.

On the other hand, Calcagnotto et al. (2011) focused on the hardness of the ferrite phase to improve the formability in dual phase steels. They suggested that hardening of the ferrite through grain refinement made the martensite deform more, further deformation of the martensite reduced deformation concentration at the martensite/ferrite interface and the grain refinement contributed to retardation of voids in the dual phase steels based on a SEM observation. The ferrite grain size was controlled by hot-rolling and annealing and the heat treatment also strongly affected the shape of martensite particles. However, they did not show unambiguous evidence. Specifically, in the coarse grained dual phase steel martensite particles surrounding ferrite grains were deformed as much as the ferrite grains, whereas in the fine grained dual phase steels equiaxed martensite particles were stretched in the tensile direction after a tensile test. The effect of martensite shape was not taken into account, even though the shape of martensite particles is one of the most important parameters to affect the interaction between the matrix and reinforcements in composite structures.

The present study therefore aims at clarifying the effect of the martensite hardness on void formation in a dual phase steel. The void formation behaviour was followed by in-situ tensile tests in a SEM where the structural evolution can be studied as a function of the given strain. These observations have revealed criteria for void formation and effect of the hardness on strain distribution in the dual phase steel.

5.2 Experimental procedures

A dual phase steel (SVM) was applied to estimate the influence of tempering treatments on void formation in the dual phase steel. In order to control the hardness of the martensite, tempering treatments at 300 to 600°C were carried out because tempering does not affect the volume fraction, size and shape of ferrite and martensite. In addition, since decohesion at the interface between the ferrite and large carbides and cracking of large carbides lead to void formation, a short holding time was chosen in order to prevent carbides from coarsening. Then some steel sheets were tempered at 300-600°C for 100s.

After tempering, the hardness of the martensite and ferrite was characterized through a Vickers hardness test and the initial microstructure was characterized by SEM and TEM observations. Void formation behaviour in the dual phase steel was followed by observation of the bulk specimens after tensile tests and in-situ tensile tests in a SEM. In addition, strain distribution in the dual phase steel was measured by TEM and EBSD method after tensile deformation to a strain of ε_t=0.05.

5.3 Results

5.3.1 Influence of tempering treatments on mechanical properties

Tempering treatments strongly affect the mechanical properties of the dual phase steel (SVM). Figs. 5.1 and 5.2 show the nominal stress-nominal strain curves and the mechanical property of the dual phase steel. Fig. 5.1 does not show the stress-strain curve after necking because the extensometer was removed when the nominal strain became larger than the uniform elongation. The total elongation is estimated based on measurement of the gauge length after the tensile test. Before tempering, the stress increases rapidly after yielding and the work hardening rate is high at a low strain. The 0.2% offset stress is defined as a yield stress (YS) as the steel does not show a yield point phenomenon before tempering. On the other hand, as tempering treatments lead to a yield point phenomenon, an upper yield stress is defined as a yield stress. To estimate the post-uniform elongation (P-El) from the onset of necking to fracture, the post-uniform elongation was calculated as the difference between the total elongation (T-El) and the uniform elongation; P-El = T-El – U-El. The ultimate tensile strength was about 680MPa before tempering treatments. Fig. 5.2 shows that tempering treatments increased all elongations, a reduction in thickness and hole-expansion ratio (λ), counterbalanced to reduction of the UTS. A tempering treatment at 600°C led to a 30% reduction of the ultimate tensile strength in SVM. However, the yield stress does not depend on tempering treatments due to a yield point phenomenon. Figs. 5.2c and d also show that tempering treatments improve the P-El more than the U-El. It appears that tempering treatments have a large effect on void formation in the dual phase steel as more voids are generally observed in a necking zone of deformed specimens. Besides, the effect of the treatments on reduction in thickness and hole-expansion ratio is also large as strains at the fracture of the specimens deformed in tension and at the edge of the hole of the hole-expanded specimens are often larger than the U-El. Whereas the effect of the treatments on P-El was relatively large, tempering treatments also affected the U-El and work hardening behaviour of the dual phase steel. Fig. 5.3 shows true stress-true strain curves and the work hardening rate ($d\sigma^t/d\varepsilon^t$) of the dual phase steel. Here the specimens without tempering, tempered at 300 and 500°C, were picked up as characteristic work hardening behaviours appeared in the specimens. It general, a criterion for the onset of necking is given by the following equation.

$$d\sigma^t/d\varepsilon^t \leq \sigma \qquad \text{Eq.[11]}$$

where σ^t and ε^t are true stress and true strain. $d\sigma^t/d\varepsilon^t$ is a work hardening rate at each strain. In general, the work hardening rate is large after yielding, gradually decreases with strain until necking and decreases rapidly after the start of necking due to a reduction of cross sections. However, the work hardening rate decreased rapidly in the specimen without tempering before the onset of necking. The rapid reduction of the work hardening rate might be related to reduction of the cross section due to void formation before the onset of the necking. Therefore, the effect is investigated in Section 5.4.4 in more detail.

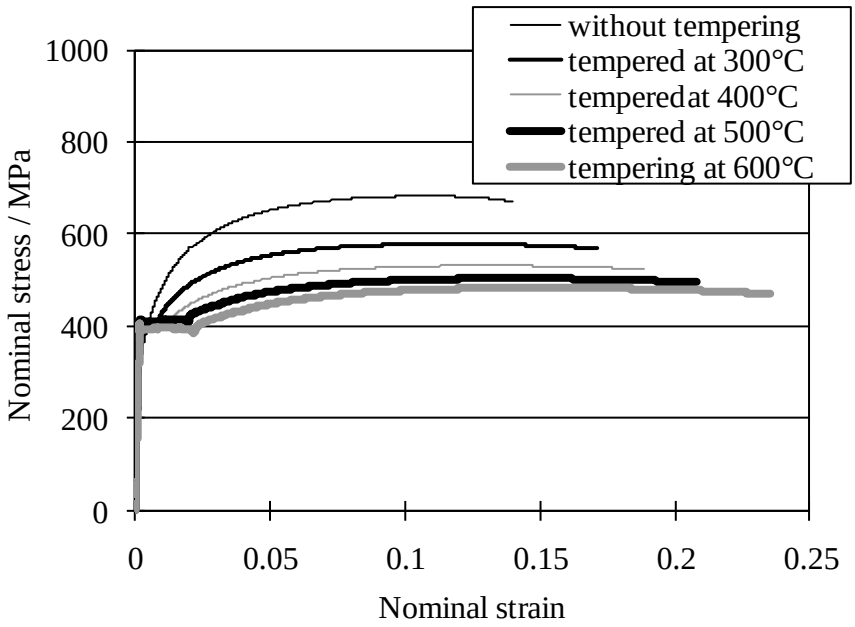

Fig. 5.1 Stress-strain curves of the dual phase steel before and after tempering treatments. Tempering treatments led to a yield-point phenomena in the tempered specimens.

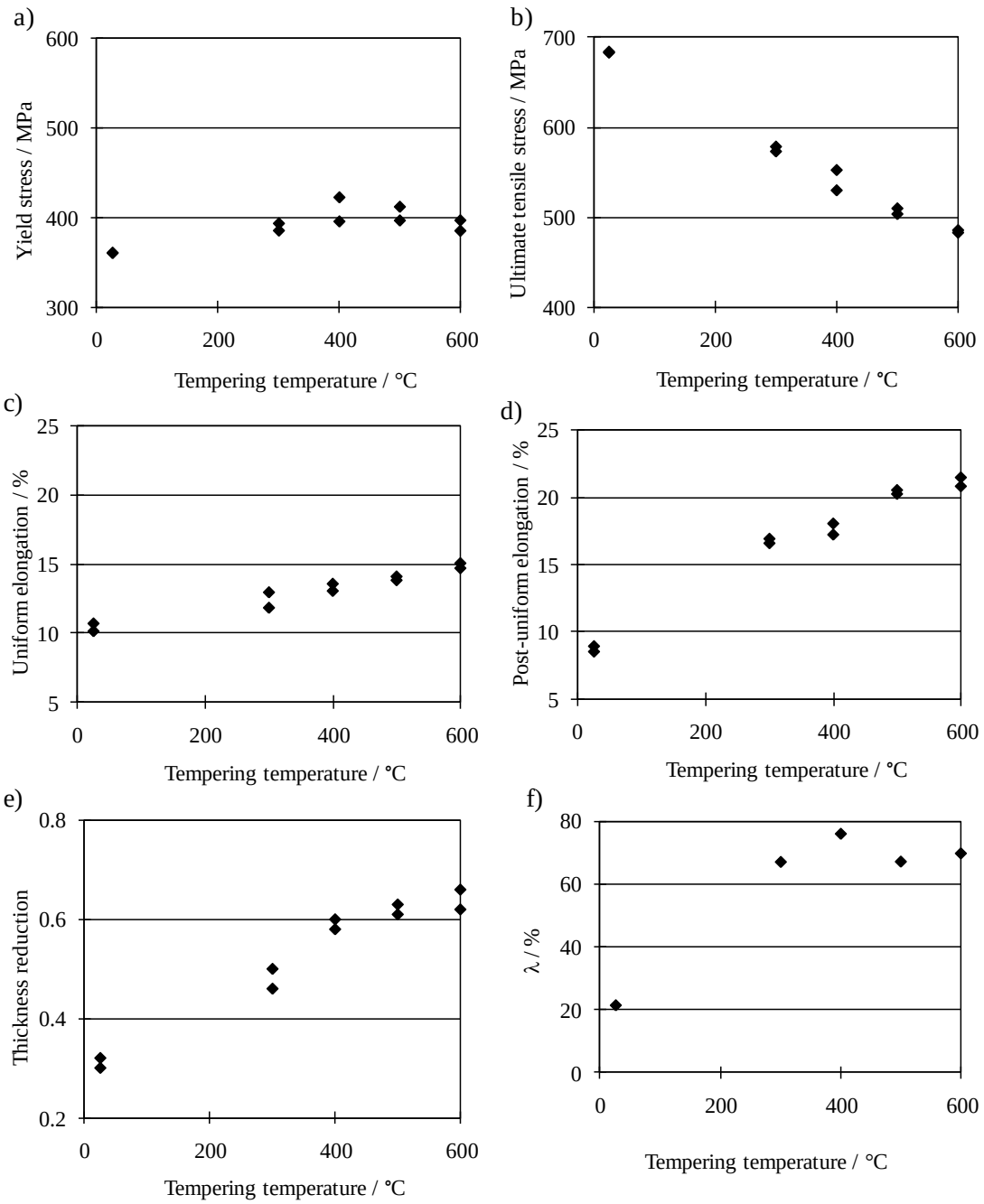

Fig. 5.2 Influence of tempering treatments on tensile properties in the dual phase steel (SVM) containing: a) yield stress, b) ultimate tensile strength, c) uniform elongation, d) local elongation, d) reduction in thickness and f) hole-expansion ratio (λ). 0.2% flow stress was defined as tempering treatments lead to yield point phenomenon.

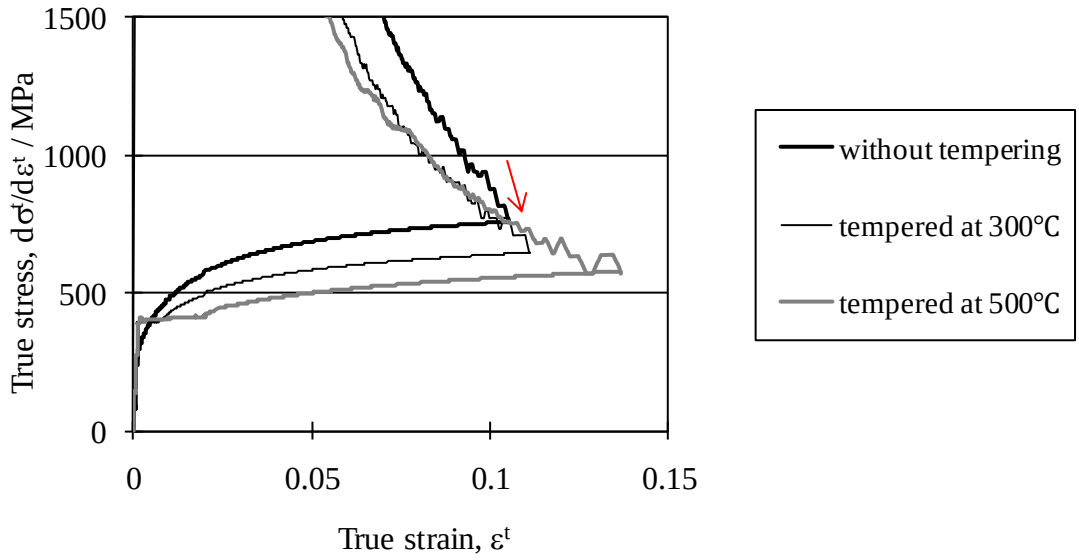

Fig. 5.3 Influence of tempering treatments on the work hardening rate ($d\sigma t/d\varepsilon\tau$) of the dual phase steel (SVM). In the specimen without tempering, rapid reduction of the work hardening rate is observed before onset of necking (marked by arrow). In the other specimens the work hardening rate decreases gradually with strain.

5.3.2 Initial microstructures

Tempering treatments significantly improved the formability, counterbalanced by a reduction of ultimate tensile strength as shown in Fig. 5.2. To clarify the effect of the tempering treatments on the tensile properties, initial microstructures and deformed microstructures were studied in more detail. The initial microstructures before deformation are shown in Fig. 5.4. In the figure, the rolling direction is a lateral direction. All microstructures consisted of a ferrite matrix (F) and martensite particles (M). After tempering the martensite phase looks brighten due to carbide precipitation. There was neither pearlite nor bainite in all specimens. Tempering treatments did not affect the volume fraction, the grain size and the shape of the ferrite and martensite. The volume fraction of martensite was 21% as reported in Table 5.1. The initial microstructures were free from voids and cracks. The shape of the two phases was also different. Ferrite grains nucleated at triple junctions and grain boundaries of austenite during cooling and have the shape of a polygon.

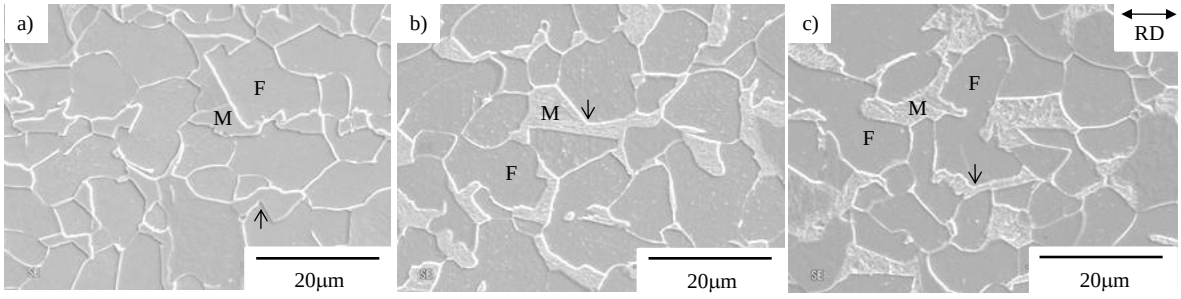

Fig. 5.4 Initial microstructure of the dual phase steel (SVM) showing equiaxed ferrite grains (F) and martensite particles (M) with concave and convex profiles (marked by arrows). The rolling direction (RD) is marked: a) without tempering, b) tempered at 300°C and c) tempered at 500°C.

Table 5.1 Volume fraction and grain size of the dual phase steel (SVM).

Volume fraction		Grain size (μm)		Aspect ratio of martensite particles
Ferrite	Martensite	Ferrite	Martensite	
0.79	0.21	7.3	3.5	2.1

On the other hand, tempering treatments affected the hardness of the martensite and ferrite as shown in Fig. 5.5. The data at 25°C are in the specimen before tempering treatments. A microhardness test shows that tempering mainly softened the martensite, but the martensite was still harder than the ferrite (Fig. 5.5.a). Fig. 5.5b shows that the difference of the hardness between the martensite and ferrite depended on the tempering temperature. It is obvious that softening of the martensite mainly leads to a reduction of ultimate tensile strength of the specimen. According to Pickering (1978), tempering treatments decrease the solution hardening by excess carbon and dislocation hardening induced by martensite transformation due to carbide precipitation and recovery of dislocations. In the present study, cementite precipitation in the ferrite and martensite was observed. Fig. 5.6 shows TEM micrographs of the microstructures of SLM before and after tempering treatments at 300 and 500°C. As shown in Figs. 5.6a-c, the martensite consisted of lathes of martensite and contained huge amounts of dislocations. The ferrite also contains a number of dislocations induced by the martensite transformation. The dislocations in the ferrite contribute to a low yield stress before tempering treatments. After tempering treatments, the martensite and ferrite contain a number of precipitates as shown in Figs. 5.6e and f. TEM observations have revealed that the precipitates in the martensite and ferrite were cementite. Fig. 5.7 exemplifies that cementite particles precipitated in the martensite after a tempering treatment at 300°C. Cementite particles were located within lathes of martensite and at the lath boundaries. Cementite particles in the martensite were smaller than in the ferrite as shown in Figs. 5.6e and f due to a large driving force for cementite precipitation in the martensite, which is related to the carbon content in the martensite. As the martensite phase had more excess carbon, the martensite was softened by tempering more than the ferrite.

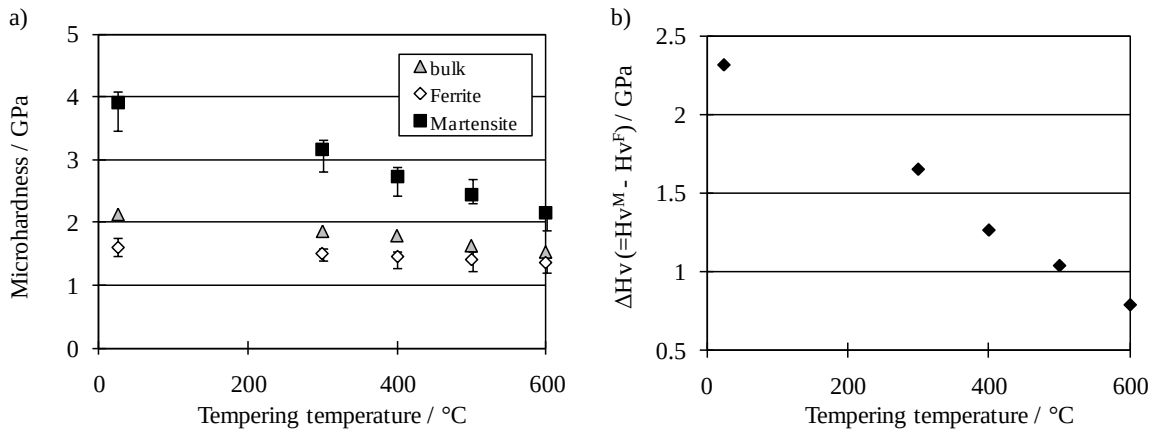

Fig. 5.5 Effect of tempering treatments on microhardness of martensite and ferrite in the dual phase steel (SVM): a) microhardness by the Vickers hardness tests and b) difference of the hardness between the martensite phase and ferrite phase. The load was 10gf to measure the hardness of the martensite and ferrite phase.

In the ferrite grains more dislocations tended to be located near the martensite/ferrite interface compared with the interior of the ferrite grains. Fig. 5.8 shows dislocations in the interior of a ferrite were less and more dislocation were located near the interface as the dislocations were induced by the martensitic transformation. Before tempering, the dislocation density near the martensite/ferrite interface (<500nm) was about $2.4\times10^{14}(1/m^2)$ and that in the interior of the ferrite was about $1.3\times10^{14}(1/m^2)$. A tempering treatment at 500°C slightly reduced the dislocation density in the ferrite, which near the interface was about $9.3\times10^{13}(1/m^2)$ and in the interior of the ferrite was about $6.2\times10^{13}(1/m^2)$. Calcagnotto et al. (2011) also suggested that more dislocations exist near the interface through an EBSD observation. On the other hand, the tempering treatments did not lead to recrystallization of the martensite due to the short holding time and the low temperature. The tempering treatments mainly affected the carbon content and dislocation density in the ferrite and martensite. Similar findings are reported by Morito et al. (1999) and Natori et al. (2005). They suggested that dislocations induced by the martensite transformation are less effective on recrystallization compared with dislocations induced by cold rolling. A cold-rolled low carbon steel is completely recrystallized, but lathes of martensite still exist in a low carbon martensite after a tempering treatment at 1023K for 0.9ks even though the average dislocation density induced by cold rolling is as many as that by the phase transformation.

As tempering treatments do not affect the volume fraction, size and shape of the martensite and ferrite, but can control the hardness of the martensite, and thereby improve the formability, the steels are suitable for a study of effect of the martensite hardness on the void formation behaviour in dual phase steels.

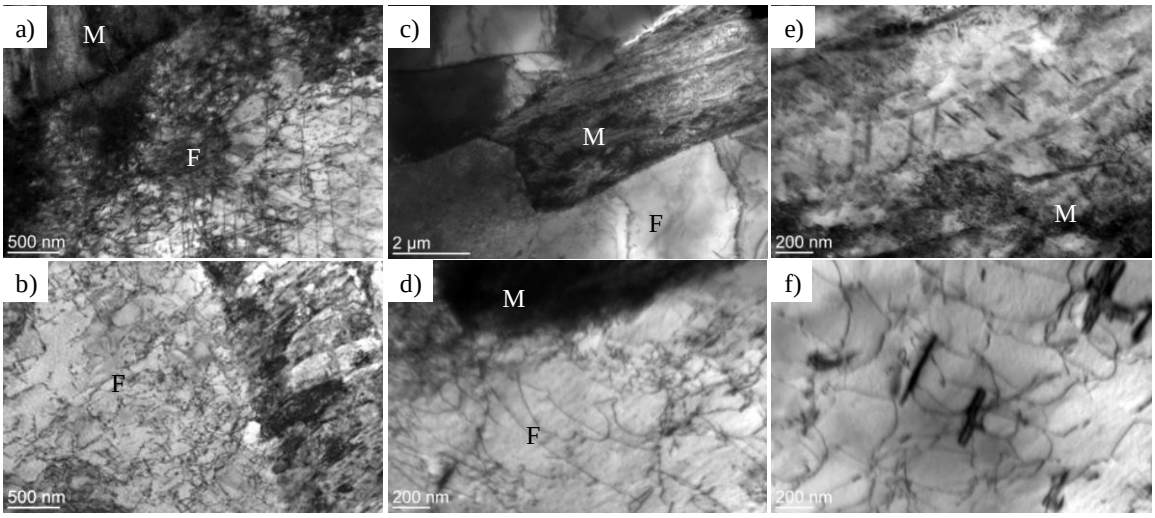

Fig. 5.6 TEM micrographs of SVM showing ferrite (F) and martensite (M) which contain huge amounts of dislocations: a) without tempering, b) tempered at 500°C, c)-f) tempered at 300°C. d), e) and f) are enlargements of c). e) and f) show that the martensite and ferrite contain carbides.

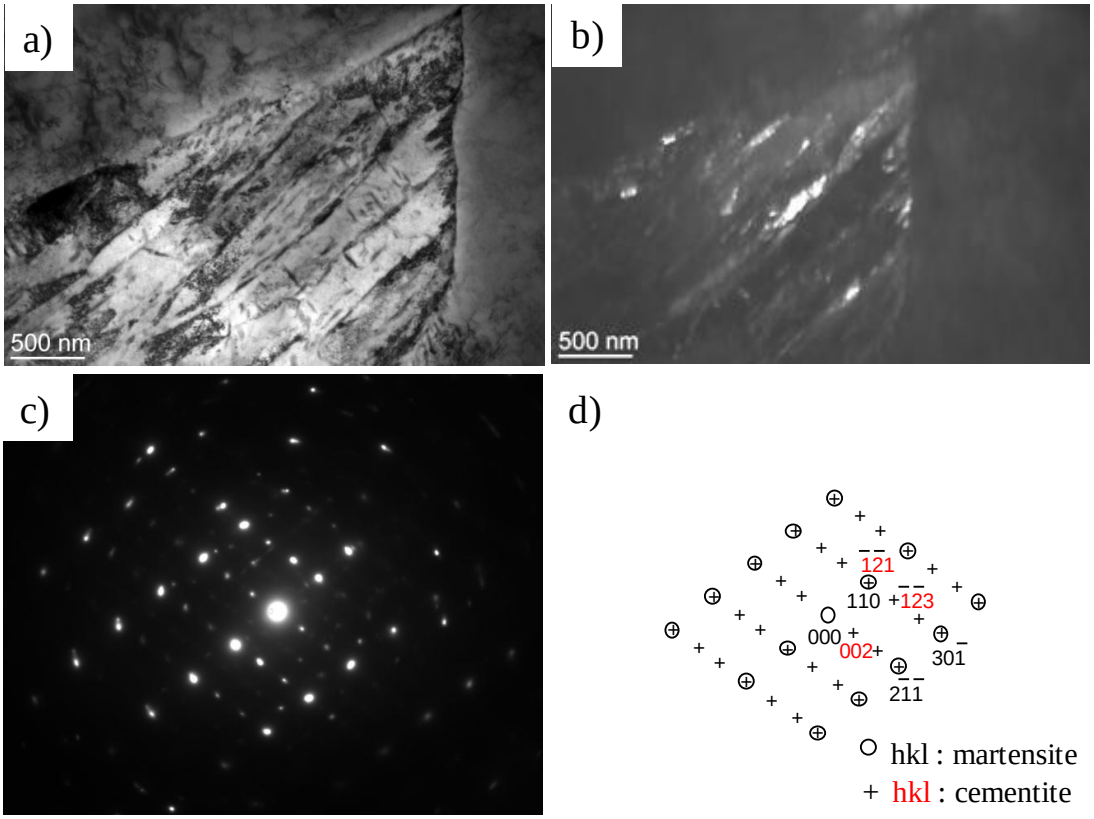

Fig. 5.7 Cementite particles in the martensite tempered at 300°C: a) bright field image of tempered martensite, b) dark field image of tempered martensite, c) diffraction pattern from lath martensite and d) diffraction patterns form lath martensite and cementite ($\left\lfloor 1\bar{1}3 \right\rfloor_M$ //$\left[1.8330 - 0.9999 - 0.0768\right]_C$).

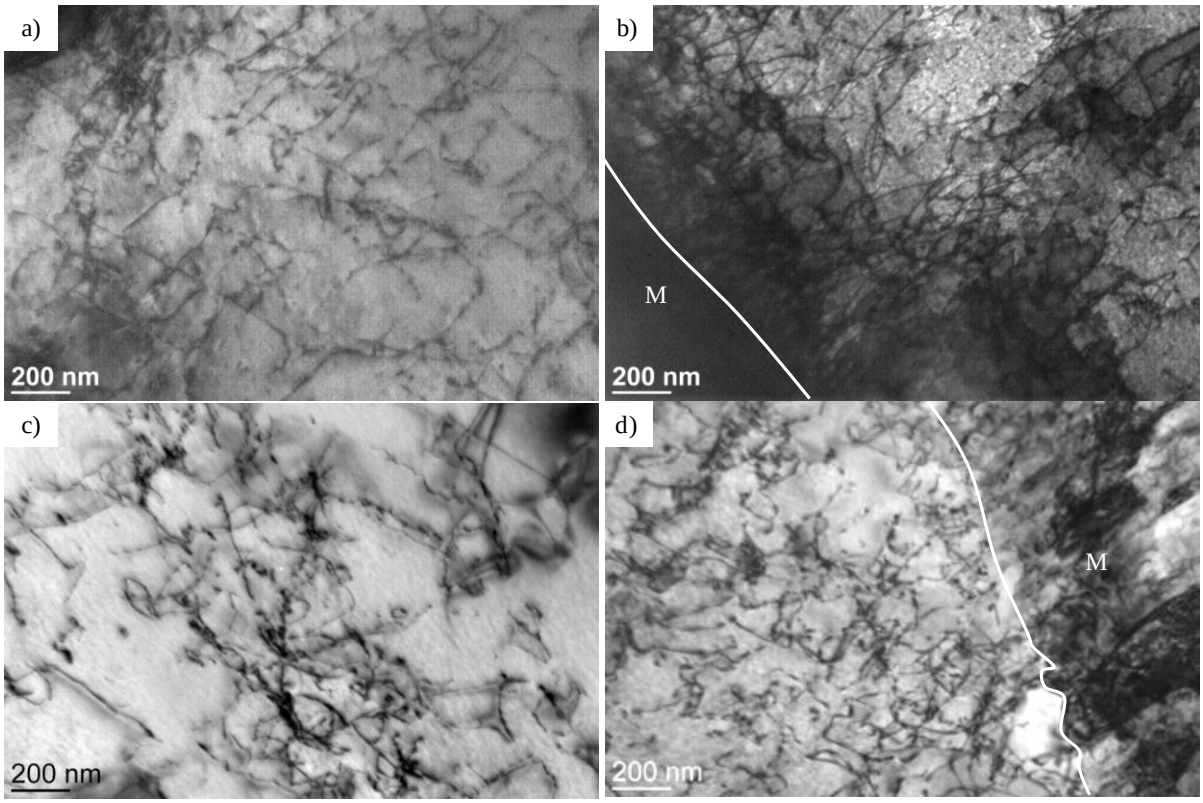

Fig. 5.8 Dislocations in a ferrite grain in SLM: a) dislocations in the interior of the ferrite grain and b) dislocations near the martensite/ferrite interface before tempering treatments, and c) dislocations in the interior of the ferrite grain and d) dislocations near the martensite/ferrite interface after tempering at 500°C.

5.3.3 Deformed microstructure after a tensile test

Figs. 5.9-11 demonstrate deformed specimens and void distribution in the specimens. Voids appear as black spots, light grey particles are the martensite phase and dark grey grains are the ferrite phase. Fig. 5.9 shows that the specimen without tempering treatments was broken after slight necking and the specimen contained a large number of voids. Fig. 5.9d shows that the specimen contained some voids at a strain of ε_t=0.111 and the voids were short. As shown in Fig. 5.9b, voids were more frequent and some voids were elongated in the tensile direction near the fracture (ε_t=0.429). It is obvious that voids formed and grew with strain. In addition, void coalescence was observed (Fig. 5.9b). Tempering treatments made the specimen deform more before fracture. Fig. 5.10a demonstrates that the specimen tempered at 300°C was broken after necking. Voids were also more frequent near the fracture (Fig. 5.10b) than at a strain of ε_t=0.429 (Fig. 5.10c). At a strain of ε_t=0.124, voids at inclusions were observed. After tempering at 500°C, the specimen was necked heavily and broken due to void formation (Fig. 5.11a). Fig. 5.11b shows that many voids existed near the fracture, but the size was smaller than in the specimen without tempering and tempered at 300°C. At a smaller strain (ε_t=0.153), voids existed at inclusions (Fig. 5.11d). At a same strain (ε_t=0.429), the number and size of voids depended on the tempering temperature. In addition, the elongated martensite particles near the fracture show that the martensite particles were deformed plastically.

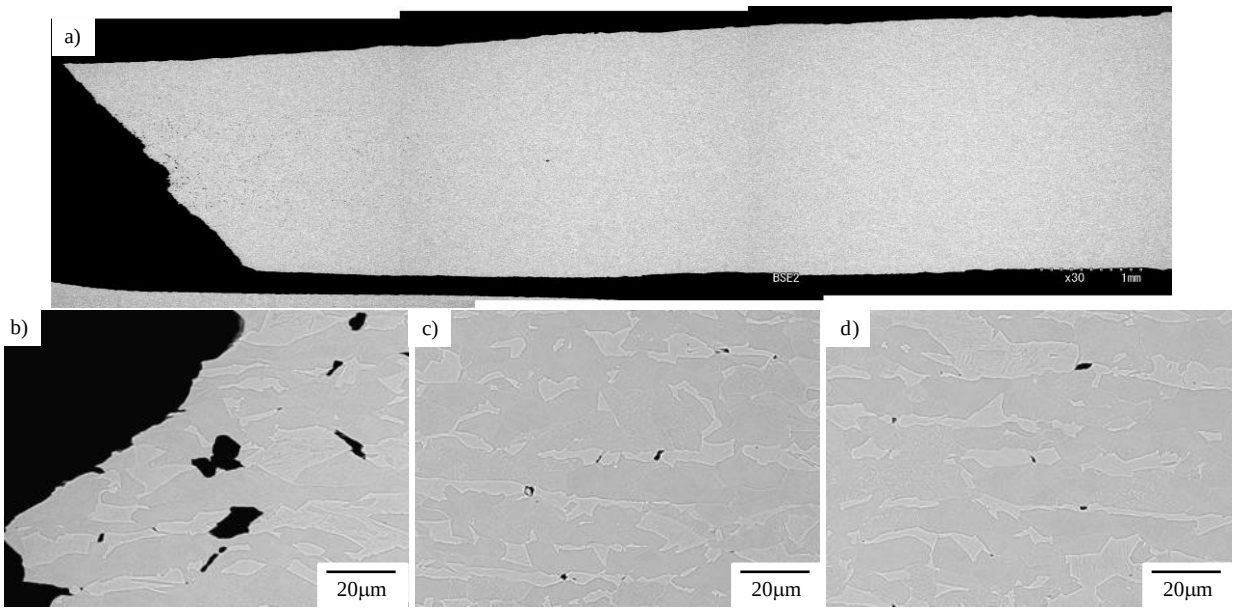

Fig. 5.9 Typical void distribution in the specimen without tempering treatments after a tensile test. a) a deformed specimen, b) ε_t=0.429, c) ε_t=0.250 and d) ε_t=0.111. The strain was calculated based of the thickness reduction of the specimen.

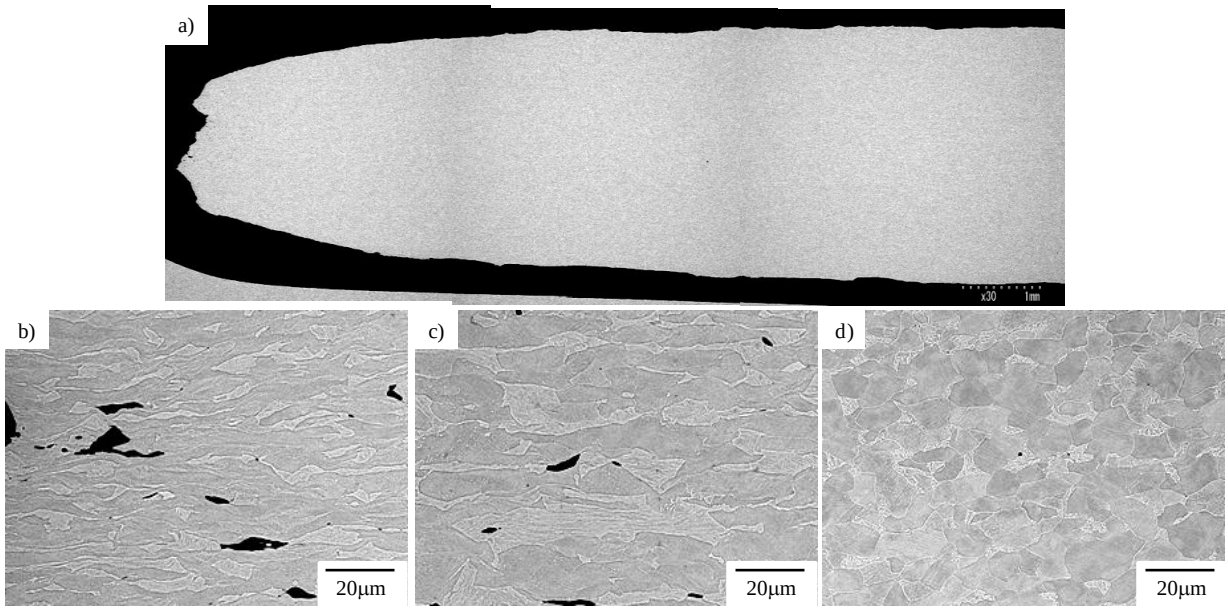

Fig. 5.10 Typical void distribution in the specimen tempered at 300°C after a tensile test. a) a deformed specimen, b) ε_t=1.000, c) ε_t=0.429 and d) ε_t=0.124. The strain was calculated based of the thickness reduction of the specimen.

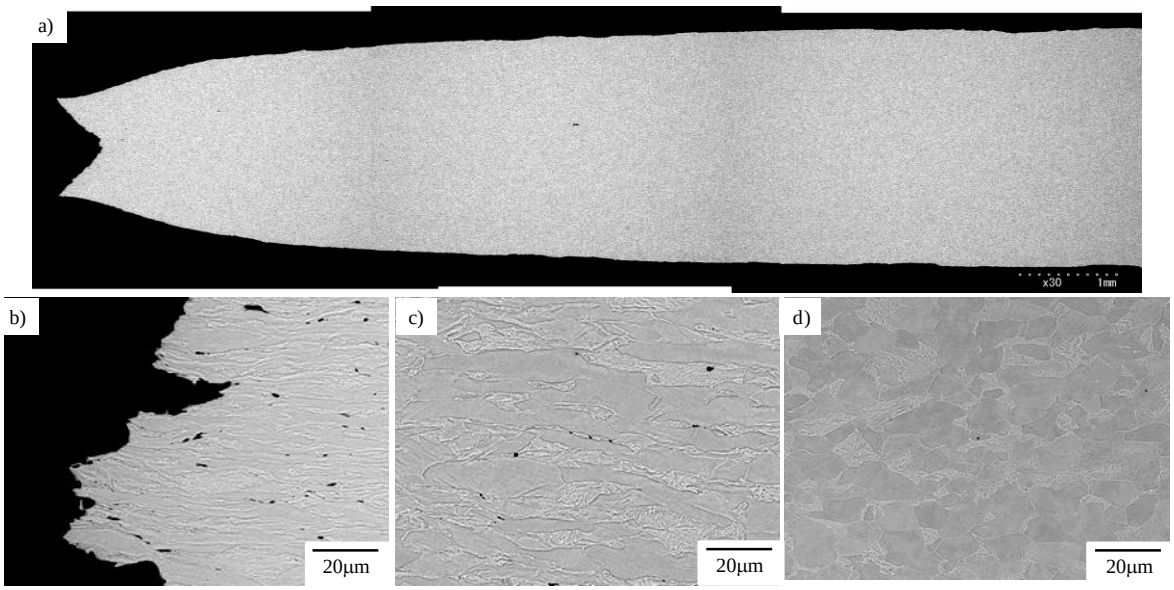

Fig. 5.11 Typical void distribution in the specimen tempered at 500°C after a tensile test. a) a deformed specimen, b) ε_t=2.500, c) ε_t=0.429and d) ε_t=0.153. The strain was calculated based of the thickness reduction of the specimen.

Void formation sites were investigated in all specimens. Fig. 5.12 demonstrates that regardless of tempering treatments, voids formed at the three different sites; (i) in the martensite, (ii) in the ferrite and (iii) at inclusions. However, further straining led to void formation in the martensite and ferrite contained in the tempered specimens. For instance, at a strain of ε_t = 0.250 a void formed at the concave part of the martensite in the specimen tempered at 300°C (Fig. 5.12d). In the specimen tempered at 500°C, voids formed in the heavily deformed martensite particle at ε_t = 0.429. On the other hand, voids at inclusions were observed frequently at a small strain of ε_t = 0.05. In particular, voids started to appear at inclusions in the ferrite earlier than in the martensite.

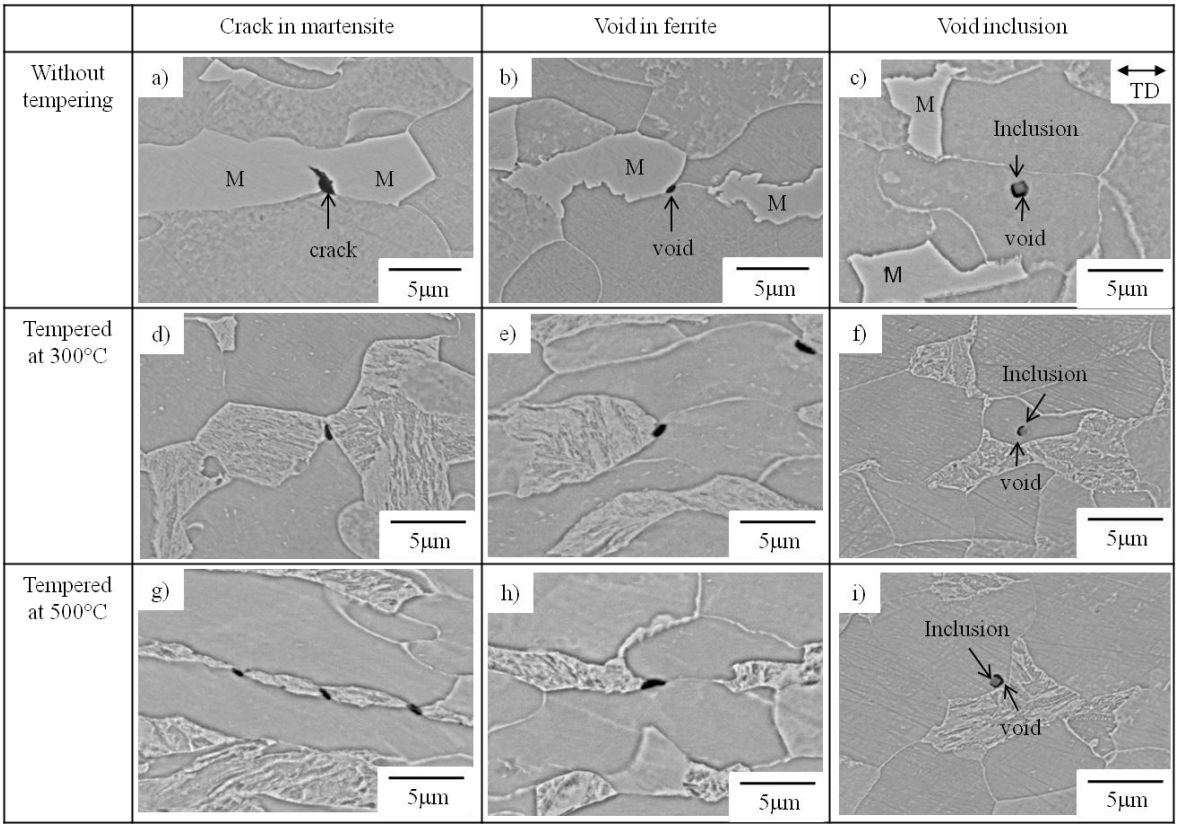

Fig. 5.12 Typical voids in the dual phase steel (SVM) deformed in tension: voids a) in the martensite, b) in ferrite and c) at an inclusion in the specimen without tempering (ε_t = 0.111), voids d) in the martensite (ε_t = 0.250), e) in ferrite (ε_t = 0.250), and f) at an inclusion (ε_t = 0.124) in the specimen tempered at 300°C martensite (ε_t = 0.429), voids g) in the martensite (ε_t = 0.429), h) in ferrite (ε_t = 0.429) and i) at an inclusion(ε_t = 0.143) in the specimen tempered at 500°C.

Fracture surfaces also depended on the tempering temperature. Fig. 5.13 shows the fracture surfaces of the deformed specimens without tempering, tempered at 300 and 500°C. The fracture surfaces consisted of two types of dimples. The first one is an elongated dimple, which appears black due to depth. The second one is a shallow dimple. It is found that the elongated dimples were related to voids in the martensite. Fig. 5.14 exemplifies that deep dimples are related to voids in the martensite and at the ferrite/martensite interface because these voids grow with strain in the tensile direction as shown in Fig. 4.4 and 4.5. On the other hand, the shallow dimples were related to secondary void formation and internal necking. The fracture surface in the tempered specimen contained more elongated dimples and shallow dimples as the fracture strain of the tempered specimens is much larger than the specimen without tempering. Plastic deformation made the martensite particles and ferrite grains thin and voids formed in the heavily deformed particles/grains tiny.

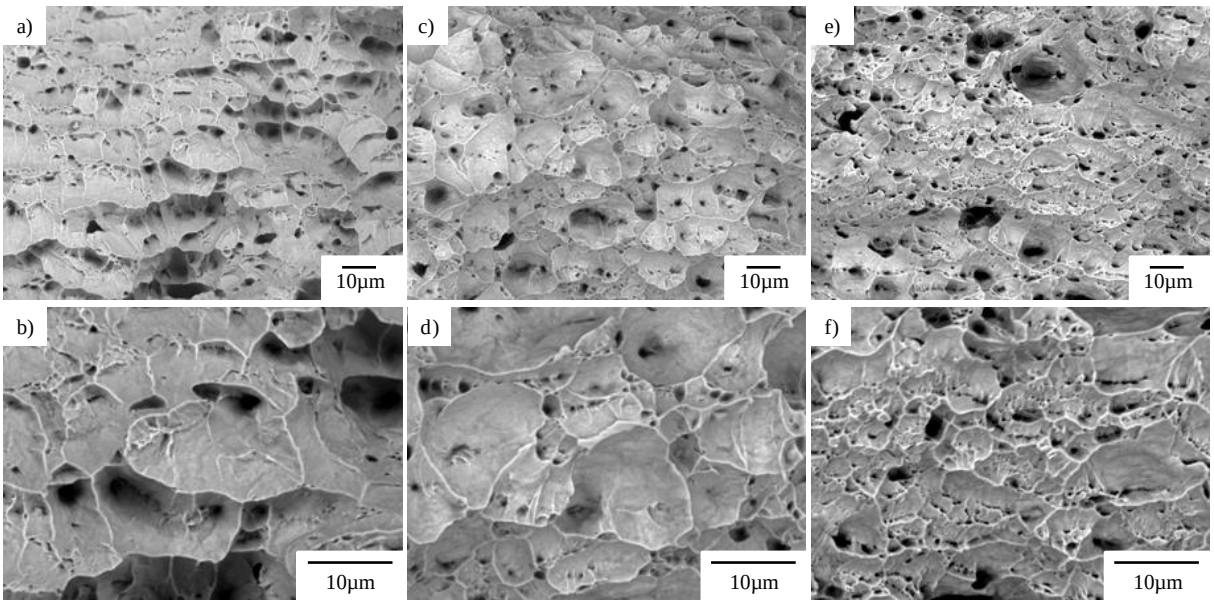

Fig. 5.13 Fracture surface of SVM after tensile tests: a) and b) without tempering, c) and d) tempered at 300°C, e) and f) tempered at 500°C. Lower row is enlargement of upper row.

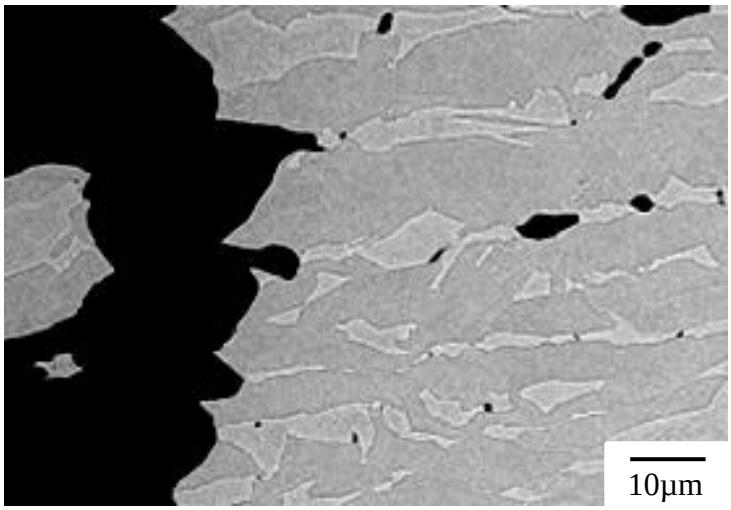

Fig. 5.14 Deformed microstructure of SVM without tempering after the tensile test. Deep dimples in Fig. 5.13 are related to voids in the martensite and at the ferrite/martensite interfaces.

5.3.4 Void formation behaviour during in-situ testing

Tempering treatments significantly affected void formation in the dual phase steel. Fig. 5.15 demonstrates the void formation behaviour induced by cracks in the martensite in the specimen tempered at 500°C. Deformation to a strain of 0.428 and 0.844 does not generate cracks and voids in the martensite and ferrite (Figs. 5.15d-i), but the martensite particle was stretched heavily. After deformation to a strain of 1.104, voids formed in the martensite particle due to cracking of the particle. It is obvious that voids formed in the martensite after the martensite particle was deformed heavily compared with voids in the specimen without tempering (Figs. 4.4 and 5). This means that the tempering treatment increases the critical strain for crack formation in the martensite and thereby retards void formation in the tempered dual phase steel. This is discussed in Section 5.4.3 in more detail.

To evaluate the effect of the tempering treatments on void formation during in-situ tensile tests, (i) number density, (ii) maximum length and (iii) area fraction of voids were measured. As an example, Fig. 5.16 shows

that tempering treatments affect void formation behaviour in SVM during in-situ observation. Here, the data in the specimen without tempering, tempered at 300 and 500°C were picked up as the data clearly showed the effect of tempering treatments. Here voids at inclusions are neglected as the void formation behaviour did not depend on tempering treatments. In the specimen without tempering, voids form predominantly in the martensite and already at a strain of ε_t=0.05 whereas few voids form in the ferrite at a strain of 0.1. This agrees with previous observations (e.g. Avramovic et al. 2009; Avramovic et al. 2010, Calcagnotto et al. 2011) showing that cracks can form in martensite before necking of the specimen while voids appear in ferrite after necking. The void number densities increase with strain before and after tempering treatments. Smaller voids were more frequent at all strains and deformation increases the number of larger voids as shown in Fig. 5.17. This indicates that voids form when local strain and stress overcome criteria for void formation and grow with strain. This continuous void formation behaviour was observed in previous works. Landron et al. (2010) observed void formation behaviour in a commercial dual phase steel by X-ray tomography. Avramovic et al. (2010) estimated the number density and area fraction of voids as a function of a strain after tensile tests. The criteria for crack formation in the martensite particles are discussed in Section 5.5.3 in more detail. Once voids formed in the ferrite and martensite, the voids grew steadily with strain until the specimen was broken. Figs. 5.16c and d show the influence of tempering treatments on void length in the tensile direction. Voids in both the martensite and ferrite grew with strain, but the maximum size of voids in the martensite was larger than in the ferrite and voids in the martensite grew more rapidly than in the ferrite. Figs. 5.16e and f also show that tempering treatments decrease the area fraction of voids due to the number density and size of voids and thereby improve the formability. Obviously, voids in the martensite dominate the number density and area fraction.

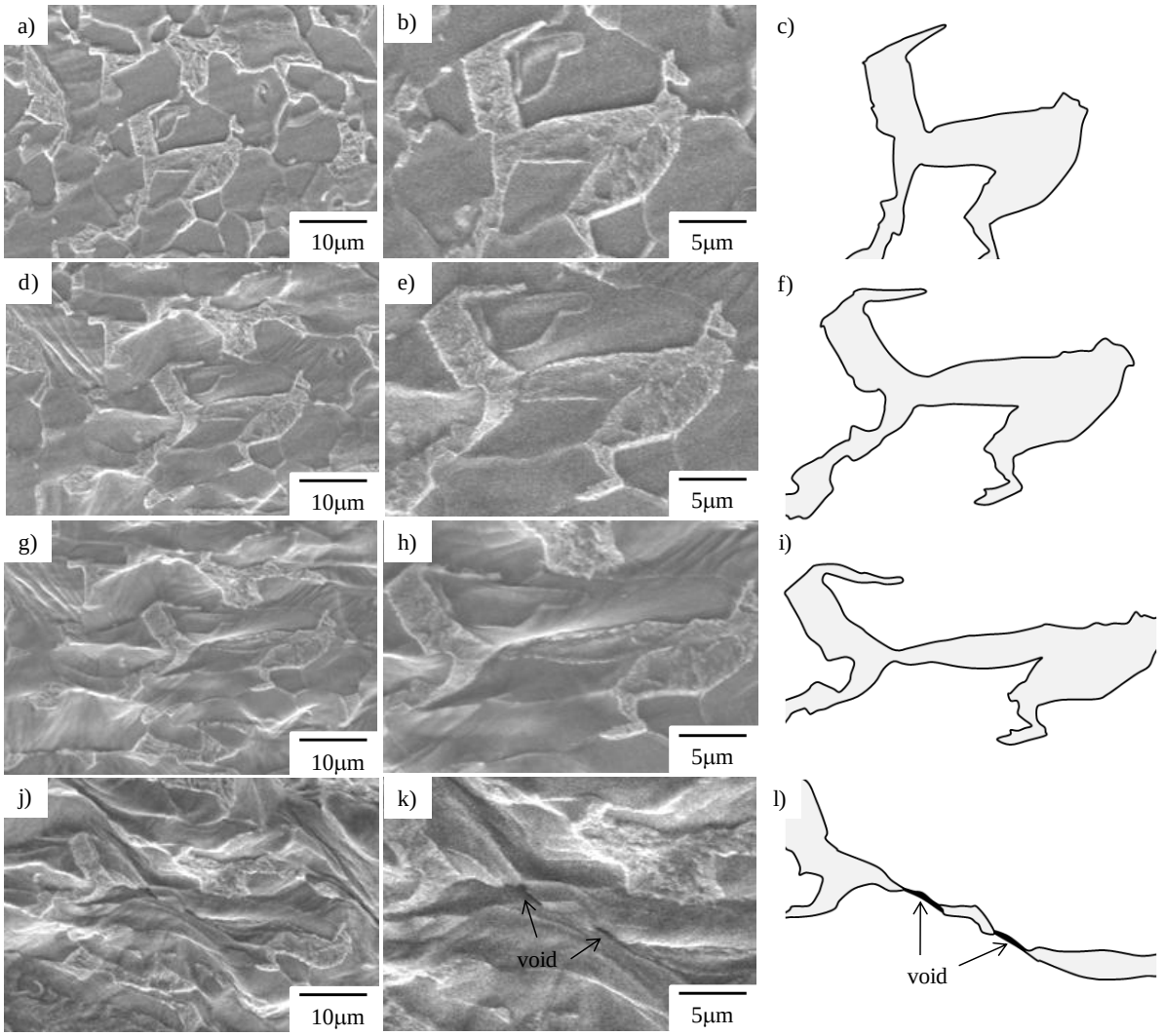

Fig. 5.15 In-situ observations of void formation in SVM tempered at 500°C during a tensile test: a) and b) initial microstructure without cracks or voids, d) and e) crack initiation in martensite (ε_h= 0.428) g) and h) crack propagation in martensite (ε_h= 0.844), j) and k) void growth and crack propagation (ε_h = 1.104), c), f), i) and l) sketches from b), e), h) and k) of the martensite particles and voids.

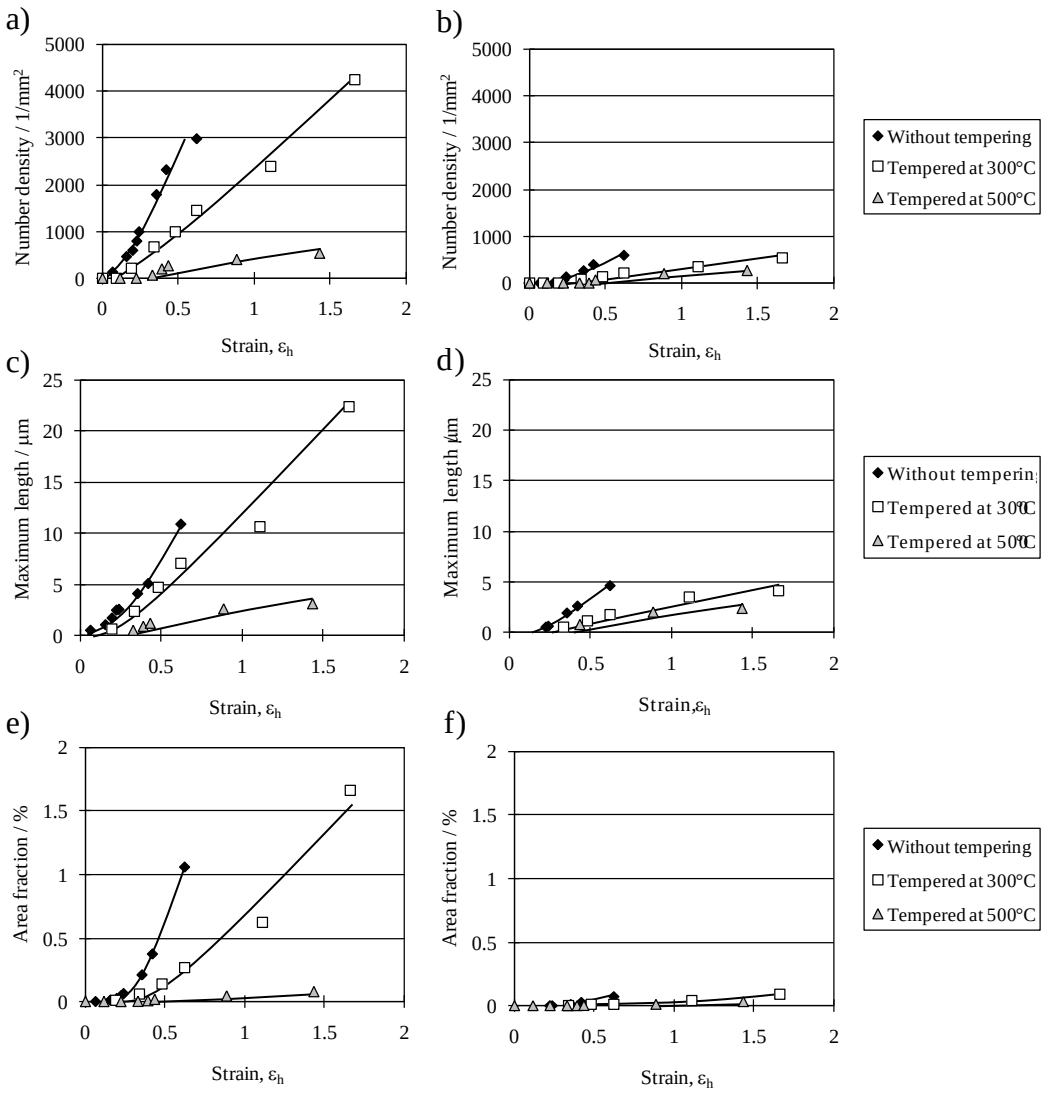

Fig. 5.16 Influence of tempering treatments on void formation behaviour in the dual phase steel during in-situ tensile tests: number density of voids a) in the martensite and b) in the ferrite, maximum length of voids c) in the martensite and d) in the ferrite, area fraction of voids e) in the martensite and f) in the ferrite.

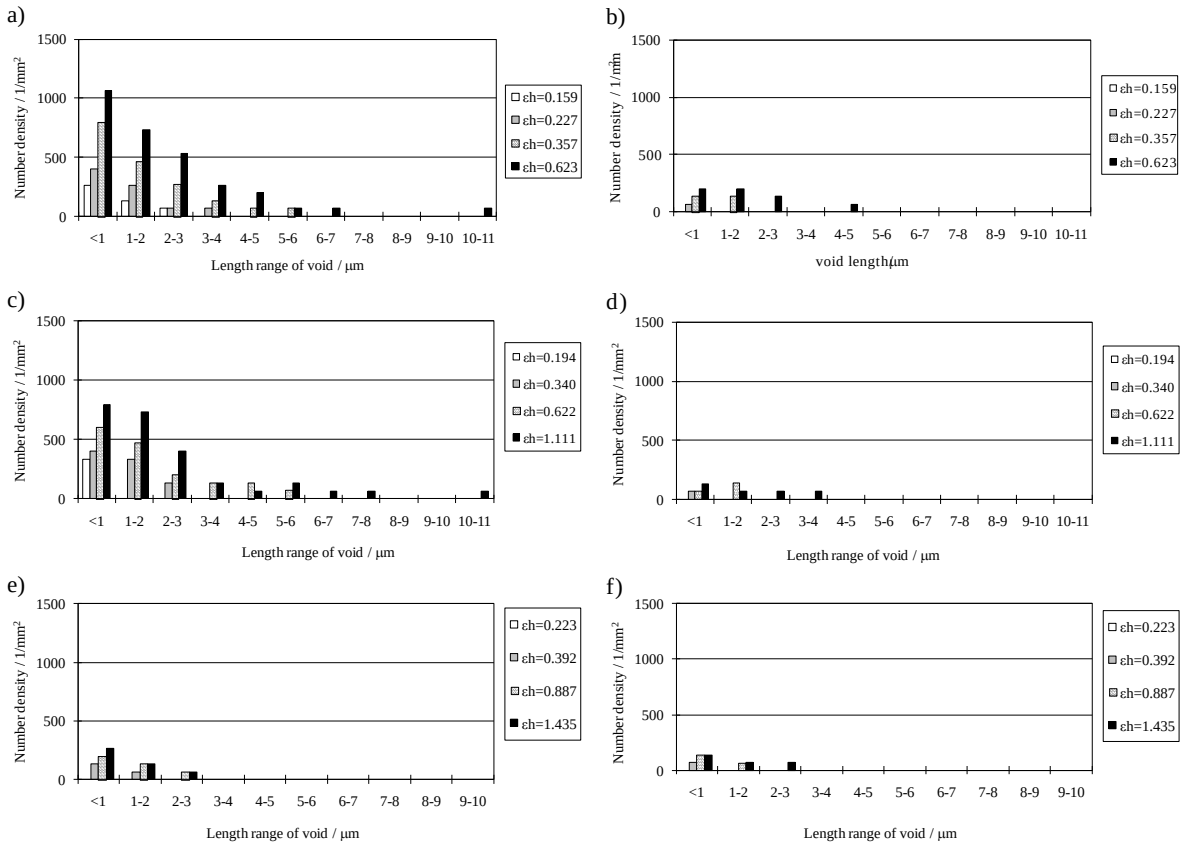

Fig. 5.17 Size distribution of voids formed in the dual phase steel during an in-situ tensile tests: a) in the martensite without tempering, b) in the ferrite without tempering, c) in the martensite after tempering at 300°C, d) in the ferrite after tempering at 300°C, e) in the martensite after tempering at 500°C, f) in the ferrite after tempering at 500°C.

5.4 Discussion

In-situ tensile tests have revealed that, regardless of tempering treatments, most voids formed in the martensite due to i) plastic deformation of martensite particles, ii) crack formation in the particles, iii) crack propagation in the particles and iv) separation of the particle fragments. Voids formed at the ferrite/martensite interface are minor. Regardless of tempering treatments, same mechanisms operate void formation in the dual phase steel. The tests have also shown that softening of the martensite through tempering treatments retard void (crack) formation in the dual phase steel and thereby improve the formability. As plastic deformation of the martensite particles proceeded void formation in the martensite, plastic deformation of the martensite has an important role on void formation in the martensite. In this section effect of softening of the martensite on deformation behaviour of the martensite and ferrite, and then a criteria for void formation in the martensite are discussed.

5.4.1 Strain partitioning between martensite and ferrite

Interaction between a matrix and reinforcements in composite structures affects deformation behaviour of the matrix and reinforcements. In the present study deformation behaviour of each phase and the effect of tempering treatments were investigated during in-situ tensile tests. Specifically, strains in the martensite phase and ferrite phase were estimated based on the length change of each particle/grain in and the influence of tempering treatments on the strains were discussed. Fig. 5.18 shows a distribution of average strain of martensite particles and ferrite grains in the specimen without tempering at a strain of ε_h=0.422. The strain in the martensite phase is much smaller than the ferrite, but martensite particles were deformed plastically.

Martensite particles and ferrite grains have different strains even though the strain given is the same. It appears that the wide distribution is related to the shape and distribution of the martensite particles as the ferrite matrix was constrained by martensite particles in the dual phase steels. For example, strains in the ferrite grains surrounded by the particles were relatively small and isolated ferrite grains were deformed more. The equiaxed martensite particles were deformed less and the particles elongated in the tensile direction were deformed more. The effect of martensite shape on strain in the martensite is discussed in Section 5.4.4. The strains were averaged at each strain.

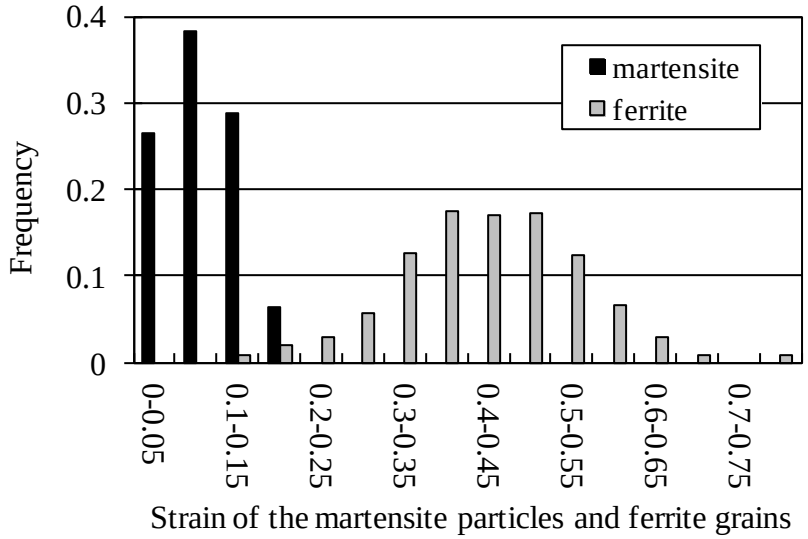

Fig. 5.18 Strain distribution in martensite particles and ferrite grains in the specimen without tempering at a strain of ε_h=0.422. Strains in the martensite particles and ferrite grains were measured as shown in Table 3.1c and d and Fig. 3.8.

Fig. 5.19 shows that strains in each phase increases with strain and tempering treatments affected strains in the martensite and ferrite. Softening of the martensite through tempering treatments assisted the martensite to deform more and decreased the strain in the ferrite due to strain compatibility. It appears that softening of the martensite led to early yielding and further straining of the martensite. Strain partitioning between the martensite and ferrite was normalized as a function of the hardness difference between the martensite and ferrite. For calculation, strains in the martensite and ferrite at each applied strain were divided by the applied strain and normalized. Fig. 5.20 shows that the strain partitioning between the martensite and ferrite depends on the hardness difference between the martensite and ferrite. In previous works the strain partitioning between the martensite and ferrite in dual phase steels is related to the hardness of the martensite (e.g. Shen et al. 1986; Su and Gurland 1987). This might affect void formation and the formability. However, an increase of the strain in the martensite by softening of the martensite overcomes criteria at a smaller strain and thereby accelerates void formation in the martensite. It contradicts to the result that tempering treatments retard void formation in the martensite. Then, local strains at the concave part of the martensite, where cracks/voids formed, were investigated in the following section.

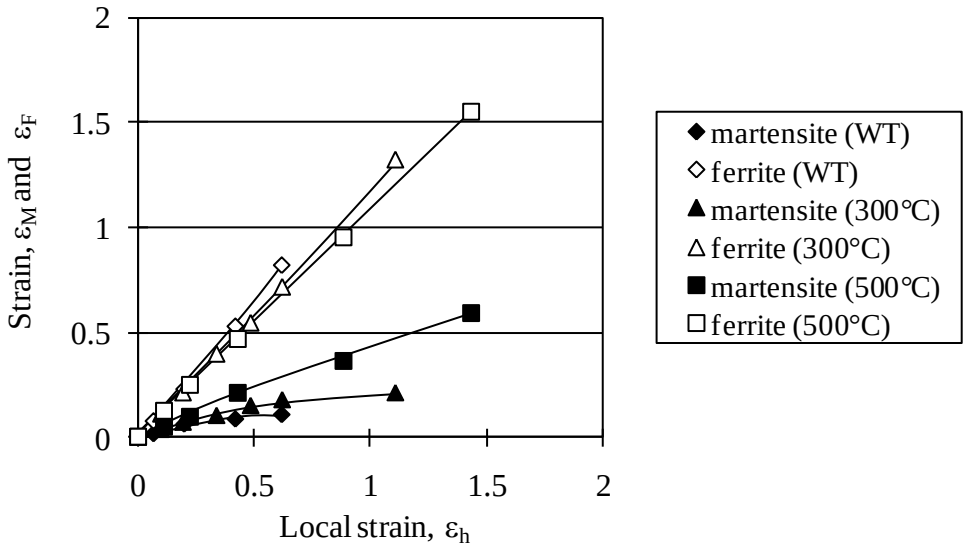

Fig. 5.19 Strain partitioning between the martensite and ferrite during in-situ tensile tests. Softening of the martensite through tempering treatments increases strain in the martensite, but deceases strain in the ferrite due to strain compatibility.

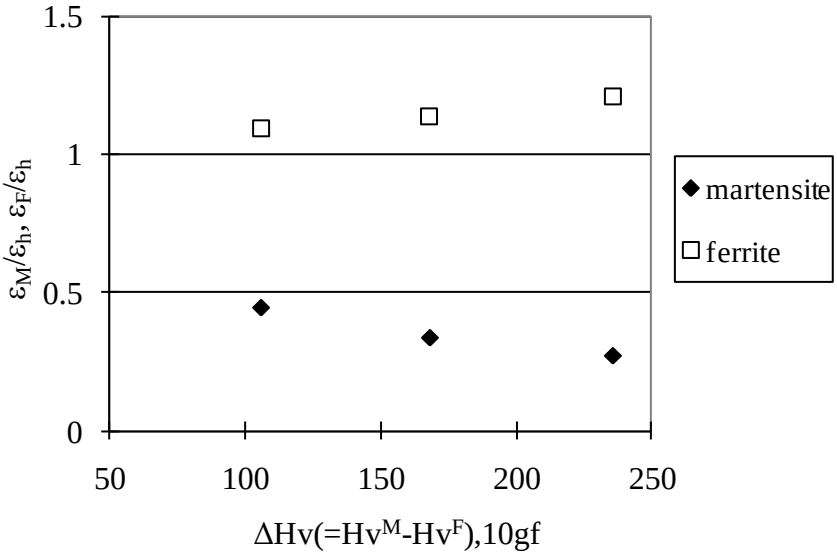

Fig. 5.20 Influence of hardness difference between the martensite and ferrite on strain partitioning between the martensite and ferrite. Hv^M: microhardness of the martensite, Hv^F: microhardness of the ferrite.

5.4.2 Strain localization

Plastic deformation of the martensite has an important role in void formation in the martensite as plastic deformation occurs at the concave part of the martensite in advance of crack formation. Strain distribution around martensite particles was estimated by EBSD measurements after tensile tests. To estimate the strain distribution before void formation, the specimen was deformed to a strain of 0.05 in tension. Fig. 5.21 shows the strain distribution in the dual phase steels before and after tensile tests. The contour maps show deviation of Euler angles at each point from the average value in each ferrite grain. The martensite was black and neglected.

The yellow region shows that the deviation is small, the deviation in the blue region is larger and the deviation in the green region is over 7°. As accumulated dislocations lead to a rotation of the crystal lattice, the large deviation means that a large number of dislocations have accumulated. Figs. 5.21a-c show strain distributions in the SVM before deformation Figs. 5.21d-f show strain distributions in the deformed specimens. Even though dislocations induced by the martensitic transformation existed in the ferrite near the martensite/ferrite interface, strains were distributed in the undeformed specimens more homogeneously than in the deformed specimens. To estimate dislocation distribution around martensite particles, local misorientation changes at the martensite/ferrite interfaces were measured in more detail. Figs. 5.22 and 23 show local strain distributions at the concave part and the tip of a martensite particle in the specimen without tempering before deformation. Figs. 5.22a and 23a show orientation maps around a martensite particle and Figs. 5.22b and 23b show band contrast maps (image quality maps) in the same area. In the band contrast map martensite particles appear black due to a large dislocation density. Figs. 5.22c and 23c show accumulated misorientation profiles at the concave interface (C-M/F) and the flat interface (F-M/F) between the martensite and ferrite, at the tip of the martensite (T-M/F) and the ferrite/ferrite grain boundary (F/F), which were measured along the lines in Figs. 21a and 22a. Figs. 5.22c and 23c show that the misorientation changed more at all martensite/ferrite interfaces than at the ferrite/ferrite grain boundaries. The misorientation changes were about 1-2.2° at 1μm away from the interface. On the other hand, the changes were less than 0.5° at 1μm away from the boundary. This is because dislocations in the ferrite were induced by the martensitic transformation during heat treatments. Tempering treatments tended to reduce the misorientation change at the martensite/ferrite interface as well as TEM observations (Fig. 5.8). After tensile deformation to a strain of 0.05, strain localized at the concave part and near the tip of the martensite particles as shown in Figs. 5.21d-f. It is obvious that the strain localization is related to void formation as voids also form at the concave part and the tip of the martensite particles. This also shows that tempering treatments retarded strain localization at the concave part and near the tip as the area fraction of the green region was reduced in the tempered specimens. In addition, green regions were often aligned across some ferrite grains and martensite particles in the 30-60° direction from the tensile direction. The strain distribution was observed in more detail. Figs. 5.24 and 25 exemplify typical misorientation change at the interface between the martensite and ferrite in the marked area in Fig. 21d. In the deformed specimen the misorientation increased at the martensite/ferrite interface. In particular, the change at the concave interface (8°/1μm) was larger than the flat interface of the martensite particle (2.7°/1μm). On the other hand, the misorientation changed less at the ferrite/ferrite grain boundary (<1°/1μm). As dislocations lead to crystal orientation changes, it is obvious that a large number of dislocations accumulated at the concave interface and the built-up stress might lead to local plastic deformation at the concave part of the martensite. As shown in Figs. 4.4-8 and 5.14, slip band formation around the concave part of the martensite particles and necking of the martensite particles also mean that deformation localized at the concave part of the martensite. It is apparent that the strain localization at the concave part of the martensite accelerated void formation in the martensite. This implies that the shape of the martensite particles is one of the most important factors to retard void formation in dual phase steels. In addition, the distribution of the martensite particles is also important because the heavily deformed areas (green regions) aligned across some ferrite grains and martensite particles.

Strain also localized near the tip of the particles as shown Fig. 5.25. Here accumulated strain was measured in the tensile direction. Fig. 5.25c shows that strain localized at the tip of the martensite particles elongated in the tensile direction. The strain localized strongly at the interface (T-M/F1) and the accumulated misorientation was 8°/1μm. On the other hand, the misorientation at another side (T-M/F2) was relatively small (2.3°/1μm) as the distribution of the particles is also important for strain localization. Specifically, deformation localized areas were often connected a tip of a martensite particle to another tip of a martensite or a concave part of a martensite particle. Therefore, whereas the shape of the martensite particle is an important parameter to control void formation in dual phase steels, the distribution of martensite particles is also important. .

A FEM analysis has also shown that deformation localizes at the martensite/ferrite interface, which faces perpendicular to the tensile direction, in a dual phase steel as hard martensite particles constraint other ferrite grains (e.g. Kadkhodapour et al. 2011).

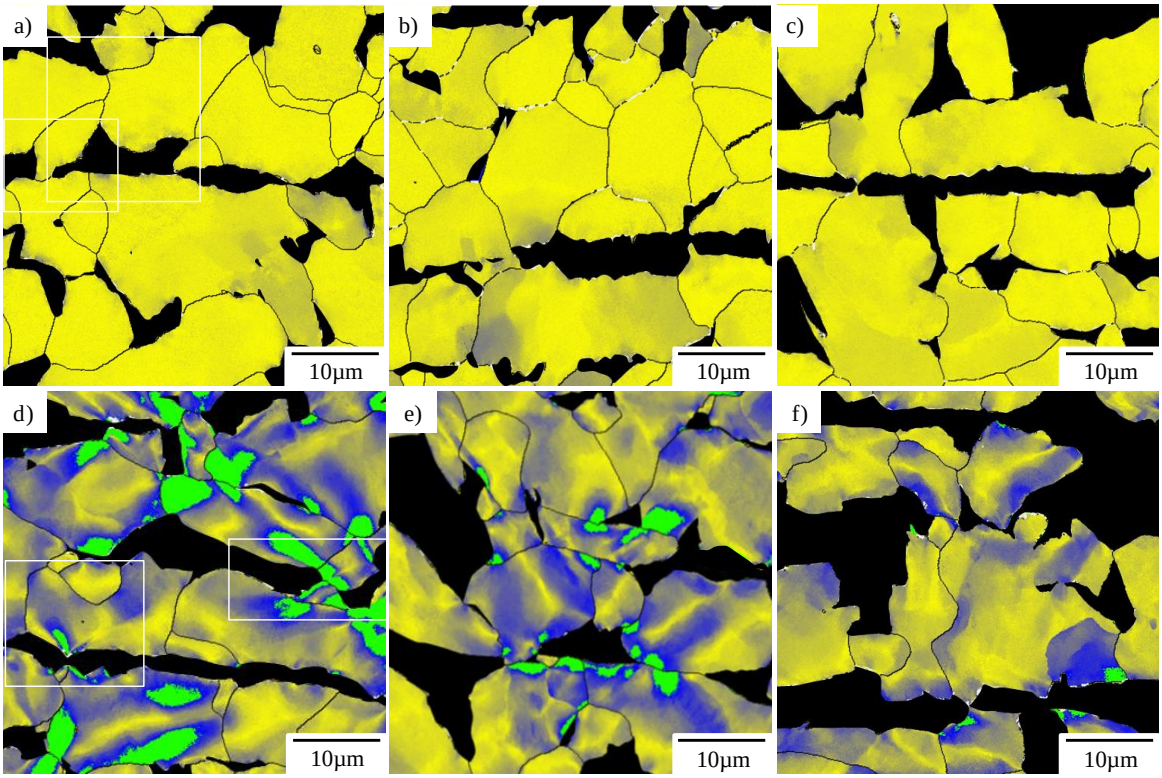

Fig. 5.21 Strain distribution, which is represented by the deviation of Euler angle at each point from the average value, in the ferrite at a strain of ε_t=0.05: initial microstructures a) without tempering, b) tempered at 300 and c) 500°C, and deformed microstructure d) without tempering treatments, e) tempered at 300 and 500°C. In the contour maps black regions are martensite and yellow, blue and green regions are ferrite. In the yellow regions the deviation was 0°, in the blue region the deviation is larger and in the green regions the deviation is over 7°.

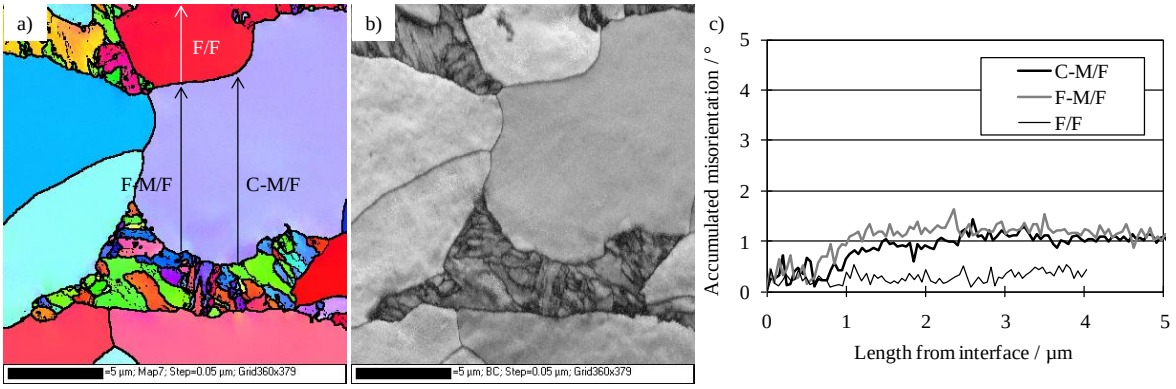

Fig. 5.22 EBSD maps of the SVM without tempering treatments before deformation: a) orientation map and b) band contrast map of a martensite particle containing concave parts and ferrite grains, and c) accumulated misorientation profiles from the concave interface between the ferrite and martensite (C-M/F), the flat interface between the ferrite and martensite (F- M/F) and the ferrite/ferrite grain boundary (F/F) to another interface. In the orientation, the colours represent the crystallographic direction. In the band contrast map, dark contrast is related to the martensite due to the large dislocation density. The tensile direction is horizontal. The step size is 50nm.

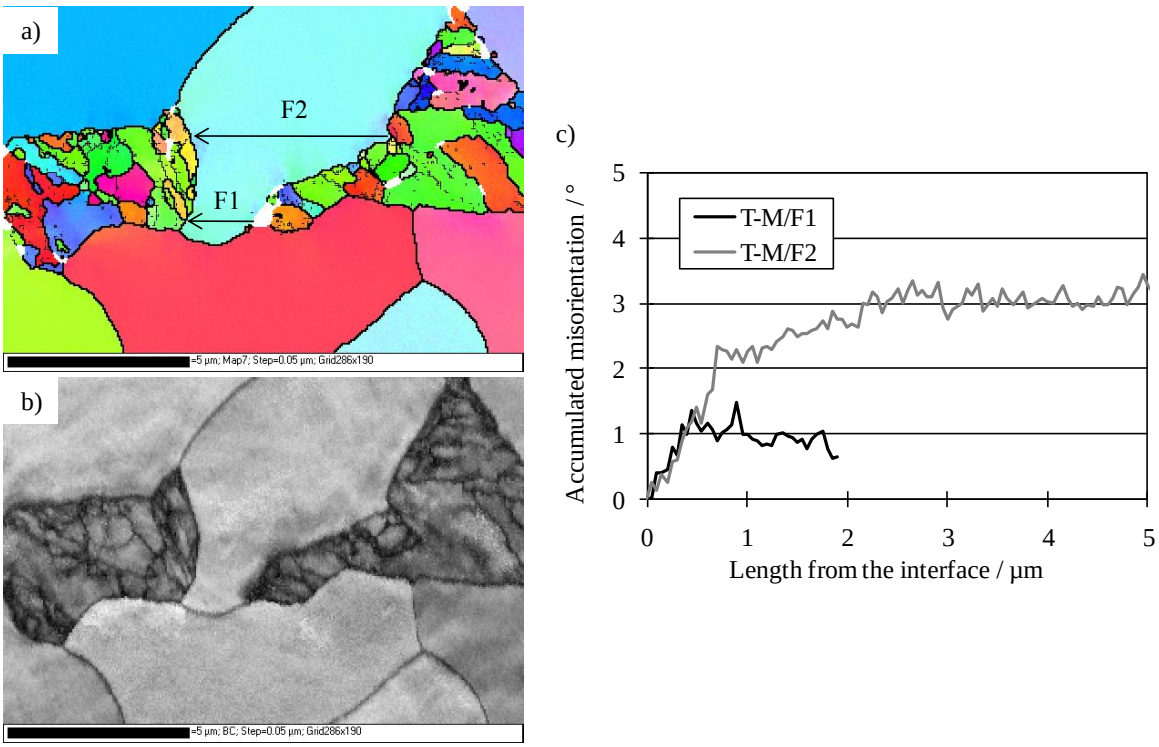

Fig. 5.23 EBSD maps of the SVM without tempering treatments before deformation: a) orientation map and b) band contrast map near the tip of a martensite particle, and c) accumulated misorientation profiles in a ferrite grain 1(F1) and 2 (F2) from the left side to the right side. The tensile direction is horizontal. The step size is 50nm.

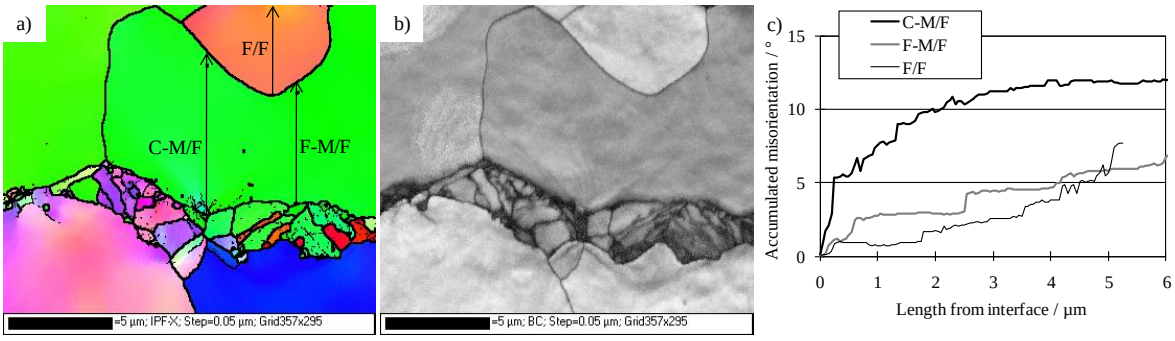

Fig. 5.24 EBSD maps of the SVM without tempering treatments after deformation to a strain of 0.05: a) orientation map and b) band contrast map of a martensite particle containing concave parts and ferrite grains, and c) accumulated misorientation profiles from the concave interface between the ferrite and martensite (C-M/F), the flat interface between the ferrite and martensite (F- M/F) and the ferrite/ferrite grain boundary (F/F) to another interface. In the orientation, the colours represent the crystallographic direction. In the band contrast map, dark contrast is related to the martensite due to the large dislocation density. The tensile direction is horizontal. The step size is 50nm.

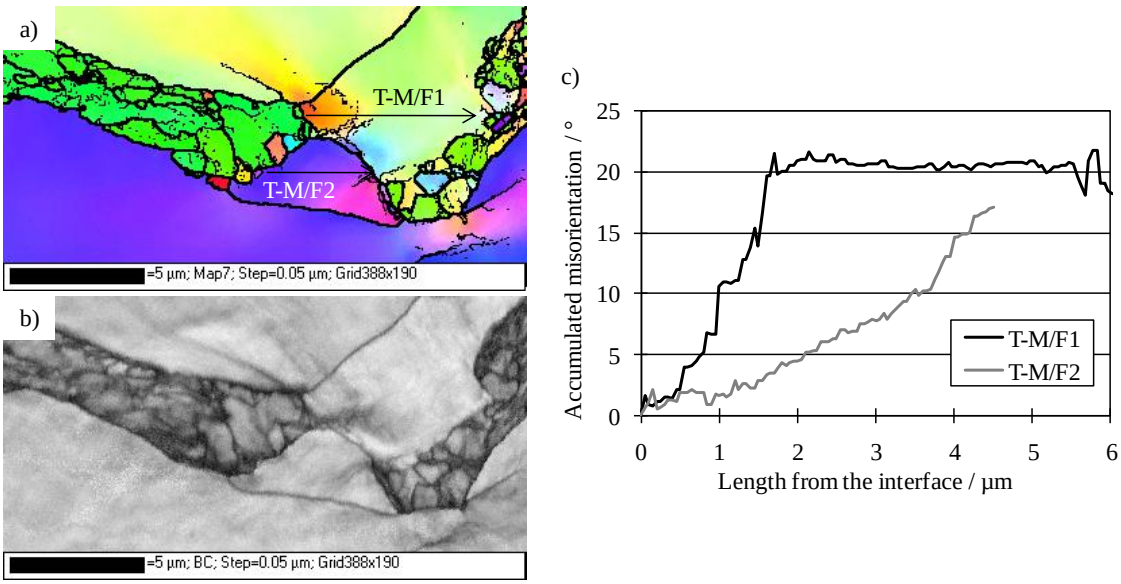

Fig. 5.25 EBSD maps of the SVM without tempering treatments after deformation to a strain of 0.05: a) orientation map and b) band contrast map near the tip of a martensite particle, and c) accumulated misorientation profiles in a ferrite grain 1(F1) and 2 (F2) from the left side to the right side. The tensile direction is horizontal. The step size is 50nm.

Tempering treatments decreased the accumulated misorientation related to strain localization at the interface. Fig. 5.26 and 27 show accumulated misorientation in the SVM tempered at 500°C after tensile testing. In the tempered specimen strain localized at the martensite/ferrite interface, but the maximum misorientation was relatively small. For example, the accumulated misorientation at the concave part of the martensite was 2.7°/1µm in Fig. 5.25c and the accumulated misorientation at the tip of the martensite was 3.5°/1µm in Fig. 5.27c. The effect of tempering treatments on the accumulated misorientation is shown in Fig. 5.28. Fig. 5.28a shows that misorientation at the martensite/ferrite interface before deformation depends on the tempering temperature, but the effect is very small. On the other hand, the misorientation after tensile tests strongly depended on the temperature. In the specimen without tempering the misorientation at the concave interface between the martensite and ferrite was about 8.5°/1µm and in the specimen tempered at 500°C the misorientation was about 2°/1µm. As the accumulated misorientation is related to dislocations accumulated at the interface, a reduction of the misorientation through tempering treatments retards void formation at the concave part and the tip of the martensite. It appears that strain partitioning between the martensite and ferrite attributes to strain localization. When the martensite is hard, strain in the martensite becomes small but strain in the ferrite becomes large. The large strain in the ferrite contributes to a large strain in ferrite grains between two martensite particles. The hard martensite allows locally the stress to overcome the yield stress of the martensite due to stress concentration at the concave part of the martensite.

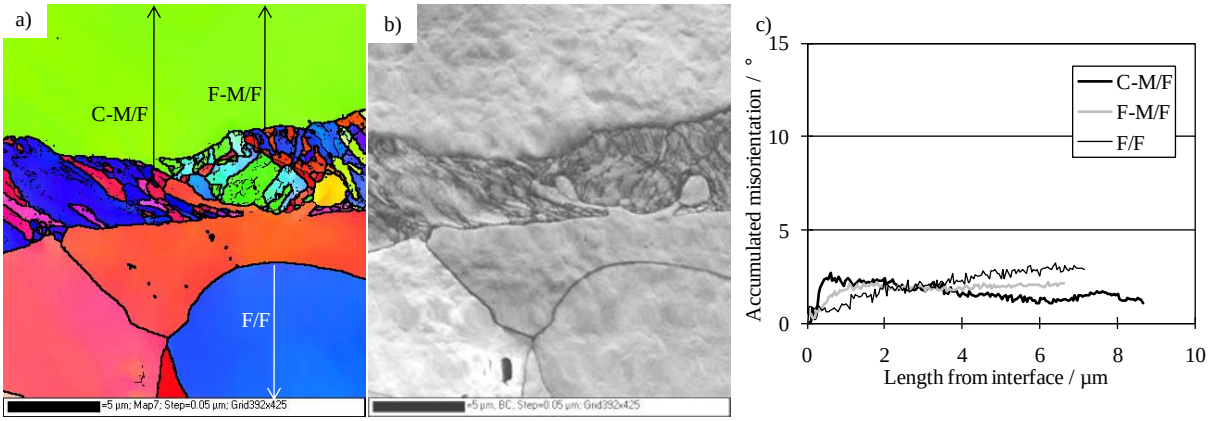

Fig. 5.26 EBSD maps of the dual phase steel temped at 500°C after deformation to a strain of 0.05: a) orientation map and b) band contrast map of a martensite containing concave parts and ferrite grains, and c) accumulated misorientation profiles from the concave interface between the ferrite and martensite (C-F/M), the flat interface between the ferrite and martensite (F-F/M) and the ferrite/ferrite grain boundary (F/F) to another interface. In the band contrast map, dark contrast is related to the martensite due to the large dislocation density. The tensile direction is horizontal. The step size is 50nm.

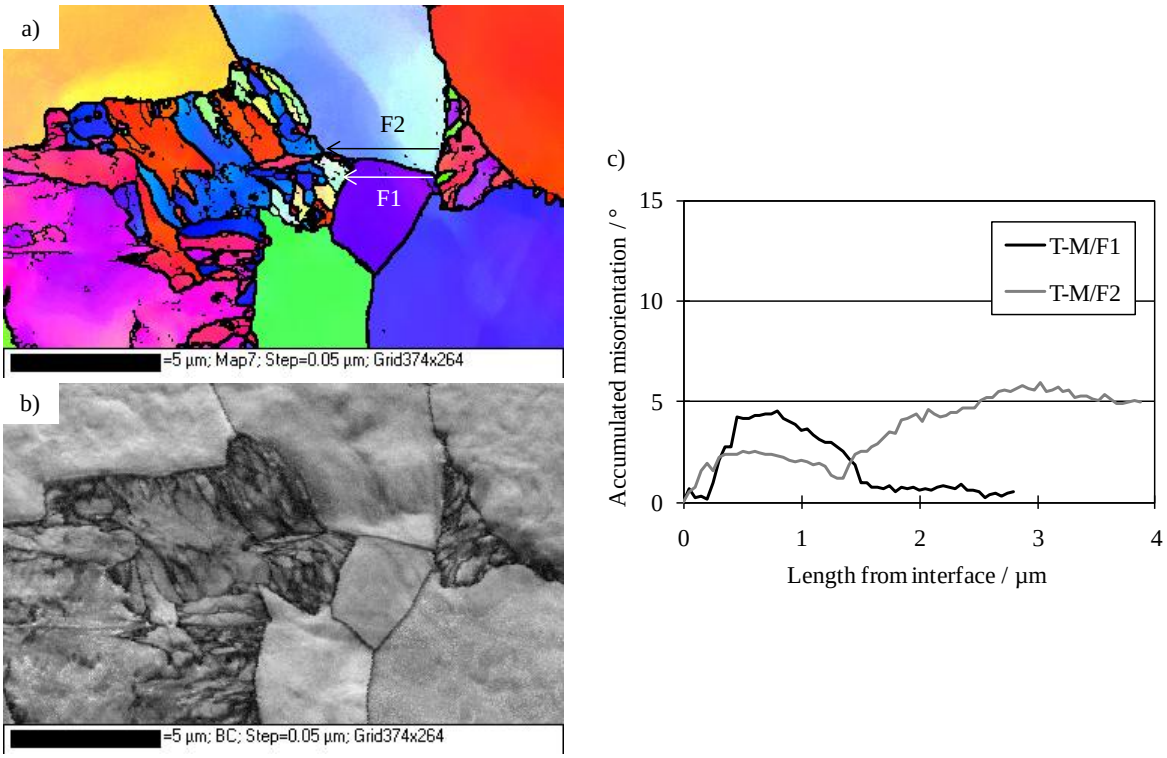

Fig. 5.27 EBSD maps of the dual phase steel temped at 500°C after deformation to a strain of 0.05: a) orientation map and b) band contrast map near the tip of a martensite particle, and c) accumulated misorientation profiles in ferrite grains 1(F1) and 2 (F2) from the left side to the right side. The tensile direction is horizontal. The step size is 50nm.

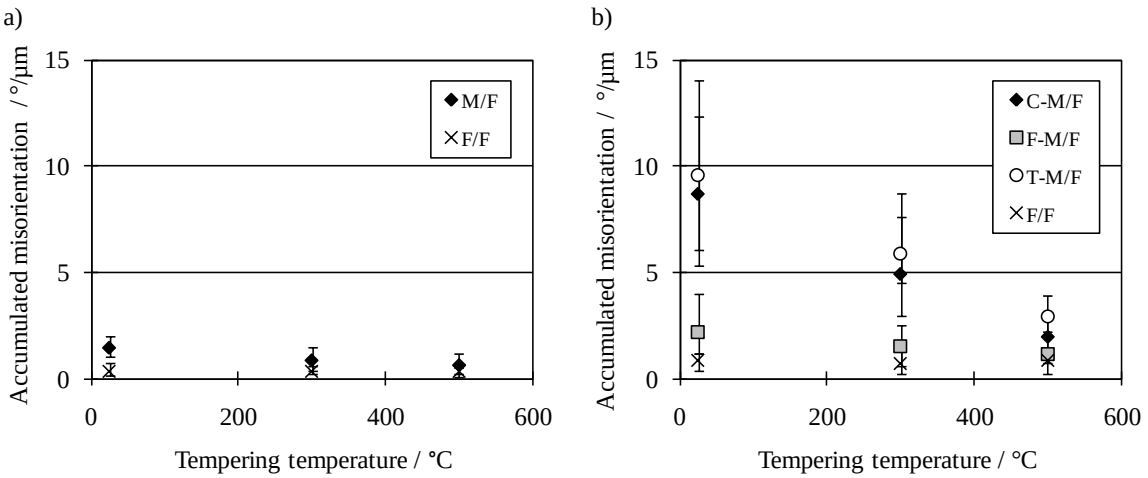

Fig. 5.28 Influence of tempering treatments on accumulated misorientation at the martensite/ferrite interfaces and ferrite/ferrite grain boundaries: a) before tensile tests and b) after tensile tests. After tensile tests, strain often localized at the concave interface between the martensite and ferrite and at the tip of the martensite particle. As strain localized heterogeneously due to the distribution of martensite particles, martensite/ferrite interfaces where strain localized were chosen. The data before tempering is shown at 25°C.

TEM observations have also revealed that deformation is localized at the concave part and the tip of the martensite particle. Fig. 5.29 exemplifies that dislocation walls representing pile-up dislocations are observed at the concave and the tip of the martensite particles in the SVM without tempering. Fig. 5.29a shows that dislocation walls were observed in the ferrite near the concave part of the martensite particle and small cells were located at the concave part of the martensite particle. The cell size became small near the concave part and the smallest size was about 0.3 μm. Dislocation walls and cell structures were observed at the tip of a martensite particle. In particular, a number of dislocation walls often crossed at the tip of martensite particles when the distance between two martensite particles was small. It appears that pile-up dislocations might lead to plastic deformation at the concave part of the martensite particles. Moreover, the minimum size of dislocation cells was about 0.9μm after tempering at 500°C and relatively large. Fig. 5.30 exemplifies that cell-block structures were observed in the SVM tempered at 500°C, but the size was relatively large. These TEM observations supplement the EBSD observation showing that strain localizes at the concave part and tip of the martensite particles, softening of the martensite through tempering treatments reduced localized strain and retarded void formation in the martensite and ferrite.

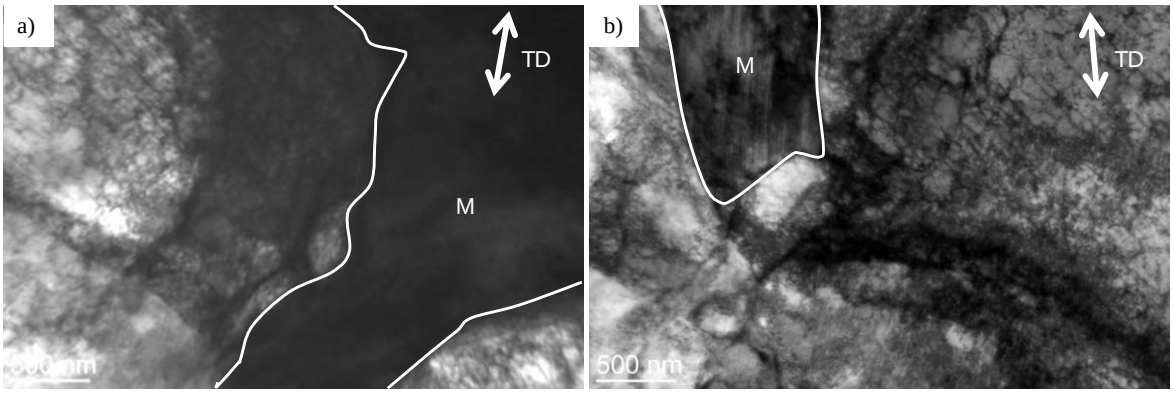

Fig. 5.29 TEM micrographs of dislocations in the SLM without tempering after deformation to a strain of 0.05: a) at the concave part of a martensite and b) the tip of a martensite particle. Dislocation walls representing the misorientation change and small cells are located at the concave part and the tip of martensite particles. The cell size often became smaller at the martensite/ferrite interface.

Vickers hardness tests also reinforced that a small built-up stress retarded void formation in the tempered dual phase steel (Fig. 5.31). The mechanical properties of martensite and ferrite have also been measured directly by Vickers hardness tests. In these tests only the hardness of large ferrite grains and martensite particles were measured because the indent size is larger than the small particles as demonstrated in Fig. 3.2. One source of error may therefore be an effect of size on the hardness suggesting that a next step could be the introduction of nano-indentation tests (e.g. Delincé et al. 2006). The hardness data for martensite and ferrite before and after tempering are illustrated in Fig. 5.31 which shows (i) that the strength of the martensite decreases significantly, thereby reducing the difference between the strength of the martensite and ferrite and (ii) that this difference is maintained at all strains. This change in mechanical properties by tempering may significantly reduce the stress which builds up at the martensite particles during straining thereby reducing the tendency for crack and void formation in the martensite.

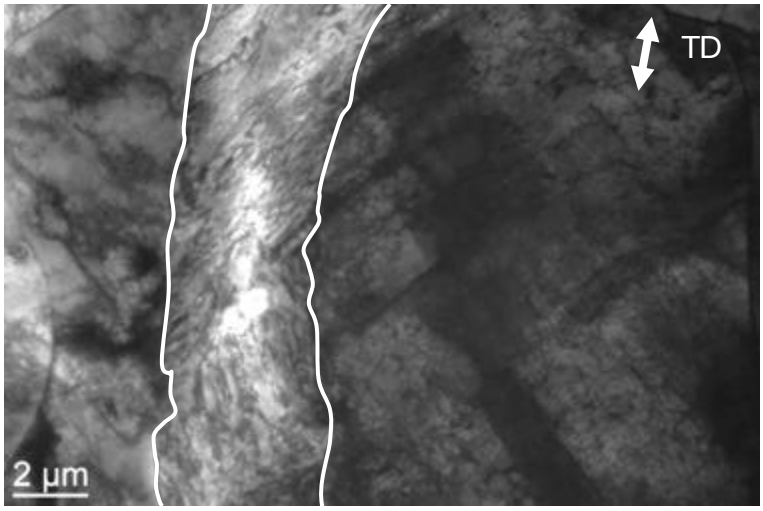

Fig. 5.30 A TEM micrograph of dislocations in the SLM tempered at 500°C after deformation to a strain of 0.05. Cell block structures were observed at the martensite/ferrite interface. The cell size in the specimen tempered at 500°C was much larger than in the specimen without tempering.

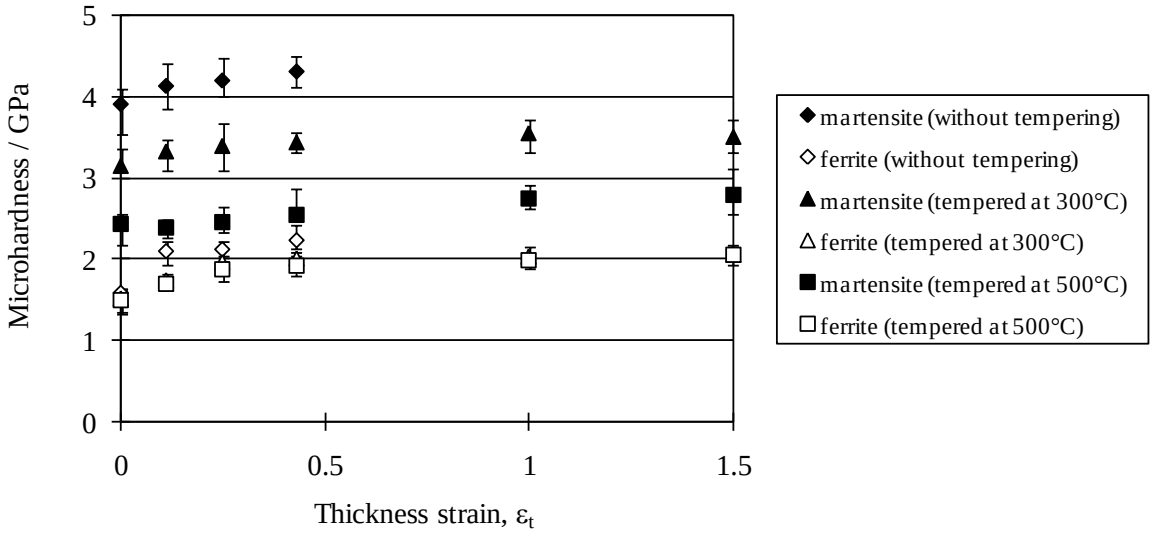

Fig. 5.31 Hardness of the martensite and ferrite in the dual phase steel before and after tempering treatments as a function of the thickness strain.

5.4.3 Critical strain for void formation in martensite

Tempering treatments affected not only strain partitioning, but also a criterion for void formation in the martensite as further straining of the martensite led to void formation in the tempered martensite. Gladman et al. (1971) and Melander and Steninger (1982) have suggested that a critical strain or stress is required for void formation. A strain of specimens when voids formed is often used as a critical strain for void formation. However, since a matrix and reinforcements interact with each other in composite structures, the hardness of the martensite affects strain partitioning between the martensite and ferrite. On the other hand, a critical strain for void formation in the martensite might depend on a property of the martensite. As the evaluation of the strain of the specimens contains two effects, it is difficult to estimate individual effects of the metallurgical parameters on plastic deformation and crack formation in the martensite. Therefore, in the present work, the local strain at the necked region of the martensite was defined as a critical strain for void formation in the martensite when a crack or a void formed in the martensite. The critical strains in about 20 martensite particles were directly measured during in-situ tensile tests. Fig. 5.32 shows that the critical strain for void formation in the martensite does not depend on the volume fraction of the martensite, but depends on the hardness of the martensite. In addition, it is also found that the critical strain did not depend on the shape, size and distribution of the martensite particles. It, therefore, appears that the critical strain is used as an intrinsic parameter to describe void formation in dual phase steels.

In the specimen without tempering treatments, the critical strain was about 0.27 and the smaller criterion led to early void formation in the martensite. On the other hand, a tempering treatment at 300°C improved it to 0.84 and the large critical strain contributed to the retardation of void formation and thereby led to the improvement of the formability. The small criterion for void formation in the martensite leads to early void formation in the martensite contained in the dual phase steel. Hadianfard (2009) has reported that cracks initiate in martensite particles contained in a dual phase steel in low cycle fatigue tests, in which the applied stress is so large that the martensite particles are deformed plastically. This result reinforces the idea that a martensite phase has a smaller criterion for void formation than in a ferrite phase.

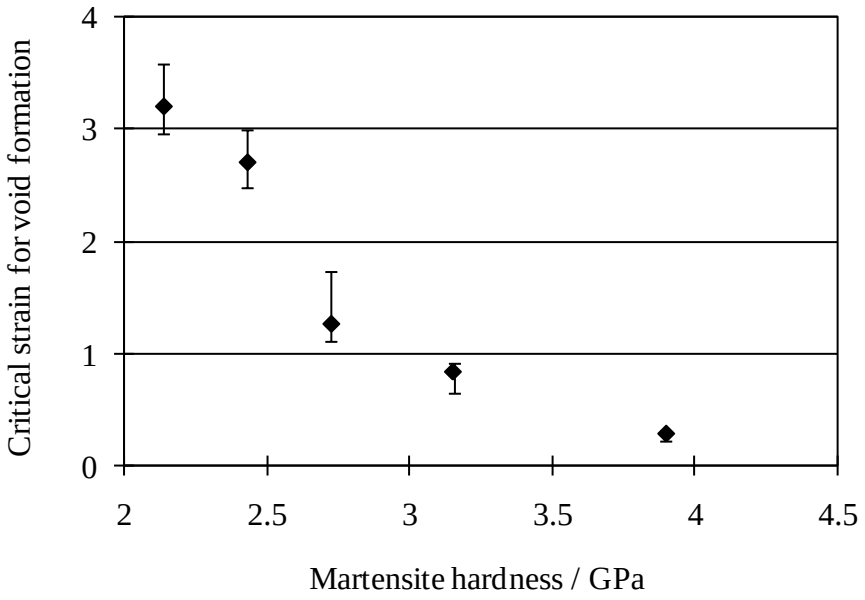

Fig. 5.32 Influence of the martensite hardness on the critical strain for crack formation in the martensite. The local strain before cracking is observed is defined as a critical strain for crack formation in the martensite.

5.4.4 Void formation behaviour in the bulk

The influence of softening of the martensite on plastic deformation of the martensite and void formation in the bulks was investigated. To estimate the effect of softening of the martensite on work hardening behaviour in the dual phase steels, the Crussard-Jaoul analysis was carried out (e. g. Lian et al. 1991, Jiang et al. 1995). Fig. 5.33 shows that a logarithmic work hardening rate ($\ln\sigma/\ln\varepsilon$) depends on a logarithmic stress ($\ln\sigma$) and the work hardening behaviours are divided into two or three regions. The first region means that the martensite is deformed elastically and the ferrite is deformed plastically. And slope changes of the work hardening rate are related to the start of plastic deformation of the martensite. However, the transition from elastic to plastic deformation of the martensite was not observed in the specimen tempered at 500°C due to a Luders deformation. In addition, as shown in Section 4.4.1, a drop of the work hardening rate related to void formation was observed in the SVM without tempering. However, the drop was not observed in the specimens tempered at 300 and 500°C due to late void formation. This means that softening of the martensite through tempering treatments improves the uniform elongation as the softening keeps the work hardening rate high close to uniform elongation. Softening of the martensite also affected the onset of plastic deformation of the martensite as shown in Fig. 5.34. It is obvious that softening of the martensite leads to early plastic deformation of the martensite. The early plastic deformation agrees with an increase of strain in the martensite (Fig. 5.19).

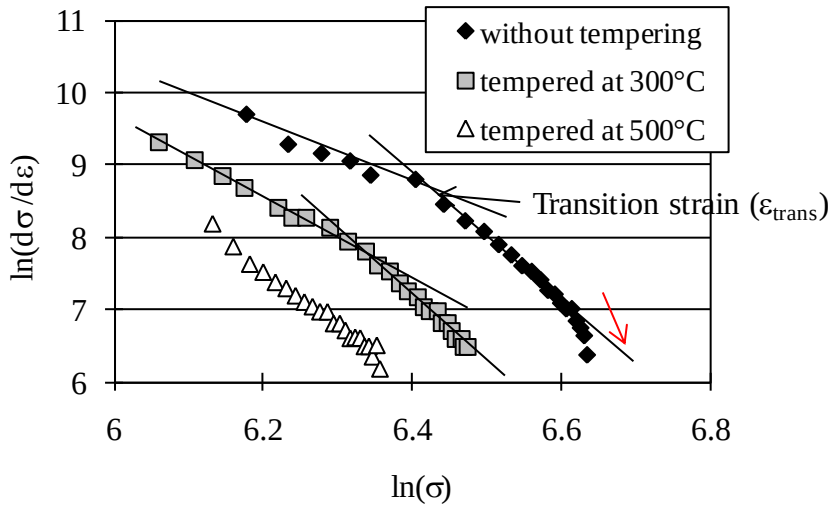

Fig. 5.33 An analysis of the work hardening behaviour in the SVM.

Finally, the void formation behaviour in bulk specimens after tensile tests was estimated based on the classification in Section 4. Fig. 5.3.3 shows that the majority of voids formed in the martensite, voids in the martensite were large and thereby the area fraction of voids in the martensite dominated. In the bulk specimens, tempering treatments also retarded void formation in the bulk specimens, reduced void growth rate and thereby reduced the area fraction of voids in the dual phase steel. The retardation of void formation by softening of the martensite contributes to improvement of the formability in the dual phase steel.

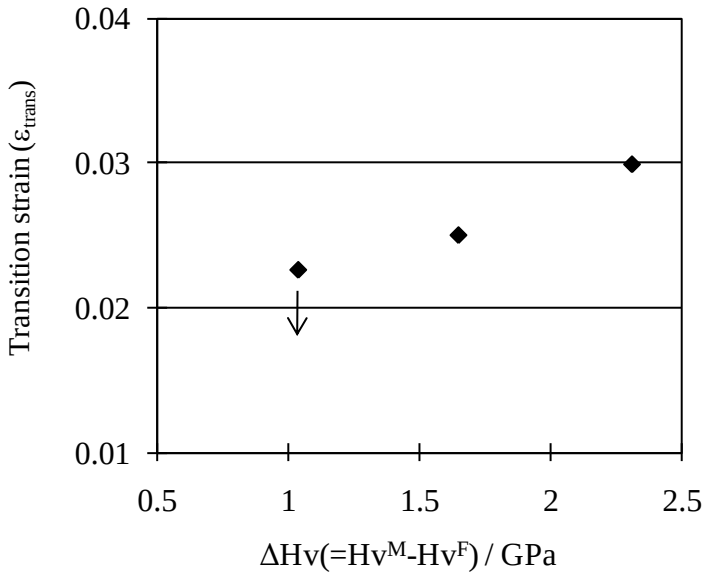

Fig. 5.34 Influence of the hardness of the martensite on the transition strain (ε_{trans}). Softening of the martensite leads to early plastic deformation of the martensite.

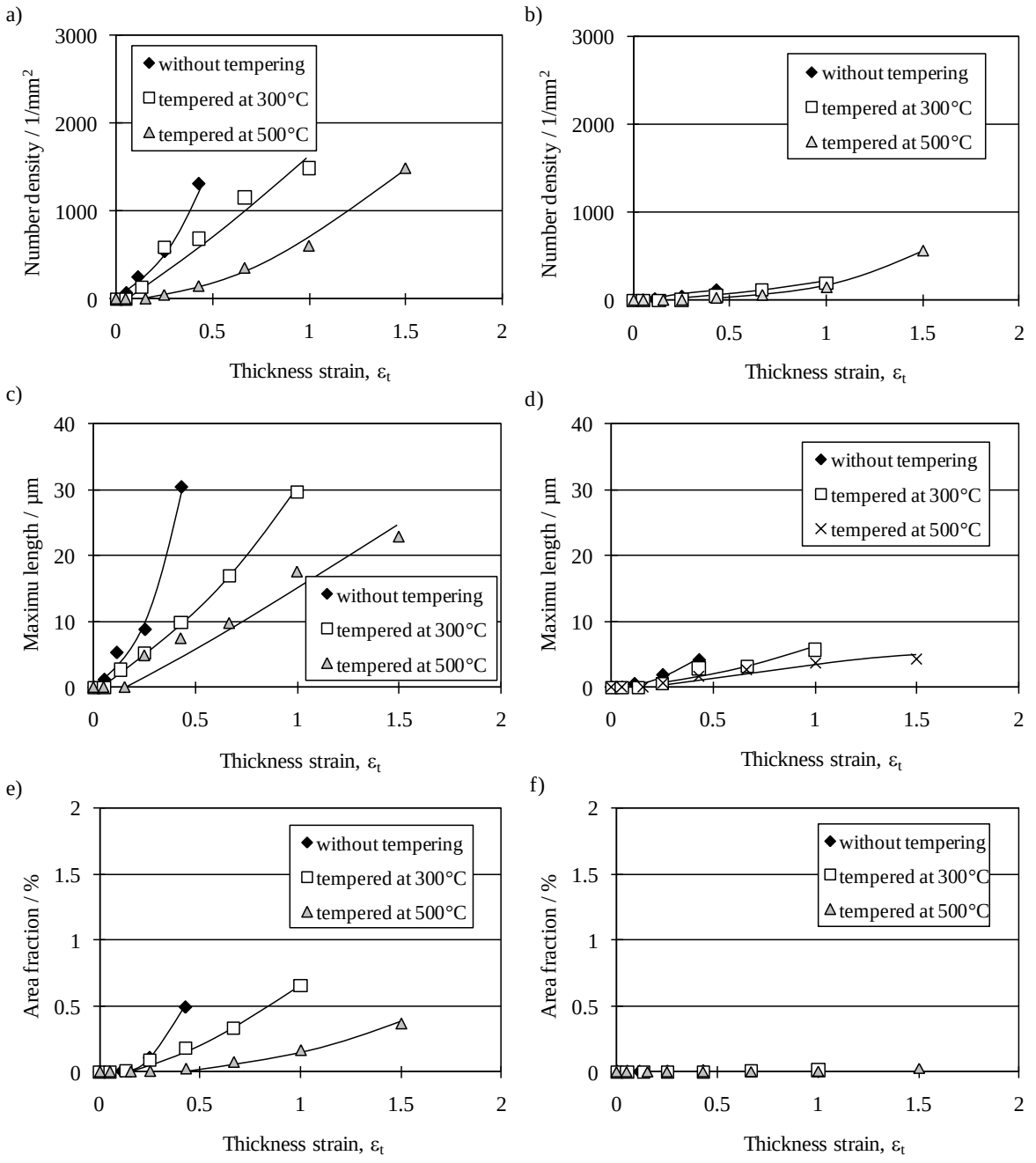

Fig. 5.35 Influence of tempering treatments on void formation in bulk specimens: number density of voids a) in the martensite and b) in the ferrite, maximum length of voids c) in the martensite and d) in the ferrite, area fraction of voids e) in the martensite and f) in the ferrite. In the bulk specimens tempering treatments retarded void formation, reduced void growth rate and thereby reduced the area fraction of voids.

5.5 Summary

In a dual phase steel, the influence of softening of the martensite through tempering treatments at 300-600°C on void formation in the martensite and ferrite has been investigated by tensile testing of bulk specimens and by in-situ tensile tests in a scanning electron microscope. Based on the microstructural observations, deformation and void formation behaviour have been related to the properties of the martensite and ferrite.

1. The tempering treatments significantly increase all elongations, counterbalanced by a reduction in strength. In particular, the post-uniform elongation is significantly improved as more voids form in the necking zone. On the other hand, the yield stress does not depend on the treatments due to a yield point effect.

2. The tempering treatments at from 300 to 600°C control the hardness of the martensite from 4 to 2.2GPa without any effect on the grain size, shape and volume fraction of the martensite due to cementite precipitation and recovery of dislocations in the martensite. On the other hand, the tempering treatments affect less the hardness of the ferrite due to the small excess carbon.

3. Cracks and voids have been observed at different sites (i) in the martensite phase, (ii) in the ferrite phase and (iii) at inclusions before and after tempering. At a given strain the majority of voids formed in the martensite, voids in the martensite were larger than in the ferrite and the area fraction of voids in the martensite thereby dominated.

4. Three factors to describe the void formation behaviour in dual phase steels have been suggested based on in-situ tensile tests and EBSD measurements; (i) strain partitioning between the martensite and ferrite, (ii) strain localization and (iii) a critical strain for void formation in the martensite.

5. In-situ tensile tests have revealed that in the dual phase steel, strain partitioned between the martensite and ferrite. Softening of the martensite allows the martensite to deform more, but makes the ferrite deform less due to strain compatibility. In addition, strain in the martensite significantly depends on the shape of the martensite particles. A decrease of the strain in the ferrite contributes to reduce the void size in the martensite and ferrite as plastic deformation of the ferrite leads to void growth in dual phase steels.

6. EBSD measurements have revealed that strain localizes at the concave part and tip of the martensite particles in dual phase steels and strain localization leads to void formation in the martensite and ferrite in the dual phase steel. Softening of the martensite retarded strain localization at the concave part and tip of the martensite particles and thereby improves the formability.

7. Local strain at the necked region of the martensite particles when a void form is defined as a critical strain for void formation in the martensite. The critical strain depends on the hardness of the martensite, but is independent of the shape and size of the martensite particles. Softening of the martensite retards void formation in the martensite due to improvement of the critical strain.

Chapter 6

Effect of volume fraction of martensite

6.1 Introduction

In this chapter, it is suggested that softening of the martensite through tempering treatments retards void formation in dual phase steels and thereby improves the formability. However, as softening of the martensite also leads to a reduction of the ultimate strength, a solution ensuring the strength should be suggested. In this chapter, an increase of the volume fraction of the martensite is focused as a method to ensure the strength.

The volume fraction of the martensite is one of the important parameters to control the strength of dual phase steels. Mazinani and Poole (2007) showed that an increase of the volume fraction ensures the tensile strength, counterbalanced to a reduction of all elongations. As the ferrite contributes to uniform elongation, the reduction of the volume fraction of the ferrite decreases the uniform elongation in dual phase steels. Whereas uniform elongation is an important parameter, post-uniform elongation is also important to ensure the formability for bending and hole-expansion. However, the effect of the martensite fraction on the void formation contributing to the formability is not shown.

On the other hand, as the hardness of the martensite also affects the strength and formability of dual phase steels. In particular, it is well-known that the post-uniform elongation, which is the elongation of the specimen from the start of necking to fracture, relates strongly to void formation and depends on the hardness of the martensite. It has been suggested that the hardness of the martensite affects void formation behaviour in dual phase steels (e.g. Mazinani and Poole 2007). However, as the hardness of the martensite is controlled through intercritical annealing, the volume fraction and the shape of the martensite are also affected by the intercritical annealing. The volume fraction of the martensite might affect void formation behaviour in dual phase steels.

Therefore, the present study focuses on the effect of the volume fraction of the martensite in dual phase steels. In the present work, the effect of the volume fraction of the martensite on void formation is investigated by using two different dual phase steels. The volume fraction of the martensite is controlled by the chemical composition and the hardness of the martensite is controlled through a hot-rolling condition and tempering treatments at 300-600°C. The void formation behaviour and deformation behaviour of the martensite and ferrite are directly followed during in-situ tests.

6.2 Experimental procedures

Two dual phase steels (SVM and LVM), which contain different volume fraction of martensite as listed in Table 3.3, were used to estimate the influence of the tempering treatments on void formation in dual phase steels. In order to control the hardness of the martensite, tempering treatments from 300 to 600°C were carried out because tempering does not affect the volume fraction and shape of the ferrite and martensite. In addition, since decohesion at the interface between the ferrite and large carbides and cracking of large carbides leads to void formation, a short holding time was chosen in order to prevent carbides from coarsening. Then some steel sheets were tempered at 300- 600°C for 100s.

6.3 Results

6.3.1 Mechanical properties

The volume fraction of the martensite affects mechanical properties of dual phase steels. Fig. 6.1 shows tensile properties of the dual phase steels and hole-expansion ratio. In is obvious that an increase of the volume fraction of the martensite increases yield stress and ultimate tensile strength, but reduced all elongations, a reduction in thickness and hole-expansion ratio. It is well-known that uniform elongation depends on the volume fraction of the ferrite as the ferrite ensures uniform elongation in dual phase steels.

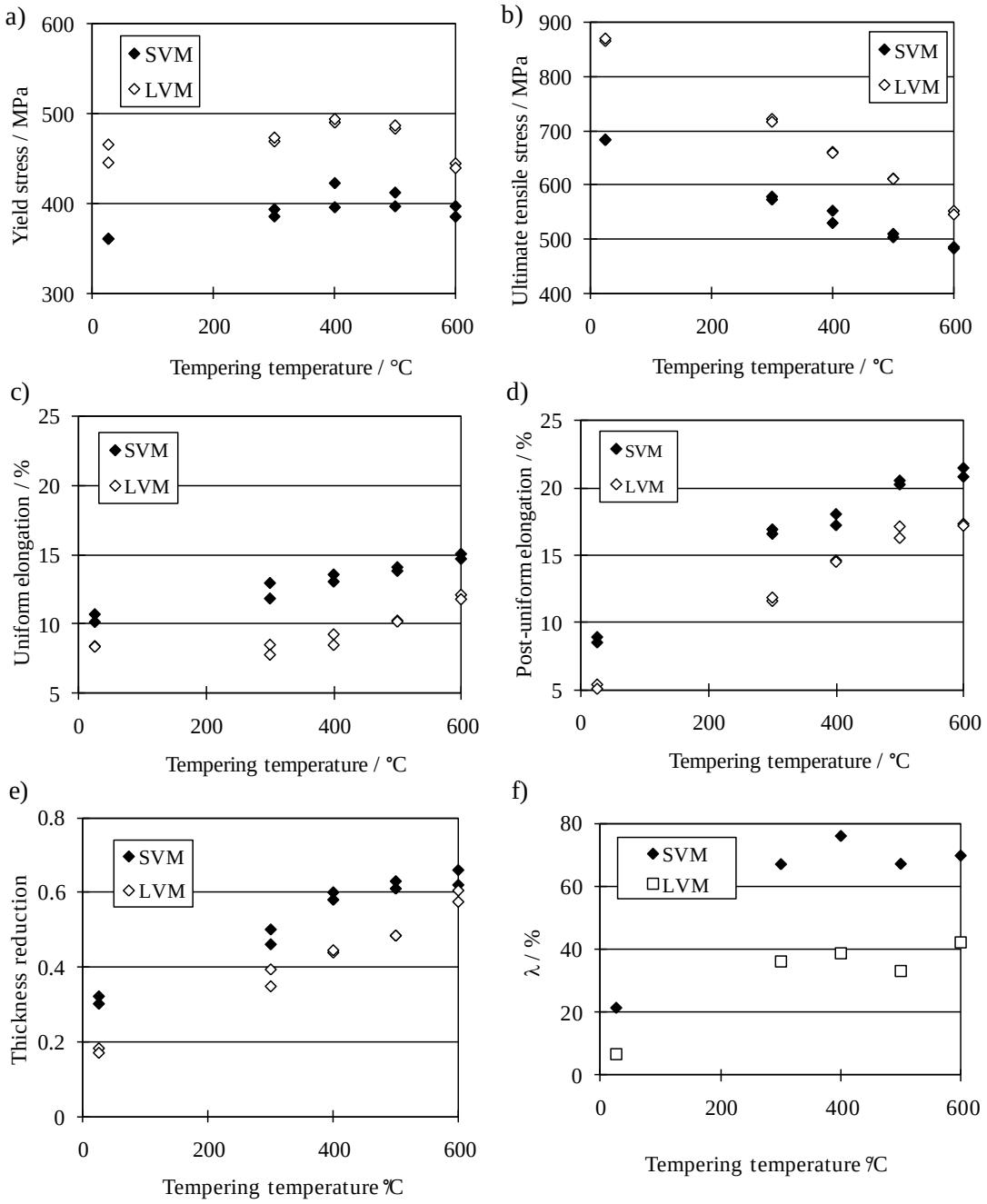

Fig. 6.1 Influence of tempering treatments on tensile properties in the dual phase steels: a) yield stress, b) ultimate tensile strength, c) uniform elongation, d) local elongation, d) reduction in thickness and f) hole-expansion ratio (λ). 0.2% flow stress was defined as tempering treatments lead to yield point phenomenon.

On the other hand, it appears that void formation is related to the volume fraction of the martensite as post-uniform elongation was affected by the volume fraction and more voids form in the necking zone. Whereas softening of the martensite affects the post-uniform elongation more than the uniform elongation, increase of the volume fraction of the martensite reduced the post-uniform elongation as much as uniform elongation. It appears that the different behaviour of post-uniform elongation is related to a different effect on void formation in the dual phase steels. Fig. 6.2 shows the nominal stress-nominal strain curves and the work hardening rate of LVM. After tempering, Lüders deformation was observed. In the LVM, a drop of the work hardening rate was

observed. The influence of the volume fraction of the martensite on void formation and plastic deformation of the martensite is discussed in Section 6.3.2 and 6.4.1 in more detail.

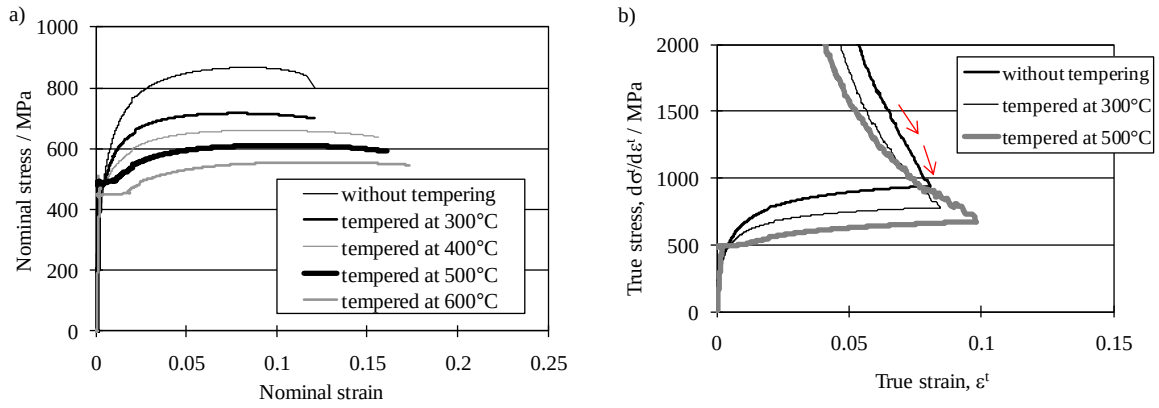

Fig. 6.2 Influence of tempering treatments on a) nominal stress-nominal strain curves and b) the work hardening rate ($d\sigma^t/d\varepsilon^t$) in LVM. In the specimen without tempering, a drop of the work hardening rate is observed (marked by arrows).

6.3.2 Void formation behaviour

In LVM as well as SVM, voids formed (i) in the martensite, (ii) in the ferrite and (iii) at inclusions, as shown in Fig. 6.3. Cracks often formed at the concave part of martensite particles and developed into voids in the dual phase steel (Fig. 6.3a)). On the other hand, voids rarely formed near the tip of martensite particles (Fig. 6.3b). In addition, few voids formed at inclusions due to decohesion and voids were often covered with inclusions (Fig. 6.3c).

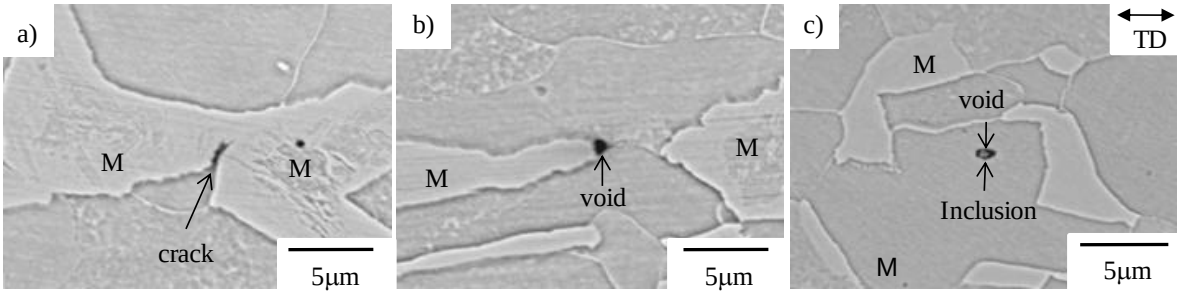

Fig. 6.3 Typical voids in LVM deformed in tension: voids a) in the martensite, b) in ferrite and c) at inclusion in the specimen without tempering ($\varepsilon_t = 0.085$).

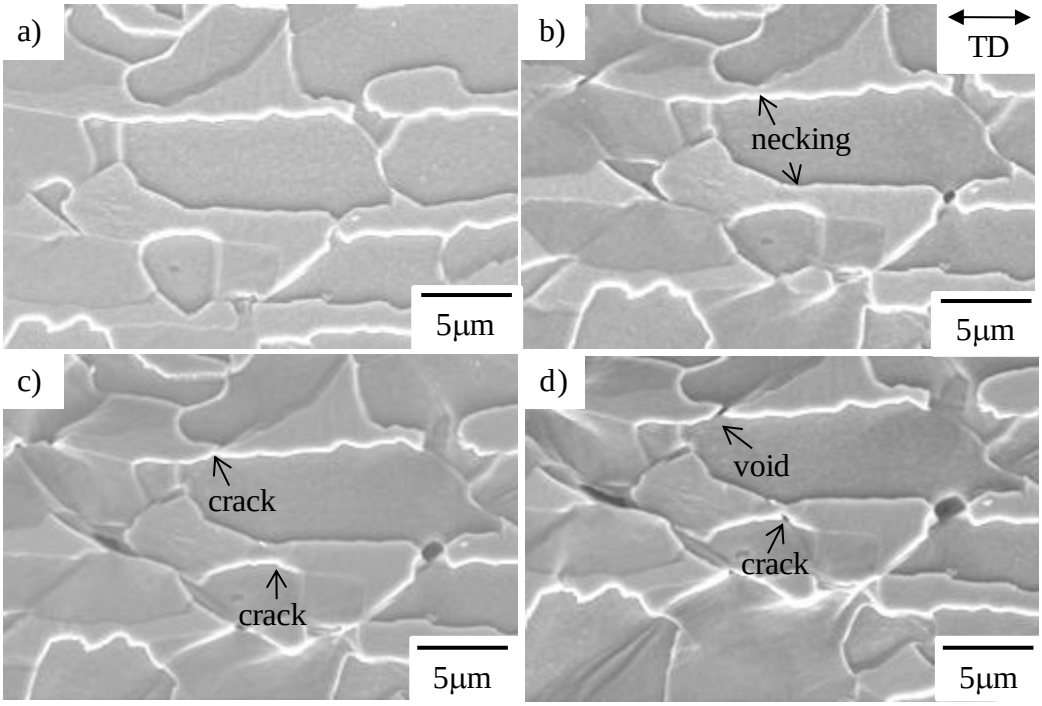

Fig. 6.4 In-situ observation of void formation in LVM without tempering during a tensile test: a) initial microstructure without cracks or voids, b) necking of a martensite particle and void formation in a martensite particle (ε_h= 0.112), c) necking, formation and growth of voids (ε_h= 0.210), d) formation and growth of voids in martensite particles (ε_h = 0.302).

Fig. 6.4 demonstrates the void formation behaviour in LVM without tempering treatments. In LVM, plastic deformation of the martensite (Fig. 6.4c) and crack formation in the martensite (Fig. 6.4c) also led to void formation in the martensite (Fig. 6.4d). Further straining made the voids grow in the tensile direction. Plastic deformation often occurred at the concave part of the martensite particles. It is obvious that the same void formation mechanism led to void formation in the dual phase steel with the large amount of the martensite. However, more voids tended to form in the LVM at a smaller strain. In addition, multiple void formation; void formation assists plastic deformation of the ferrite grains next to the broken martensite and further deformation in the ferrite grains induces crack/void formation in other martensite particles, was also observed as well as in Fig. 4.5.

After tempering treatments, plastic deformation and crack formation in the martensite led to void formation in the martensite in LVM. Fig. 6.5 demonstrates the typical void formation behaviour in LVM tempered at 500°C. Here the martensite appears bright due to cementite precipitation. The initial microstructure is free from cracks and voids in Fig. 6.5a. Fig. 6.5b shows that at a deformation to a strain of ε_h =0.364 martensite particles and ferrite grains were elongated in the tensile direction and thinned. In particular, the concave part of the martensite was heavily deformed due to deformation localization. In addition, slip bands representing strain localization were also observed at the concave part. After deformation to a strain of ε_h=0.471, a crack initiated at the concave part of the martensite particle and propagated in the martensite (Fig. 6.5c). It is apparent that plastic deformation of the martensite had a key role for crack formation in the martensite. Fig. 6.5d shows that further straining (ε_h= 0.994) made the crack develop into a void and the void grew in the tensile direction. A number of slip bands were located at the void and the outline of the void was zigzag. The zigzag profile is evidence that dislocations contribute to void growth in dual phase steels at ambient temperature.

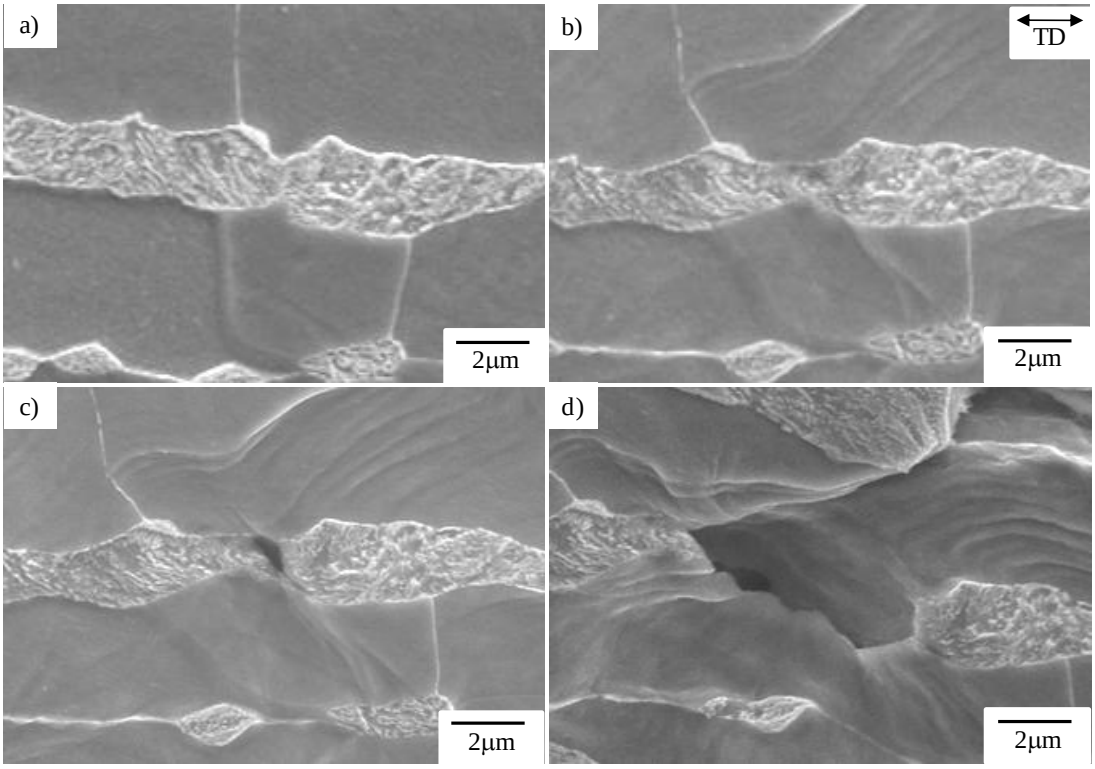

Fig. 6.5 Void formation behaviour in the LVM tempered at 500°C during in-situ testing: a) initial microstructure without cracks or voids, b) plastic deformation of the martensite (ε_h= 0.364), c) crack formation and growth in the martensite (ε_h= 0.471) and d) void growth in the tensile direction (ε_h= 0.994). The martensite appears bright due to cementite precipitation.

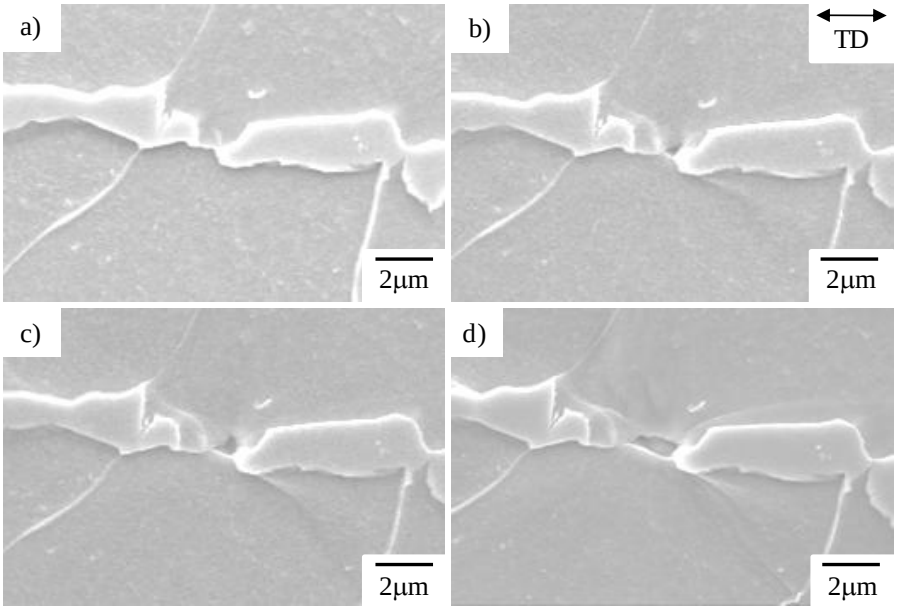

Fig. 6.6 In-situ observation of void formation in LVM without tempering during a tensile test: a) initial microstructure without cracks or voids, b) void formation and slip-band formation near the end of a martensite particles (ε_h= 0.118), c) void growth in the ferrite (ε_h= 0.210) and d) void growth in the ferrite (ε_h= 0.302).

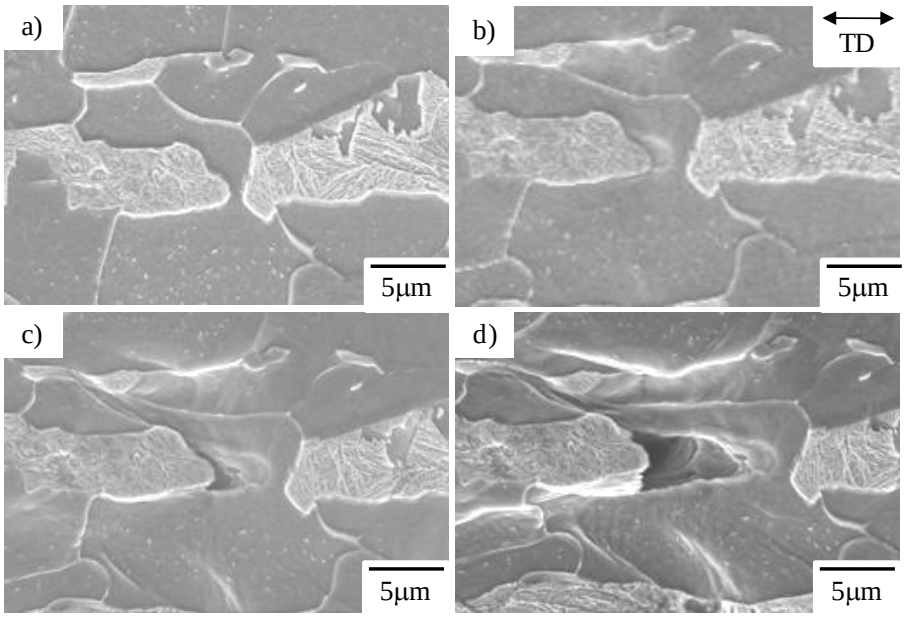

Fig. 6.7 In-situ observation of void formation in LVM tempered at 300°C during a tensile test: a) initial microstructure without cracks or voids, b) void formation and slip-band formation near the end of a martensite particles (ε_h= 0.481), c) void growth in the ferrite (ε_h= 0.642) and d) void growth in the ferrite (ε_h= 0.880).

In addition, void formation in the ferrite was rarely observed in LVM. Figs. 6.6 and 7 demonstrate void formation behaviour at a martensite/ferrite interface on the ferrite side in LVM without tempering and tempered at 300°C. During in-situ tensile tests, voids initiated at the martensite/ferrite interface and grew in the tensile direction with strain. However, voids did not reach other martensite particles as well as in SVM. In addition, voids formed at the triple junction of a martensite and two ferrite grains (Fig. 6.6) and the martensite/ferrite interface, where a ferrite/ferrite grain boundary did not touch. Kadkhodapour et al. (2011) suggested that decohesion between the ferrite/ferrite grain boundaries leads to void formation in a dual phase steel based on a structural evolution and a FEM analysis. However, the in-situ tests have revealed that decohesion at the ferrite/ferrite grain boundary was not dominant in the dual phase steels. Fig. 6.8 shows quantitative analyses of void growth in the ferrite. Here length change between two martensite particles, of the ferrite between the martensite particles and voids were followed. As mentioned in Section 4.4.5, void formation and growth did not shorten the ferrite between two martensite particles and the void, thereby, did not lead to void formation between two martensite particles. These observations also supplement the idea that most voids form in the martensite in dual phase steels.

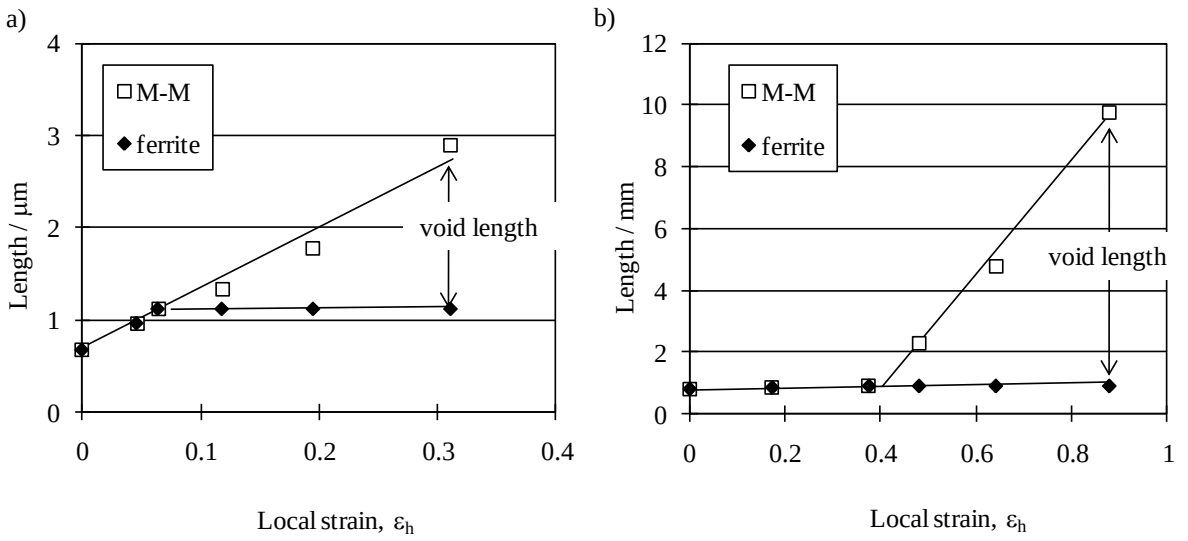

Fig. 6.8 Void growth behaviour in the ferrite: a) in LVM without tempering treatments (in Fig. 6.6) and b) in LVM tempered at 500°C (in Fig. 6.7). Voids formed at the martensite/ferrite interface did not reach another martensite particle.

In LVM, tempering treatments also affected the void formation and growth. Fig. 6.9 exemplifies the effect of tempering treatments on void formation in LVM. As shown in Figs. 6.9a and b, tempering treatments retarded void formation in the martensite and ferrite and most voids formed in the martensite, regardless of tempering treatments. Figs. 6.9c and d show that tempering treatments also decreased void growth rates in the martensite and ferrite. The length in the martensite was much larger than in the ferrite. Therefore, tempering treatments reduced the area fraction of voids in the martensite and ferrite (Figs. 6.9e and f). As shown in Fig. 5.16, tempering treatments also had a similar effect on void formation in SVM. It is obvious that the volume fraction and hardness of the martensite affects void formation and growth in the dual phase steels.

To clarify the effect of the martensite volume fraction on the void formation behaviour in the martensite and ferrite, (i) number density, (ii) maximum length, (iii) average length and (iv) area fraction were directly measured during in-situ tensile tests. Fig. 6.10 shows typical void formation behaviour in LVM without tempering. Voids frequently formed in the martensite and an increase of the volume fraction of the martensite accelerated void formation in the martensite (Fig. 6.10a), made voids in the martensite and ferrite larger (Figs. 6.10c and d) and area fraction of voids in the martensite thereby dominates (Fig. 6.10c). It appears that the maximum length of voids is related to the void growth rate in the martensite and ferrite. After tempering treatments, an increase of the volume fraction of the martensite made more voids form in the martensite and the length of voids larger.

The large increase of void number density in the martensite implies that not only void initiation site density, but also other parameters affected void formation in the martensite. For instance, the volume fraction in LVM (=0.38) is about twice as large as in SVM (=0.21) but the number density of voids in the martensite in LVM is about four times as large as in SVM. In addition, it is obvious that the void growth rate represented to the slope of the maximum length change is affected by the volume fraction of the martensite. These points are discussed in more detail in the following section.

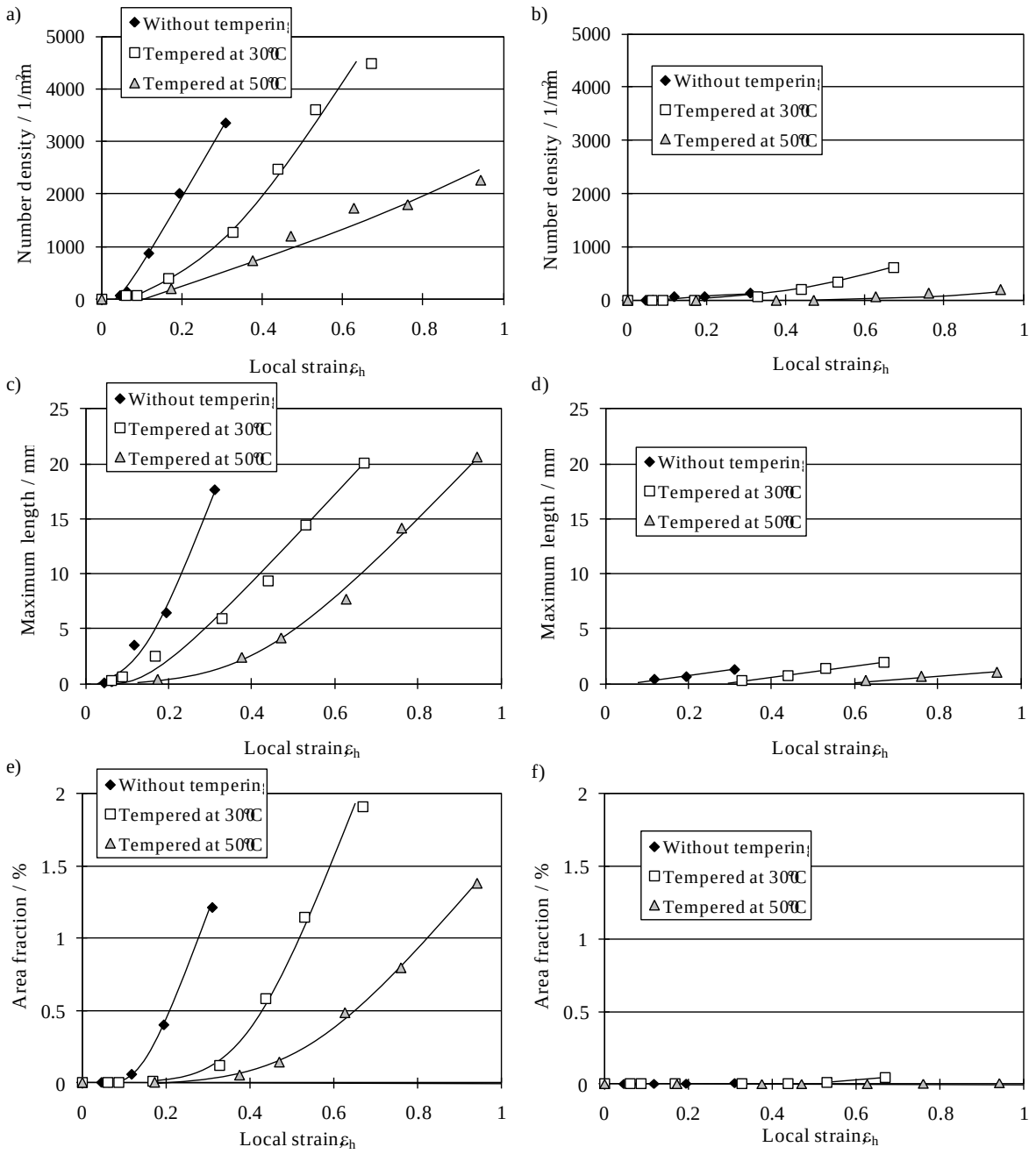

Fig. 6.9 Effect of tempering temperature on void formation in LVM: void number density a) in the martensite and b) in the ferrite, maximum length of voids c) in the martensite and d) in the ferrite, area fraction of voids e) in the martensite and f) in the ferrite.

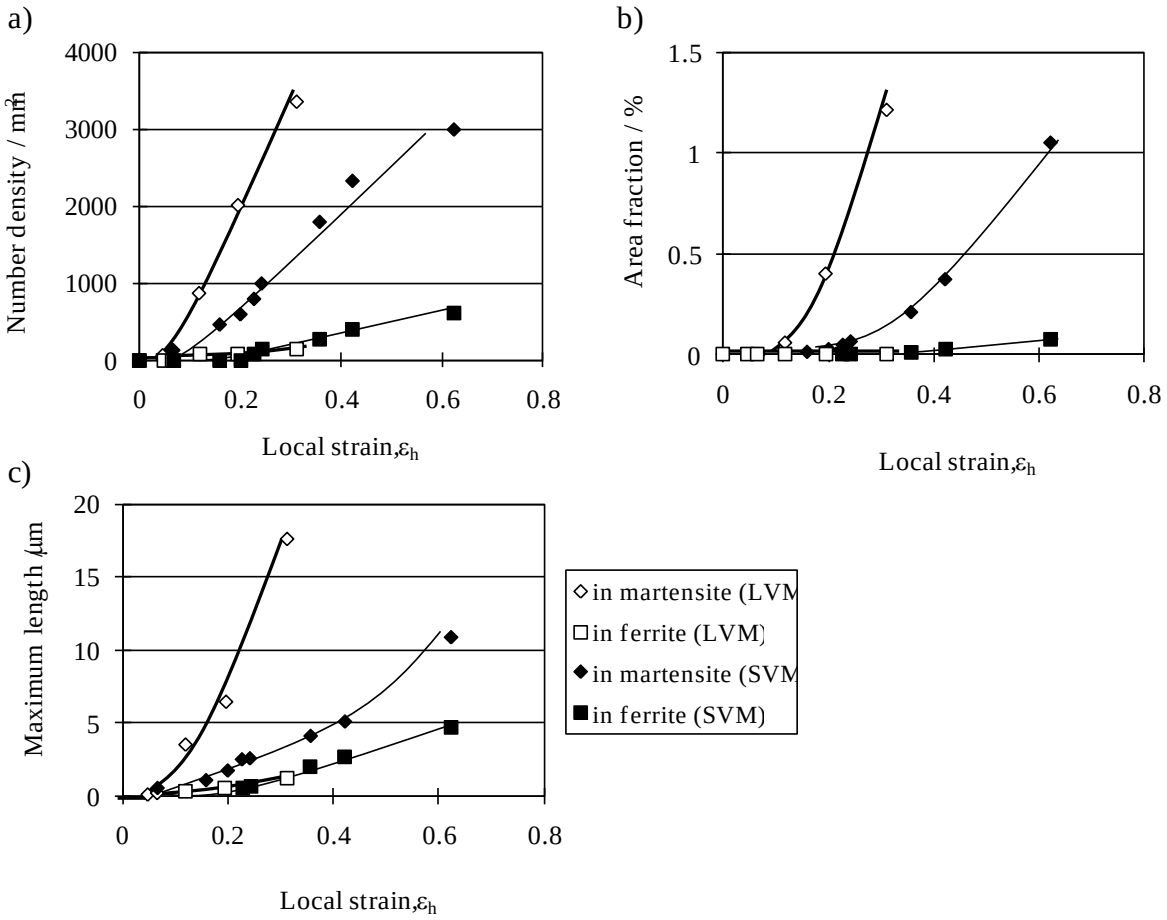

Fig. 6.10 Effect of volume fraction of the martensite on void formation behaviour in the dual phase steels without tempering treatments: a) number density of voids in the martensite and ferrite, b) area fraction of voids in the martensite and ferrite, c) maximum length and d) average length of voids in the martensite and ferrite.

6.4 Discussion

6.4.1 Critical strain for void formation in martensite

Gladman et al. (1971) and Melander et al. (1982) suggested that a critical strain or stress is required for void formation. In this study, the local strain at the necked region of the martensite was defined as a critical strain for void formation in the martensite when a crack or a void formed in the martensite. The critical strains in about 20 martensite particles were directly measured during in-situ tensile tests. Fig. 6.11 shows that the critical strain for void formation in the martensite does not depend on the volume fraction of the martensite, but depends on the properties of the martensite. In addition, it is also found that the critical strain did not depend on the shape, size and distribution of the martensite particles. It, therefore, appears that the critical strain is used as an intrinsic parameter to describe void formation in dual phase steels.

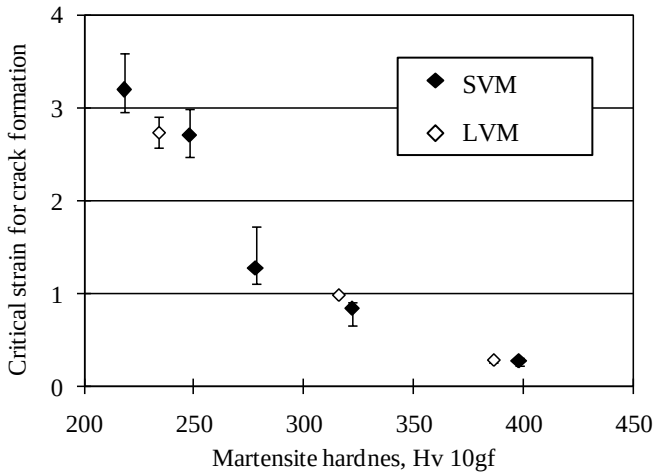

Fig. 6.11 Critical strain for void formation in the martensite. The critical strain does not depend on the volume fraction of the martensite, but depends on the hardness of the martensite.

6.4.2 Strain partitioning between martensite and ferrite

Plastic deformation of the martensite and ferrite depended on the volume fraction of the martensite. Fig. 6.12 shows the work hardening behaviour of LVM and influence of the volume fraction on the transition strain related to the onset of plastic deformation of the martensite. Fig. 6.12a demonstrates the work hardening behaviour of LVM is also divided into two or three regions based on the modified Crussard-Jaoul analysis (e.g. Lian et al. 1991, Jiang et al. 1995). In all specimens the martensite was deformed elastically and a small deformation makes the martensite deform plastically. Fig. 6.12b demonstrates that the volume fraction of the martensite affected the onset of plastic deformation of the martensite. In the dual phase steel containing a large amount of the martensite plastic deformation started at less than ε_{trans}=0.02, which is a strain of tensile specimens. In addition, the specimens without tempering and tempered at 300°C show a rapid drop of the work hardening rate due to void formation. It appears that void formation affected the work hardening rate at a large strain more due to large area faction of voids.

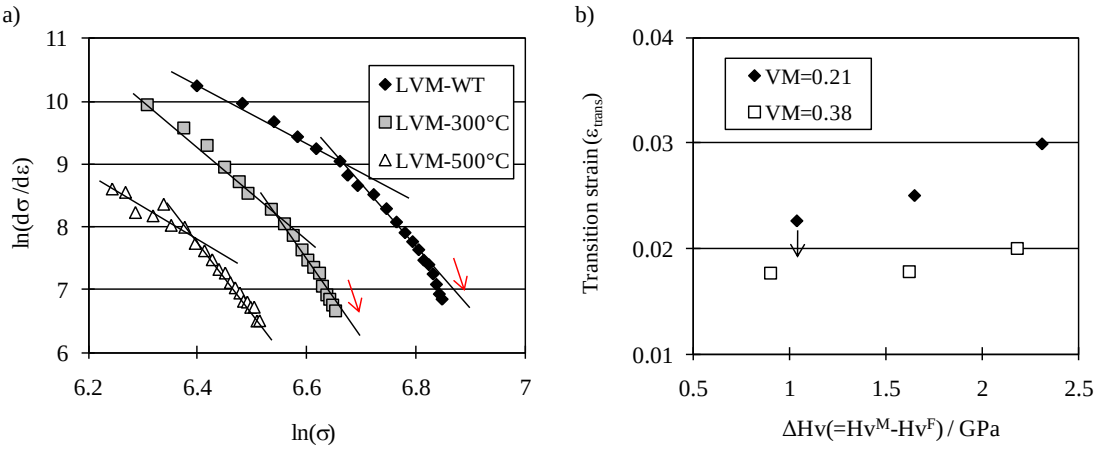

Fig. 6.12 Influence of volume fraction of the martensite on plastic deformation of the martensite; a) Work hardening behaviour of the LVM a) and b) influence of volume fraction of the martensite on the transition strain (ε_{trans}) related to the onset of plastic deformation of the martensite in the dual phase steels.

Strains in the martensite and ferrite were measured at each strain based on the length changes of about 200 grains/particles and the averaged values were normalized by applied local strains (ε_h) of the specimens. Fig.

6.13 shows that the strain in the martensite was relatively small and an increase of the volume fraction of the martensite and ferrite deformed more. It appears that an increase of the hard martensite led to further deformation of the ferrite due to strain compatibility, further deformed ferrite contributed to straining of the martensite due to the large work hardening in the ferrite. Therefore, the large volume fraction increases the strain in the martensite, allows the strain to overcome the critical strain shown in Fig. 6.11 at smaller applied strains of the specimens and thereby leads to early void formation. The previous works supplement that strain partitioning between the martensite and ferrite depends on the volume fraction of the martensite. Tasan et al. (2010) showed that during an in-situ tensile test the strain in the martensite is much smaller than in the ferrite contained in a dual phase steel, where the martensite fraction is less than the SVM. Ghadbeigi et al. (2010) pointed out that the martensite is deformed as much as the ferrite in a dual phase steel containing 50 vol.% martensite during an in-situ tensile test. The tendencies in their works are the same as in the present study even though the hardness of the martensite and ferrite is not shown in their papers. Besides, it is also found that in bulk specimens, the volume fraction of the martensite affected strain partitioning between the martensite and ferrite, which was estimated based on the thickness reduction of the martensite particles and ferrite grains.

In addition, strain partitioning between the martensite and ferrite contributes to void growth in the martensite and ferrite. As shown in Fig. 6.13, the strain in the ferrite was also affected by the volume fraction of the martensite. As plastic deformation of the ferrite matrix leads to separation of the broken martensite particles and void growth in the ferrite, the increase of the strain in the ferrite assists void growth in the martensite and ferrite. Moreover, deformation localization at voids accelerates void growth in dual phase steels as void formation leads to local softening. Therefore, the void growth rate in the LVM is larger than in the SVM.

Finally, the deformation behaviour of each grain/particle also depended on the shape and distribution of the martensite particles. Specifically, ferrite grains surrounded by martensite particles were deformed less, whereas isolated ferrite grains, which did not touch martensite particles, were deformed more. Strains in equiaxed martensite particles were smaller than in elongated particles and particles with concave parts. It, therefore, appear that the shape of the martensite particles is one of the most important parameters to affect the strain partitioning between the martensite and ferrite.

This result also implies that the effect of the martensite hardness, which is controlled by intercritical annealing, on void formation is underestimated. The increase of volume fraction of the martensite makes the martensite soft due to a reduction of the carbon content in the martensite, and thereby increases the critical strain for void formation in the martensite. On the other hand, the increase contributes to further straining of the martensite leading to early void formation. Therefore, the volume fraction of the martensite should be constant in order to estimate accurately the effect of the martensite hardness on void formation in dual phase steels. A tempering treatment is a better method to estimate the effect of the martensite hardness on void formation in dual phase steels.

The difference between the tempering treatments, which affect the critical strain and strain partitioning, and volume fraction of the martensite, which affects only strain partitioning, leads to different effects on void formation in dual phase steels and strength of specimens. The combination of softening of the martensite and increasing of the martensite fraction enables one to develop advanced dual phase steels with high strength and better formability.

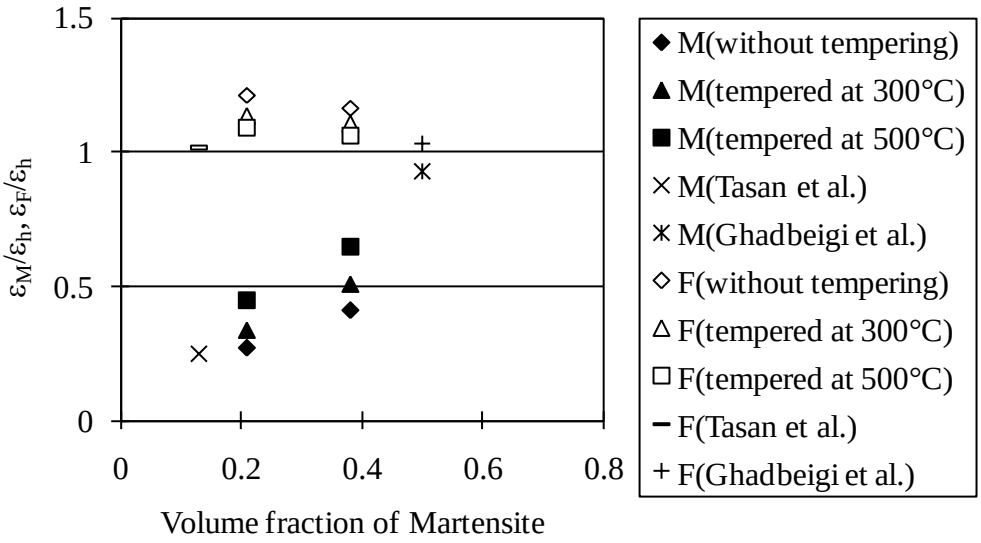

Fig. 6.13 Influence of the volume fraction of the martensite on strain in the martensite and ferrite. The strain partitioning between the martensite and ferrite depends on the volume fraction of the martensite. The hardness of the martensite also affects the strain partitioning. Strain partitioning behaviour in other dual steels, which were carried out by Tasan et al. (2010) and Ghadbeigi et al. (2010), is also compared.

6.5 Summary

The influence of the volume fraction of the martensite on void formation has been investigated by tensile testing of bulk specimens and by in-situ tensile tests in a scanning electron microscope. The hardness of the martensite was controlled through tempering treatments at 300-600°C. Based on the microstructural observations, influence of the volume fraction and hardness on void formation and growth has been discussed. The following conclusions are reached.

1. Increasing of the martensite fraction from 21 to 38 vol.% increases the yield stress and ultimate tensile strength, and is counterbalanced by a reduction of all elongations. However, the tempering treatments did not affect the yield stress due to a yield point phenomenon.

2. Regardless of volume fraction of the martensite, a majority of voids formed in the martensite and the area fraction of voids in the martensite dominated in the dual phase steels. Voids rarely formed at the martensite/ferrite interface, but did not lead to void formation between two martensite particles.

3. The increase of the volume fraction of the martensite significantly accelerated void formation in the martensite, enlarged voids in the martensite and ferrite in dual phase steels and thereby increased the area fraction of voids in the martensite.

4. A critical strain for void formation in the martensite depends on the properties of the martensite, but is independent of the volume fraction, shape, size and distribution of the martensite. The strain partitioning between the martensite and ferrite depends on the volume fraction, hardness and shape of the martensite.

5. The increase of the volume fraction of the martensite makes the martensite and ferrite deform more and further straining of the martensite contributes to early void formation in dual phase steels. Further straining of the ferrite increases the void growth rate in the ferrite and martensite. Therefore, an increase of the volume fraction of the martensite has a negative effect on the formability.

Chapter 7

Effect of the shape of martensite particles on deformation

7.1 Introduction

In the last chapter, it is suggested that the morphology of the hard particle is a key parameter for void formation in dual phase steels and equiaxed martensite particles are preferable to retard void formation and thereby, improve formability for tensile tests, hole-expansion tests and bending tests. The morphology of the martensite particles also affects the void formation behaviour in dual phase steels. As mentioned above, voids predominantly formed at the concave part of the martensite particles and in the elongated particles after plastic deformation of the particles. This obviously shows that martensite shape is one of the most important parameters for void formation in dual phase steels. Then, the shape of the martensite particles was characterised and deformation behaviour of each particle was followed during in-situ loading.

7.2 Experimental procedures

SVM was used to estimate the influence of particle morphology on the deformation behaviour of martensite particles in the dual phase steel. In order to estimate the straining behaviour of equiaxed particles and elongated particles in the dual phase steel, length change of the particles were directly followed during in-situ loading and the strain in each particle was estimated as a function of applied strain on specimens. As mentioned the chapter 3, the morphology of martensite particles in the dual phase steel was complicated. Fig. 7.1 exemplifies typical morphologies of martensite particles in the dual phase steel and are categorized as; a) equiaxed particles, b) elongated particles in the tensile direction, c) elongated particles perpendicular to the tensile direction and d) less regular particles. The martensite particles whose aspect ratio is from 0.5 to 2.0 were defined as equiaxed particles (Fig. 7.1a). If the aspect ratio is over 2.0 and aligned in the tensile direction, the particles are defined as elongated particles in the tensile direction (Fig. 7.1b). The population was dominant in the dual phase steel because the sheet was deformed in the rolling direction during the hot-rolling process. When the aspect ratio of the particles is less than 0.5 in the tensile direction, the particles are called elongated particles perpendicular to the tensile direction (Fig. 7.1c). On the other hand, some particles have branches and large concave parts. They are defined as a less regular shape (Fig. 7.1d). To estimate the deformation behaviour of martensite particles with different shapes, SVM tempered at 500°C was chosen to follow the strain at larger given strains as the critical strain for void formation in the martensite is large and it is easy to follow the length change. The straining behaviour of each particle was estimated as a function of given strains during in-situ loading.

7.3 Results and Discussion

The typical deformation behaviour of 4 types of martensite particles is shown in Figs. 7.2 -5. Deformation behaviour of each martensite particle strongly depends on the shape. Fig. 7.2 shows the deformation behaviour of an equiaxed particle during the in-situ tensile test. After deformation to strains of ε_h=0.33 and 0.887, the shape was almost identical to the initial shape and the equiaxed particle was deformed less. On the other hand, the shape of elongated particles depended on the applied strain. Fig. 7.3 shows that an elongated particle was stretched in the tensile direction and became thinner with strain. However, when the particle was aligned perpendicular to the tensile direction, the particle was not deformed much (Fig. 7.4). Some elongated particles were bent and rotated by plastic deformation of the surrounding ferrite grains. A less regular shape of the martensite led to more complicated deformation as shown in Fig. 7.5. The thinner part aligned in the tensile direction was deformed more than the other parts perpendicular to the tensile direction. Even though not only the shape but also the distribution affects the strain distribution in dual phase steels as shown in Table 4.1, strain of the elongated and less regular shaped martensite particles tend to be larger than of the equiaxed particles (Fig.

7.6). Therefore, the strain of the particles elongated in the tensile direction overcomes a critical strain for void formation in the martensite at a smaller strain and voids form in the elongated particles at a smaller strain than in the equiaxed particles even though a dual phase steel contains equiaxed particles and elongated particles. The results also imply that spheroidizing of the particles retards void formation in the martensite and thereby improves the formability in dual phase steels as it appears that the critical strain for void formation in the martensite does not depend on the martensite shape. As shown in Figs. 4.4 and 4.5, rapid void formation in elongated particles shows that martensite morphology is a key parameter for void formation in dual phase steels. It seems that martensite morphology is not important only for the formability, but also for strength of dual phase steels due to strain/stress partitioning between hard particles and soft matrix related work hardening behaviour of composite materials. He et al. (1984) and Sun et al. (2002) pointed out that flow stress in a dual phase steel containing elongated martensite particles is larger than in a dual phase steel with fine spherical particles, but voids form at a smaller strain in the steel with elongated particles and the elongation is small. In metal matrix composites, mechanical properties and void formation behaviour depends on shape of reinforcements. Clyne and Withers (1993) pointed out that elliptical particles often contain cracks and decohesion tends to occur between metals and spherical particles. Mishnaevsky Jr (2007) suggested that flow stress in the composites with elliptical particles is larger than in the composite containing spherical particles and the elliptical particles are broken at a smaller strain through a FEM analysis.

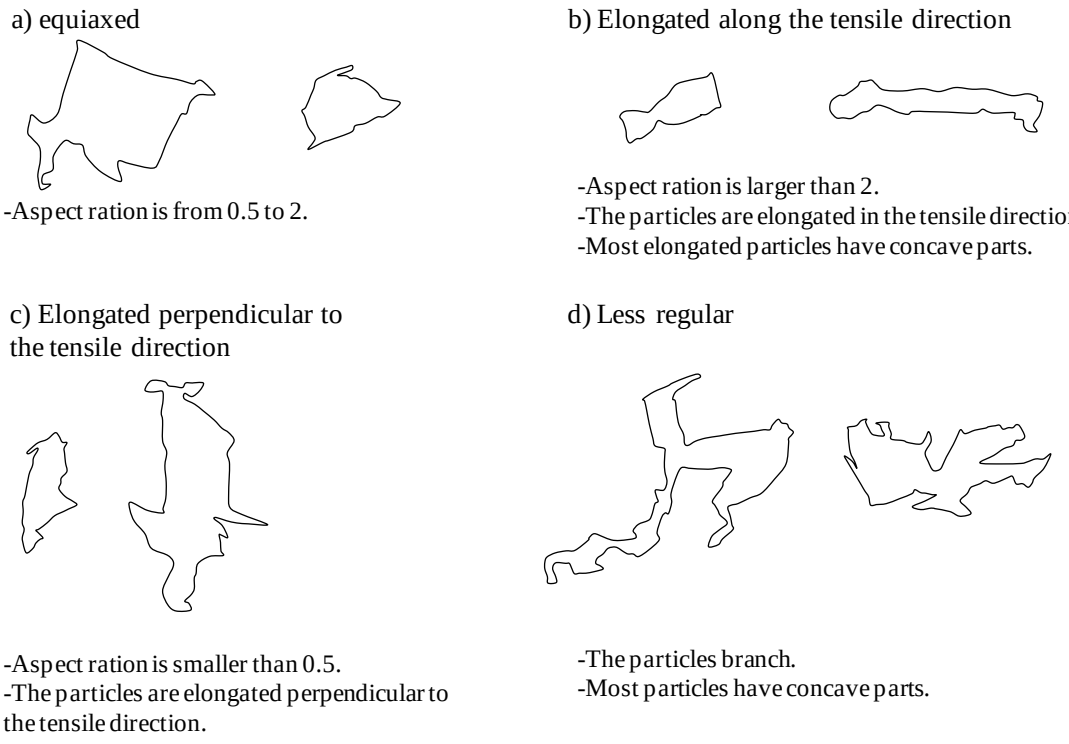

Fig. 7.1 Morphologies of martensite particles in the SVM: a) equiaxed particles, b) elongated particles in the tensile direction, c) elongated particles perpendicular to the tensile direction and d) less regular particles.

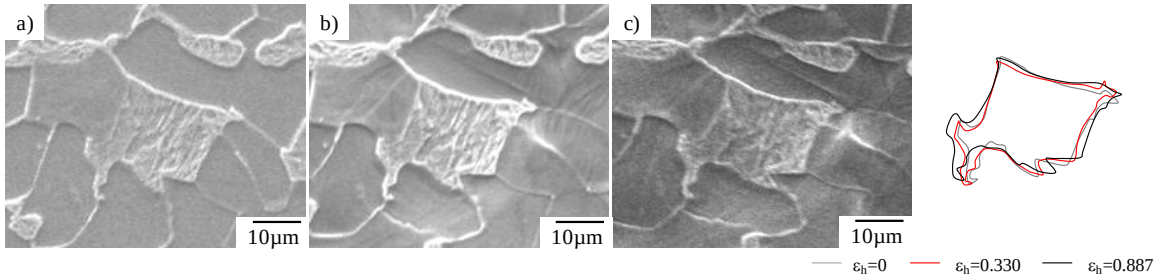

Fig. 7.2 Deformation behaviour of equiaxed martensite particles: a) before deformation, b) ε_h=0.330, c) ε_h=0.887 and d) schematic illustration of martensite shape at each strain. The tensile direction is horizontal.

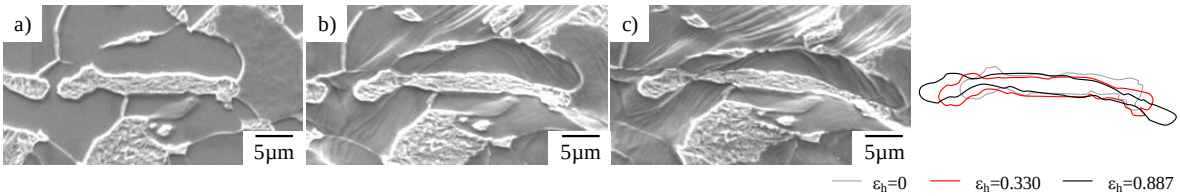

Fig. 7.3 Deformation behaviour of elongated particles in the tensile direction: a) before deformation, b) eh=0.330, c) eh=0.887 and d) schematic illustration of martensite shape at each strain. The tensile direction is horizontal.

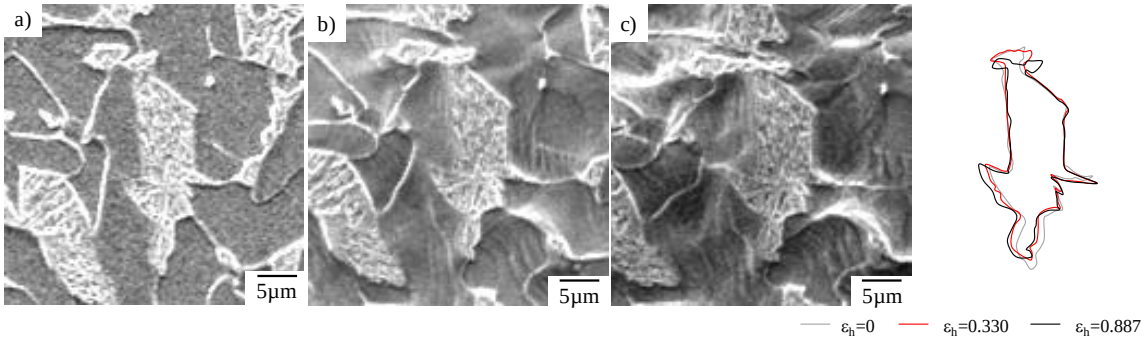

Fig. 7.4 Deformation behaviour of elongated particles perpendicular to the tensile direction: a) before deformation, b) eh=0.330, c) eh=0.887 and d) schematic illustration of martensite shape at each strain. The tensile direction is horizontal.

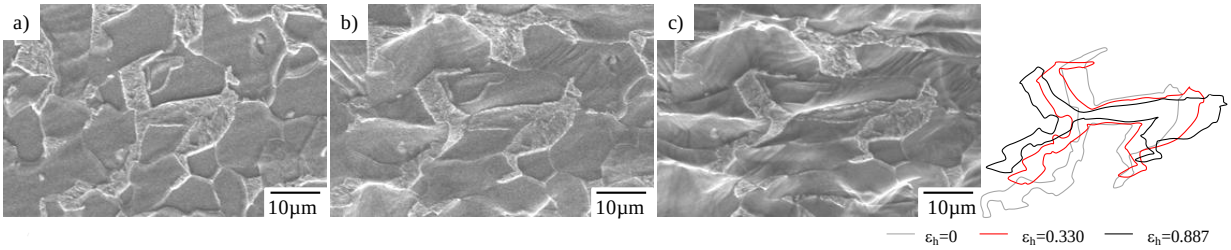

Fig. 7.5 Deformation behaviour of elongated particles perpendicular to the tensile direction: a) before deformation, b) eh=0.428, c) eh=0.844 and d) schematic illustration of martensite shape at each strain. The tensile direction is horizontal.

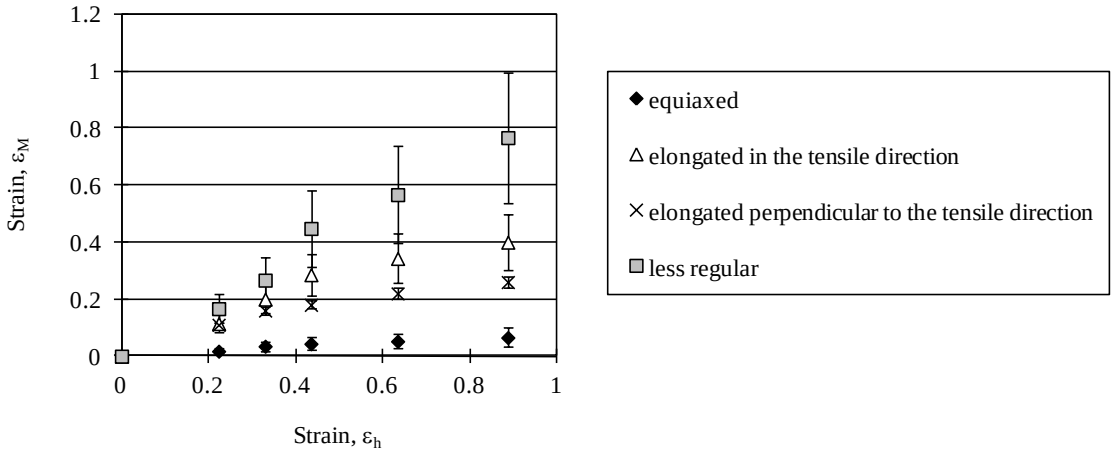

Fig. 7.6 Deformation behaviour of martensite particles with different shapes.

In addition, the complicated 3D-structure in a dual phase steel makes morphological control more important. Landron et al. (2010) and Adachi et al. (2012) showed that martensite particles in dual phase steels were elongated in the rolling direction, often connected to other particles and had many concave parts through X-ray holotomography and serial sectioning even though martensite particles were equiaxed in 2D-images. In particular, band-like structures are often observed in higher strength dual phase steels due to Mn segregation zones (Avramovic-Cingara et al. 2010). However, since 3D-structures of dual phase steels are still ambiguous, estimation of 3D-structures in commercial dual phase steels, non-destructive observation of void formation and deformation behaviour in bulk samples and analysis of the deformation behaviour of the constituents in dual phase steels are future works.

7.4 Summary

The influence of the morphology of the martensite particles on deformation has been investigated by in-situ tensile tests in a scanning electron microscope. The morphology of martensite particles was categorized as a) equiaxed particles, b) elongated particles in the tensile direction, c) elongated particles perpendicular to the tensile direction and d) less regular particles. The straining behaviour of each particle was estimated as a function of given strains. Based on the microstructural observation, the influence of the martensite morphology on void formation has been discussed. The following conclusions are reached.

1. The strain partitioning between the martensite and ferrite strongly depends on the shape of the martensite particles. Martensite particles elongated in the tensile direction are deformed more than the equiaxed particles and particles aligned perpendicular to the tensile direction. Equiaxed particles are less deformable and voids rarely form in these particles. On the other hand, the critical strain for void formation in martensite depends on the hardness.

2. The strain partitioning behaviour in each particle and the intrinsic critical strain for void formation lead to rare void formation in equiaxed martensite particles even though martensite particles have various kinds of morphology.

Chapter 8

Conclusions

The purpose of the present work is to classify void formation mechanisms, characterise which metallurgical factors are important to describe void formation and reveal the effect of metallurgical parameters on void formation in dual phase steels. The deformation behaviour of the constituents and void formation behaviour in the matrix and reinforcements were followed by tensile testing of bulk specimens and by in-situ tensile tests in a scanning electron microscope.

At first, the structural evolution has revealed that there are three typical void formation sites; (a) in the martensite phase, (b) in the ferrite phase and (c) at inclusions, as shown in Fig. 8.1. At a given strain both the frequency and the area fraction of voids in martensite dominate. The void formation in the martensite evolves in four steps; (i) plastic deformation of martensite, (ii) crack initiation at the martensite/ferrite interface, (iii) crack propagation leading to fracture of martensite particles and (iv) void formation by separation of particle fragments (Fig. 8.1a). The in-situ observations have allowed void nucleation to be related directly to plastic deformation and cracking of martensite particles. The voids in ferrite are predominantly formed near the end of the martensite particles and were proceeded by voids in the martensite (Fig. 8.1b). Void formation in the ferrite does not lead to void formation between two martensite particles. Decohesion of the martensite/ferrite interfaces and ferrite/ferrite grain boundaries is not observed. Void formation at inclusions is minor due to the high purity, but voids formed at the smallest strain at the metal/inclusion interface due to a weakly bonded interface (Fig. 8.1c). This characteristic void formation has revealed that void formation in the martensite dominates in bulk samples. Whereas void formation affects post-uniform elongation more as voids form with strain, early void formation decreases the work hardening rate of the dual phase steels and uniform elongation.

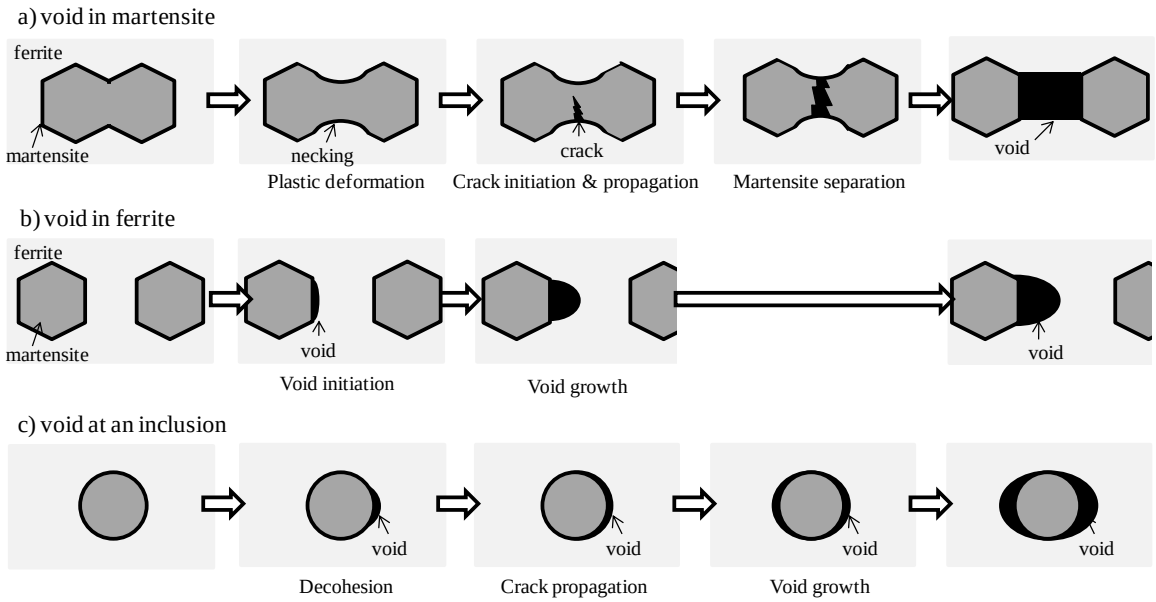

Fig. 8.1 Void formation behaviour in dual phase steels; a) in the martensite, b) in the ferrite and c) at an inclusion.

Second, three factors related to void formation are suggested based on structural evolutions by in-situ testing and EBSD observations; (i) strain partitioning between the martensite and ferrite, (ii) strain localization and (iii) a critical strain for void formation in the martensite. During deformation, the strain often localizes at the concave part and tip of the martensite particles and voids form in the martensite when a localized strain

overcomes a critical value for void formation in the martensite. The critical strain for void formation in the martensite is an intrinsic parameter to describe void formation in the martensite and depends on the properties of the martensite, but is independent of the volume fraction, morphology and size of the martensite particles. As plastic deformation of the martensite leads to crack formation in the martensite, strain in the martensite is important. In particular, strain partitions between the martensite and ferrite due to the different mechanical properties of the martensite and ferrite. The strain partitioning between the martensite and ferrite was estimated as a function of the hardness and volume fraction of the martensite. Whereas strain partitioning is an important parameter, strain localization related to the shape and distribution of the martensite particles is another important parameter. Strain localizes at the concave part of the martensite and necking of the martensite particles leads to void formation in the martensite during tensile tests. Localized strain at the tip of a martensite particle also contributes to void at the martensite/ferrite interface in dual phase steels due to stress concentration and stress relaxation by void formation. These parameters are bases for both analyzed and numerical modelling in order to optimize forming performance and related to metallurgical parameters such as the hardness, volume fraction and shape of the martensite particles.

Thirdly, softening of the martensite is suggested as a method to improve the formability of dual phase steels. This is exemplified that softening of the martensite through tempering treatments at 300-600°C significantly improves the formability, counterbalanced by a reduction of ultimate tensile strength in the dual phase steels. In particular, the improvement of post-uniform elongation is remarkable. The structural evolution has revealed a relationship between the hardness of the martensite and the three factors related to void formation. Softening of the martensite increases the strain in the martensite and decreases the strain in the ferrite due to strain compatibility. Reduction of strain in the ferrite contributes to slow void growth in the martensite and ferrite. The more mild strain partitioning by softening of the martensite reduces the localized strain at the concave part and tip of the martensite and thereby retards void formation in the martensite and ferrite. In addition, improvement of the property of the martensite representing to the hardness significantly retards void formation in the martensite. Reduction of localized strain and the large critical strain contributes to retardation of void formation in the martensite and ferrite and thereby improves the formability in dual phase steels.

Moreover, it is shown that an increase of volume fraction of the martensite (0.21->0.38) mainly affects strain partitioning between the martensite and ferrite, and thereby affects void formation in dual phase steels and mechanical properties of dual phase steels. In particular, a larger strain in the martensite phase accelerates the void formation in the martensite in dual phase steels containing a large amount of martensite particles. On the other hand, the critical strain for void formation in the martensite does not depend on the martensite fraction, but martensite hardness. A combination of softening of the martensite and an increase of the martensite fraction enables one to develop advanced dual phase steels with high strength and better formability due to the different effects on the three factors due to a different effect of martensite hardness and martensite fraction on the critical strain and the strain partitioning in dual phase steels. For instance, a combination of tempering treatment at 400°C and volume fraction change (0.21->0.38) increases the post-uniform elongation from 8.7 to 14.8% and hole-expansion ratio from 20 to 40% without changing the ultimate tensile strength.

Finally, control of martensite morphology is suggested as a method to retard void formation in dual phase steels. In particular, martensite particles elongated in the tensile direction deform more and can lead to void formation at a smaller strain in dual phase steels.

Acknowledgement

The authors thank Nippon Steel Corporation for financial support and for producing the steel sheets used in this study, as well as acknowledging support from the Danish National Research Foundation and the National Natural Science Foundation of China (Grant No. 50911130230) for the Danish-Chinese Centre for Nanometals, within which part of this work was performed.

Outlook

In this section, the hope of non-destructive observation of the deformation and fracture behaviour in advanced materials is discussed. As shown in the present study, to clarify void and crack formation mechanisms is significantly important to improve the formability. In addition, to reveal strain partitioning between a matrix and hard particles in multi-phase materials is of great importance to understand the stress-strain relationship in advanced materials. As Landron et al. (2010) suggest that stress-triaxiality affects macroscopic void formation behaviour, void formation behaviour such as formation rate and growth rate of voids in bulk samples might be different from on surfaces. Therefore, non-destructive observations of deformation and fracture behaviour in advanced materials is of great importance. However, to reveal the mechanisms is limited by lack of non-destructive observation of deformation and fracture behaviour in bulk samples. This causes the deformed microstructures of dual phase steels are very complicated and thereby there is no suitable observation technique. Figs. 5.20-26 show that deformation localizes at the tip of and at the concave part of martensite particles and the change of the accumulated misorientation is about 3-14° per 1μm. On the other hand, as spatial resolution of X-ray tomography and 3D-XRD (X-Ray Diffraction), which are well known as typical non-destructive observations, is about 1μm×1μm×1μm, it might be difficult to detect each deformed ferrite grain and martensite particle, and strain localization related to martensite particles during deformation. In addition, advanced high strength steels consist of ultra-fine grains and particles. As reported by Calcagnotto et al. (2011), the grain size is often less than 1μm. Void formation and deformation behaviour in bulk samples are still puzzling; where voids form and interact with the constituents, even though Maire et al. (2008) estimate the size, number density and volume fraction of voids in a dual phase steel by X-ray tomography. Moreover, computational analysis such as finite element modelling is also helpful to optimize the formability of advanced materials based on 3D-structure measured by X-ray tomography, 3D-XRD and serial sectioning. Therefore, it is hoped that non-destructive observation such as X-ray tomography and 3D-XRD have been developed more and applied more frequently for the characterization for deformation and fracture mechanism in advanced metals.

Table 3D/4D observation techniques

Technique	Type	Parameters	issues
In-situ SEM	non-destructive	Deformation on surfaces Void formation on surfaces	Not observing deformation and fracture behaviour in bulks
Serial sectioning	destructive	3D microstructure	Not following deformation and fracture behaviour
X-ray tomography	non-destructive	Void formation in bulks	Not distinguishing the ferrite with the martensite in dual phase steels
3D-XRD	non-destructive	Strain distribution	Spatial resolution Too small grains, too many grains

References

Adachi1 Y., Sato N., Mayumi Ojima M., Nakayama M. and Wang Y. T. Development automated serial-sectioning 3D microscope and topological approach to pearlite and dual-phase microstructure in steels. In *proceedings of international conference of 3D materials Science.* 2012. 37-42.

Akisue O. and Hada T. Past Development and Future Outlooks of Automotive Steel Sheets. *Nippon Steel Technical Report.* 1995, 64, 1-6.

Akbarpour M. R. and Ekrami A. Effect of ferrite volume fraction on work hardening behaviour of high bainite dual phase (DP) steels. *Mat. Sci. Eng. A,* 2008, 477A, 206-10.

Akisue O. and Usuda M. New types of steel sheets for automobile weight reduction. *Nippon Steel Technical Report,* 1993, 57, 11-15.

Ahmad E., Manzoor T. and Hussain N. Thermomechanical processing in the intercritical region and tensile properties of dual-phase steel. *Mater. Sci. Eng. A,* 2009, A508, 259-65.

Avramovic-Cingara G., Saleh C. H. A. R., Jain M. K. and Wilkinson DS. Void nucleation and growth in dual-phase steel 600 during uniaxial tensile testing. *Metal Mater. Trans. A,* 2010, 40A, 3117- 27.

Avramovic-Cingara G., Ososkov Y., Jain M. K. and Wilkinson D. S. Effect of martensite distribution on damage behaviour in DP600 dual phase steels. *Mater. Sci. Eng. A,* 2009, A516, 7-16.

Babout L., Maire E., Buffiere J. Y. and Fougeres R. Characterization by X-ray computed tomography of decohesion, porosity growth and coalescence in model metal matrix composites. *Acta Matell.,* 2001, 49, 2055-63.

Babout L., Maire E., Buffiere J. Y. and Fougeres R. Damage initiation in model metallic materials: X-ray tomography and modelling. *Acta Mater.,* 2004, 52, 2475-87.

Calcagnotto M., Adachi Y., Ponge D. and Raabe D. Deformation and fracture mechanisms in fine- and ultrafine-grained ferrite/martensite dual-phase steels and the effect of aging . *Acta Metall.,* 2011, 59, 658-70.

Christman T., Needleman A., Nutt S. and Suresh S. On microstructural evolution and micromechanical modelling of deformation of a whisker-reinforced metal-matrix composite. *Mater. Sci. Eng. A,* 1989, A107, 49-61.

Clyne T. W. and Withers P. J. In *An introduction to metal matrix composites.* Cambridge University Press; 1993, 231-34.

Davies R.G. In *Formable HSLA and Dual Phase Steels*. TMS-AIME, (ed. Davenport A. T.)Warrendale, PA; 1977, 25-39.

Davies R. G. The deformation behaviour of a Vanadium-strengthened dual phase steel. *Metall. Trans. A,* 1978, 9A, 41-52.

Delincé M., Jacques P. J. and Pardoen T. Separation of size-dependent strengthening contributions in fine-grained dual phase steels by nanoindentation. *Acta Metall.,* 2006, 54, 3395-04.

Delincé M., Bréchet Y., Embury J. D., Geers M. G. D., Jacques P. J. and Pardoen T. Structure-property optimization of ultrafine-grained dual-phase steels using a microstructure-based strain hardening model. *Acta. Metall.,* 2007, 55, 2337-50.

Erdogan E. The effect of new ferrite content on the tensile fracture behaviour of dual phase steel. *J. Mater. Sci.,*2002, 37, 3623-30.

Fang X., Fan Z., Ralph B., Evans P. and Underhill R. Effects of tempering temperature on tensile and hole expansion properties of a C-Mn steel. *Mater. Proc. Tech.*, 2003, 132, 215-18.

Gerbase J., Embury J. D. and Hobbs R. M. In *Structure and Properties of Dual-Phase Steels*, (eds. Kot R. A. and Morris J.W.) TMS-AIME, New York, 1979, 118–144.

Ghadbeigi H., Pinna C., Celotto S. and Yates J. R. Local plastic strain evolution in a high strength dual-phase steel. *Mater. Sci. Eng.*, A 2010, 527A, 5026-32.

Gladman T., Holmes B. and Mclvor I. D. In *Effect of Second-Phase particles on Mechanical Properties of Steel.*ISI Publication, Londaon, 1971, 68.

González C. and Llorca J. An analysis of the effect of hydrostatic pressure on the tensile deformation of aluminum-matrix composites. *Mater. Sci. Eng.*, 2002, A341, 256-263.

Gurland J. Observations on the fracture of cementite particles in a spheroidized 1.05%C steel deformed at room temperature. *Acta Metall.*, 1972, 20, 735-41.

Jardim O. R., Longo W. P. and Chawla K. K. Fracture behaviour of a Tempering dual phase steel. *Metallography*, 1984, 17, 123-130.

Jena A. K. and Charturvedi M. C. On the effect of the volume fraction of the martensite on the tensile strength of dual-phase steel. *Mat. Sci. Eng.*, 1988, 100, 1-6.

Jia N., Cong Z. H., Sun X., Cheng S., Nie Z. H., Ren, Liaw R. K. and Wang Y. D. An in-situ high-energy X-ray diffraction study of micromechanical behaviour of multiple phases in advanced high-strength steels. *Acta Mater.*, 2009, 57, 3965-3977.

Jiang Z., Guan Z. and Lian J. Effects of microstructural variables on the deformation behaviour of dual-phase steel . *Mater. Sci. Eng.*, A 1995, A190, 55-64.

Joarder A., JHA J. N., Ojha S. N. and Sarma D. S. The tempering behaviour of a plain carbon Dual-Phase steel. *Mater. Chara.*, 1990, 25, 199-209.

Kadkhodapour J., Butz A., Ziaei-Rad S. and Schmauder S. A micro mechanical study on failure initiation of dual phase steels under tension using single crystal plasticity model. *Int. J. Plast.*, 2011, 59, 2575-2588.

Kim S. and Lee S. Effects of Martensite Morphology and Volume Fraction on Quasi-Static and Dynamic Deformation Behaviour of Dual-Phase Steels. *Metall. Mater. Trans. A*, 2000, 31A, 1753-1760.

Kishida K. High strength steel sheets for light weight vehicle. *Nippon Steel Technical Report*, 2000, 81, 12-16.

Hadianfard M. J. Low cycle fatigue behaviour and failure mechanism of a dual-phase steel. *Mater. Sci.Eng. A*, 2009, 499A, 493-499.

Han S. K. and Margolin H. Void formation, void growth and tensile fracture of plain carbon steel and a dual-phase steel. *Mater. Sci. Eng. A*, 1989, A112, 133-41.

Han S., Byoungchul H., Sunghak L., Chang G. L. and Kim S. J. Effect of martensite morphology and tempering on dynamic deformation behaviour of dual-Phase steels. *Metall. Trans. A*, 2004, vol.35A, 2371-2382.

Hasegawa K., Kawamura K., Urabe T. and Hosoya Y. Effects of microstructure on stretch-flange-formability of 980MPa grade cold-rolled ultra high strength steel sheets. *ISIJ Int.*, 2004, 44, 603-09.

Hayashi K., Miyata K. and Katsuki F. Deformation behaviour in high-strength dual-phase steel sheets during bending test. *Tetsu-to-Hagane*, 2012, vol.98, No. 6, pp. 82-88.

He X. J., Terao N. and Berghezan A. Influence of martensite morphology and its distribution on mechanical properties and fracture mechanisms of Fe-Mn-C dual phase steels. *Mater. Sci.*, 1984, 18, 367-73.

Hosseini S. B., Temmel C., Karlsson B. and Ingesten N. G. An in-situ scanning electron microscopy study of the bonding between MnS inclusions and the matrix during tensile deformation of hot-rolled steels. *Metal. Mater. Trans. A*, 2007, 34A, 982-89.

Jiang Z., Guan Z. and Lian J. Effects of microstructural variables on the deformation behaviour of dual-phase steel. *Mater. Sci. Eng. A*, 1995, 190, 55-64.

Kadkhodapour J., Butz A., Rad S. Z. and Schmauder S. Experimental and numerical study on geometrically necessary dislocations and non-homogeneous mechanical properties of the ferrite phase in dual phase steels. *Int. J. Plast.*, 2011, 59, 2575-88.

Kang J., Ososkov Y., Embury J. D. and Wilkinson D. S. Digital image correlation studies for microscopic strain distribution and damage in dual phase steels. *Scripta Mater.*, 2007, 56, 999-1002.

Kelestemur O., Kelestemur M. H. and Yildiz S. Improvement of Mechanical Properties of Reinforcing Steel Used in the Reinforced Concrete Structures. *J. Iron Steel Res. Inter.*, 2009, 16, 55-63.

Kim S. and Lee. S. Effects of martensite morphology and volume fraction on quasi-static and dynamic deformation behaviour of dual phase steels. *Metal. Mater. Trans. A*, 2000, 31A, 1753-1760.

Koo J. Y. and Thomas G. In *Formable HSLA and Dual Phase Steels.* (ed. Davenport A. T.) TMS-AIME, Warrendale, PA, 1977, 25-39.

Korzekwa D. A., Lawson R. D., Matlock D. K. and Krauss G. A consideration of models describing the strength and ductility of dual-phase steels. *Scripta Metal.* 1980, 14, 1023-1028.

Kosco J. B. and Koss D. A. Ductile fracture of mechanically alloyed iron-yttria alloys. *Metall. Mater.*, 1993, A 24, 681-87.

Landron C., Bouaziz O., Maire E. and Adrien J. Characterization and modeling of void nucleation by interface decohesion in dual phase steels. *Scripta Metall.*,2010, 63, 973-76.

León-Garcia O., Petrov R. and Kestens L. A. I. Void initiation at TiN precipitates in IF steels during tensile deformation. *Mater .Sci. Eng. A* 2010, A527, 4202-09.

Li B. L., Godfrey A. and Liu Q. Investigation of Macroscopic Grain Sub-Division of an IF-Steel during Cold-Rolling. *Mater. Sci. Forum*, 2002, 408-412, 1185-1190.

Mishnaevsky Jr L. In *Computational Mesomechanics of Composites.* John Wiley & Sons. Ltd. 2007, 161-165.

LeRoy G., Embury J. D., Edward G. and Ashby M. F. A model of ductile fracture based on the nucleation and growth of voids. *Acta Metal.*, 1981, 29, 1509-22.

Lian J., Jiang Z. and Liu J. Theoretical model for the tensile work hardening behaviour of dual-phase steel. *Mater. Sci. Eng. A*, 1991, A147, 55-65.

Lubarda V. A., Schneider M. S., Kalantar D. H., Remington B. A. and Meyers M. A. Void growth by dislocation emission. *Acta Metall.*, 2004, 52, 1397-08.

Maire E., Bouaziz O., Michiel M. D. and Verdu C. Initiation and growth of damage in a dual-phase steel observed by X-ray microtomography. *Acta Metall.*, 2008, 56, 4954-64.

Marder A. R. and Bramfitt B. L. In *Structure and Properties of Dual-Phase Steels*. (eds. Kot R. A., Morris J. W.) TMS-AIME, Warrendale, PA; 1979, 145-82.

Matsuoka S., Hasegawa K. and Tanaka K. Newly-developed ultra-high tensile strength steels with excellent formability and weldability. *JFE Technical Report*, 2007, 10, 13-18.

Mazinani M. and Poole W. J. Effect of martensite plasticity on the deformation behaviour of a low-carbon dual phase steel. *Metall. Mater. Trans. A*, 2007, 38A, 328-39.

Melander A. and Steninger J. The roles of surfides, oxides and pearlite in the ductile fracture of a niobium microalloyed steel. *Mater. Sci. Eng.* 1982, 52, 239-248.

Meyers M. A., Traiviratana S., Lubarda V. A., Benson D. J. and Bringa E. M. The role of dislocations in the growth of nanosized voids in ductile failure of metals . *JOM*, 2009, 61, 35-41.

Miyahara K., Matsuoka S. and Hayashi T. Nanoindentation as a Strength Probe-a study on the hardness dependence of indent size for fine-grained and coarse-grained ferritic steel. *Metal. Mater. Trans.*, 2001, 32A, 761-768.

Morito S., Tanaka H., Furuhara T. and Maki T. In *Proc. of Int. Sympo.* on in Honer Professor Krauss G., ASM, Cincinnati, 1999, 631.

Morito S., Nishikawa J. and Maki T. Dislocation Density within Lath Martensite in Fe-C and Fe-Ni Alloys. *ISIJ-Int.*, 2003, 43, 1475-.1477

Morito S., Tanaka H., Konishi R.. Furuhara T. and Maki T. The morphology and crystallography of lath martensite Fe-C alloys. *Acta Mater.*, 2003, 51, 1789-1799.

Morooka, S., Umezawa, O., Harjo, S., Hasegawa, K. and Toji , Y. Quantitative analysis of tensile deformation behaviour by in-situ neutron diffraction for ferrite-martensite type dual-phase steel. *Tetsu-to-Hagane*, Vol. 2012, vol. 98, pp.311-319.

Movahed P., Kolahgar S., Marashi S. P. H., Pouranavari M. and Parvin N. The effect of intercritical heat treatment temperature on the tensile properties and work hardening behaviour of ferrite-martensite dual phase steels. *Mat. Sci. Eng. A*, 2009, A518, 1-6.

Nakagawa A. H. and Thomas G. Microstructure-mechanical property relationships of dual-phase steel wire. *Metall. Trans. A*, 1985, 16A, 831-40.

Natori M., Futamura Y., Tsuchiyama T. and Takaki S. Difference in recrystallization behaviour between lath martensite and deformed ferrite in ultralow carbon steel. *Scripta Mater*., 2005, 53, 603-606.

Kishida K. High Strength Steel Sheets for Light Weight Vehicle. *Nippon Steel Technical Report.* 2000, 81, 12-16.

Nishimoto A. Hosoya Y. And Nakaoka K. In *Fundamentals of Dual-Phase Steels*, (eds. Kot R.A., Bramfitt B.L.) TMS-AIME, Warrendale, PA, 1981, 447-455.

Nutt Sr. and Needleman A. Void nucleation at fibre ends in Al-SiC composites. *Scripta Metall.*, 1987, 21, 705-10.

Poruks P., Yakubtsov I. and Boyd J. D. Martensite-ferrite interface strength in a low-carbon bainitic steel. *Scripta Mater.*, 2006, 54, 41-45.

Osokov Y., Wilkinson D. S., Jain M. and Simpson T. In-situ measurement of local strain partitioning in a commercial dual-phase steel. *Int. J. Mater. Res.*, 2007, 98, 664-673.

Qiu H., Mori H., Enoki M. and Kishi T. Evolution of ductile fracture of structural steels by microvoid model. *ISIJ Int.*, 1999, 39, 358-64.

Pickering F. B. In *Hardenability Concepts with Application to Steel.* (ed. Daone D. V. and Kirkaldy J. S.) AIME, 1978, 179.

Rashid M. S. In *Formable HSLA and Dual-Phase Steels,* (ed. Davenport A. T.) TMS-AIME, New York, 1979, 1-24.

Ray R. K. Tensile fracture of a dual-phase steel. *Scripta Metall.,* 1984, 18, 1205-09.

Roberts W. Lehtinen B. and Easterling K. E. An in-situ SEM study of void development around inclusions in steel during plastic deformation. *Acta Metall.,* 1976, 24, 745-58.

Sabirov I. and Kolendnik O. The effect of inclusion size on the local condition for void nucleation near a crack tip in a mild steel. *Scripta Metall.,* 2005, 53, 1373-78.

Saito T., Takahashi M., Miyazaki Y., Mizuhashi N. and Sakiyama T. Welding Technology for Uncoated and Coated Steel Sheets for Automobiles. *Seitetsu Kenkyu*, 1987, 34, 327-32.

Samuel F. H. Effect of Dual-Phase treatment and tempering on the microstructure and mechanical properties of a high strength, low alloy steel. *Metall. Trans.,* 1985, 75, 51-66.

Sarwar M. and Priestner R. Influence of ferrite-martensite microstructural morphology on Tensile properties of dual-phase steel. *J. Mater. Sci.,* 1996, 31, 2091-95.

Sarwar M., Manzoor T., Ahamd E. and Hussain N. The role of connectivity of martensite on the tensile properties of a low alloy steel. *Material and design*, 2007, 28, 1928-33.

Shen H. P., Lei T. C. and Liu J. Z. Microscopic deformation behaviour of martensitic-ferritic dual-phase. *Mater. Sci. Tech.,* 1986, 2, 28-33.

Shimada S., Takada Y., Lee J. and Tanaka T. Trial of Evaluate Wettability of Liquid Zn with Steel Sheets Containing Si and Mn. *ISIJ-Int.,* 2008, 48, 1246-1250.

Speich G. R. and Miller R. L. In *Structure and Properties of Dual-phase Steels,* (eds. Kot R.A., Morris J.W.) TMS-AIME, New York, NY, 1979, 145-182.

Steinbergunner D. L., Matlock D. K. and Krauss G. Void formation during tensile testing of dual phase steels. *Metal. Trans. A,* 1988;19A:579-89.

Stelmashenko N. A., Walls M. G., Brown L. M. and Milman Y. U. V. Microindentations on W and Mo oriented single crystals: AN STM study. *Acta Metall. Mater.,* 1993, 141, 2855-2865.

Su Y. L. and Gurland J. Strain partition, uniform elongation and fracture strain in dual-phase steels. *Mater. Sci.Eng.,*1987, 95, 151-65.

Sun S. and Pugh M . Properties of thermomechanically processed dual-phase steels containing fibrous martensite. *Mater. Sci. Eng. A*, A335 (2002) 298-308.

Sugimoto K., Sakaki T., Fukusato T. and Miyagawa O. Influence of Martensite Morphology on Initial Yielding and Strain Hardening in a 0.11C-1.36Mn Dual phase Steel. *Tetsu-to-hagane,* 1985, 71, 994-1001.

Szewczyk A. F. and Gurland J. A study of the deformation and fracture of a dual-phase steel. *Metall. Trans. A,*1982, 13A, 1821-26.

Takada Y., Shimada S., Lee J. Kurosaki M. and Tanaka T. The Effect of Si and Mn Content on Dynamic Wetting of Steel with Liquid Zn. *ISIJ-Int.,* 2009, 49, 100-104.

Tasan C. C., Hoefnagels J. P. M. and Geers M. G. D. Microstructural banding effects clarified through microscopic digital image correlation. *Scripta Metall.,* 2010, 62, 835-38.

Tasan C. C., Hoefnagels J. P. M. and Geers M. G. D. Experimental analysis of strain path development ductile damage mechanics and forming limit. *Mechanics and Mater.,* 2009, 41, 1264-1276.

Toji Y., Takagi S., Yoshino K., Hasegawa K. and Tanaka Y. Evaluation of hydrogen embrittlement for high strength steels. *Tetsu-to-Hagane,* 2009, 95, 81.

Thomas G. and Koo J. Y. In *Structure and Properties of Dual phase Steels.* (eds. Kot R. A and Morris J. W.), TMS-AIME, Warrendale, PA, 1979, 183-201.

Tomota Y., Yoshino H. and Kuroki K. Effect of ductility of the second phase on ductile fracture. *Scripta Metall.*,1977,11, 853-56.

Traiviratanav S., Bringa E. M., Benson D. J. and Meyers M. A. Void growth in metals: Atomistic calculations original. *Acta Metall.,* 2008, 56, 3874-86.

Uthaisangsuk V., Prahl U. and Bleck W. Micromechanical modelling of damage behaviour of multiphase steel. *Comp. Mater. Sci.,* 2008, 43, 27-37.

Yamazaki K., Mizuyama Y., Oka M., Tsuchiya H. and Yasuda H. Recent advance in ultrahigh-strength sheet steels for automotives. *Nippon Steel Technical Report,* 1995, 64, 37-44.

Vajragupta N., Uthaisangsuk V., Schmaling B., Munstermann S., Hartmaier A. and Bleck W. A Micromechanical damage simulation of dual phase steels using XFEM. *Comput. Mater. Sci.,* 2012, 54, 271-279.

Vasudevan A. K. and Richmond O. The influence of hydrostatic pressure on the ductility of Al-SiC composite. *Mater. Sci. Eng.*, 1989, A107, 63-69.

Whitehouse A. F. and Clyne T. W. Cavity formation during testing starting of particulate and short fiber metal matrix composites. *Acta Metall.,* 1993, 41, 1701-11.

Danmarks Tekniske Universitet
DTU Vindenergi
Nils Koppels Allé
Bygning 403
2800 Kgs. Lyngby
Telefon 45 25 25 25
info@vindenergi.dtu.dk
www.vindenergi.dtu.dk